

CHEMICAL CONSTITUENTS OF *Knema angustifolia* STEM AND BIOLOGICAL ACTIVITIES



A Thesis Submitted in Partial Fulfillment of the Requirements
for the Degree of Master of Science in Chemistry
Department of Chemistry
Faculty of Science
Chulalongkorn University
Academic Year 2019
Copyright of Chulalongkorn University

องค์ประกอบทางเคมีของลำต้นกำลังเลื้อยตม *Knema angustifolia* และฤทธิ์ทางชีวภาพ



วิทยานิพนธ์นี้เป็นส่วนหนึ่งของการศึกษาตามหลักสูตรปริญญาวิทยาศาสตรมหาบัณฑิต

สาขาวิชาเคมี ภาควิชาเคมี

คณะวิทยาศาสตร์ จุฬาลงกรณ์มหาวิทยาลัย

ปีการศึกษา 2562

ลิขสิทธิ์ของจุฬาลงกรณ์มหาวิทยาลัย

ดุง เล ทิ คิม : องค์ประกอบทางเคมีของลำต้นกำลังเลื้อยค้ำ *Knema angustifolia* และ
ฤทธิ์ทางชีวภาพ. (CHEMICAL CONSTITUENTS OF *Knema angustifolia* STEM
AND BIOLOGICAL ACTIVITIES) อ.ที่ปรึกษาหลัก : ผศ. ดร.วรินทร์ ชวนศิริ

สมุนไพรกำลังเลื้อยค้ำ *Knema angustifolia* ถูกใช้เป็นยาตามความเชื่อของแพทย์แผน
โบราณสำหรับการบำบัดเชื้อโรคต่างๆ มีรายงานข้อมูลทางเคมีของพืชชนิดนี้น้อย ได้แยกพาราเบน
ไซควิโนนตัวใหม่ชื่อ angustiquinone (3) และสารที่ทราบสูตรโครงสร้างแล้วสิบสาร ได้แก่
rapanone (1), embellin (2), quercetrin (4), kaempferol (5) bergenin (6), 11-O-acetyl
bergenin (7), catechin (8), isovanillic acid (9), protocatechuic acid (10) และ gallic acid
(11) จากสิ่งสกัดเฮกเซนและเอทิลแอสีเทตของลำต้น *K. angustifolia* ได้ศึกษาโครงสร้างของสาร
ที่แยกได้ด้วยการวิเคราะห์ด้วย 1D และ 2D เอ็นเอ็มอาร์, HRMS และการเปรียบเทียบข้อมูลจาก
เอกสารอ้างอิง ได้ทดสอบฤทธิ์ยับยั้งเอนไซม์ tyrosinase และ α -glucosidase ของสารประกอบ
1-2 และ 4-11 พบว่า quercetrin (4) และ kaempferol (5) เป็นสารยับยั้ง tyrosinase ที่มี
ศักยภาพ ด้วยค่า IC_{50} 42.3 ± 0.26 และ 156.5 ± 0.34 μ M สำหรับ rapanone (1) และ embellin
(2) แสดงฤทธิ์ยับยั้ง α -glucosidase ที่ดีมาก ด้วยค่า IC_{50} 1.3 ± 0.17 และ 9.25 ± 0.26 μ M
ตามลำดับ ซึ่งมีฤทธิ์ดีกว่า acarbose ที่เป็นยาที่ใช้ทั่วไป 93.6 ± 0.49 μ M

จุฬาลงกรณ์มหาวิทยาลัย
CHULALONGKORN UNIVERSITY

สาขาวิชา เคมี
ปีการศึกษา 2562

ลายมือชื่อนิสิต

ลายมือชื่อ อ.ที่ปรึกษาหลัก

6072199823 : MAJOR CHEMISTRY

KEYWORD: Knema angustifolia/ embelin/ rapanone/ anti-tyrosinase/ α -glucosidase inhibitory activity

Dung Le Thi Kim : CHEMICAL CONSTITUENTS OF *Knema angustifolia* STEM AND BIOLOGICAL ACTIVITIES. Advisor: Asst. Prof. WARINTHORN CHAVASIRI, Ph.D.

The medicinal plant *Knema angustifolia* has been used in Thai folk medicine for the treatment of various diseases, especially related to body tonic or blood tonic agent. Chemical data on this plant are scarce. A novel *para*-benzoquinone, angustiquinone (3), along with ten known compounds, rapanone (1), embelin (2), quercetin (4), kaempferol (5), bergenin (6), 11-*O*-acetyl bergenin (7), catechin (8), isovanillic acid (9), protocatechuic acid (10) and gallic acid (11) were isolated from the *n*-hexane and EtOAc extracts of the stems of *K. angustifolia*. Their structures were unambiguously elucidated using extensive 1D and 2D NMR analyses, high-resolution mass spectrometry along with comparison with literature data. Compounds 1-2 and 4-11 were tested for anti-tyrosinase and α -glucosidase inhibitory activity. Quercetin (4) and kaempferol (5) revealed as potent inhibitors of tyrosinase activity, in which the IC_{50} 42.3 ± 0.26 , 156.5 ± 0.34 μ M, respectively. Notably, rapanone (1) and embelin (2) exhibited excellent α -glucosidase inhibitory activity with IC_{50} 1.3 ± 0.17 and 9.25 ± 0.26 μ M, respectively which much higher than commercial drug acarbose (93.6 ± 0.49 μ M).

Field of Study: Chemistry

Student's Signature

Academic Year: 2019

Advisor's Signature

ACKNOWLEDGEMENTS

First of all, the author would like to give special thanks to her advisor, Assistant Professor Dr. Warinthorn Chavasiri. Detailed guidance, tremendous support and heartening encouragement during the progress of this thesis have been vital in its success. Furthermore, thankfulness is also prolonged to the Center of Excellence in Natural Products Chemistry, Department of Chemistry for providing the best facilities to complete the extensive research performed.

The author expresses sincere gratitude to Associate Professor Dr. Vudhichai Parasuk, Associate Professor Dr. Pattara Thiraphibundet and Associate Professor Dr. Pongtip Sithisarn for being her chairman and committees, as well as for their advice.

The author wishes to express appreciation toward the ASEAN scholarship 2018 for subsidizing her Master's program. Besides, it would be tremendous and progress-driving for the author to receive the Overseas Research Experience Scholarship from Graduate school and Faculty of Science, Chulalongkorn University, which provides a chance not only to broaden and further knowledge but also an opportunity to explore the culture of Japan.

The author also admits Professor Dr. Mamoru Koketsu, Faculty of Engineering, Gifu University, for his kind assistance and sharing his extensive knowledge. Further acknowledgment is sent to all members of WC's lab for their mental and physical help through her study. Notably, the author would like to thank the Ph.D. student, Asshaima Paramita Devi, who responsible for testing the biological activities of her samples.

Finally, words cannot describe the feeling of the utmost profound gratitude dedicated to her family, who have always been beside her, and share the difficulties when the author is dedicated to complete research for the good of science away from home. They try to enable the best conditions for her to finish the course of research.

Dung Le Thi Kim

TABLE OF CONTENTS

	Page
.....	iii
ABSTRACT (THAI).....	iii
.....	iv
ABSTRACT (ENGLISH).....	iv
ACKNOWLEDGEMENTS.....	v
TABLE OF CONTENTS.....	vi
LIST OF TABLES.....	ix
LIST OF FIGURES.....	xi
LIST OF SCHEMES.....	xiii
LIST OF ABBREVIATIONS.....	xiv
Chapter 1 Introduction.....	1
1.1 Characteristics and traditional usage of plants in <i>Knema</i> genus.....	2
1.2 Chemical constituents of <i>Knema</i> genus.....	4
1.3 Bioactive compounds from <i>Knema</i> genus.....	8
1.4 Botanical aspects and traditional usage of <i>Knema angustifolia</i>	10
1.5 Previous study on <i>K. angustifolia</i>	11
1.6 Biological activity.....	12
1.6.1 Anti-tyrosinase activity ²²	12
1.6.2 α -glucosidase inhibitory activity.....	13
1.7 The goal of this research.....	14
Chapter 2 Experimental.....	16

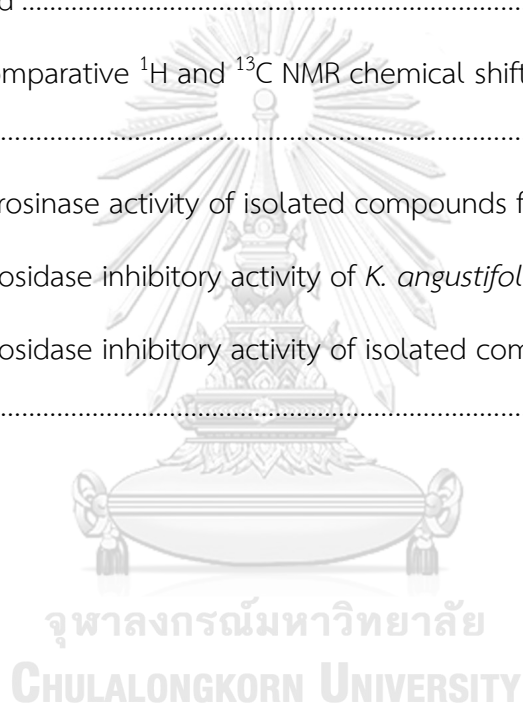
2.1 Plant material.....	16
2.2 Chemical and enzymes.....	16
2.3 Instruments and equipment.....	17
2.4 Extraction procedure of the <i>Knema angustifolia</i> stems.....	17
2.5 Bioassay Procedures.....	22
2.5.1 Anti-tyrosinase activity.....	22
2.5.2 α -glucosidase inhibitory activity.....	23
Chapter 3 Results and discussion.....	25
3.1 Preliminary study of crude extracts.....	25
3.2 Chemical constituents from <i>K.angustifolia</i> stems.....	26
3.2.1 Separation of <i>n</i> -hexane extract.....	26
3.2.1.1 Separation of fraction H5.....	26
3.2.2 Separation of ethyl acetate extract.....	29
3.2.2.1 Separation of fraction E2.....	30
3.2.2.2 Separation of fraction E3.....	31
3.2.3 Structural elucidation of isolated compounds.....	33
3.2.3.1 Structural elucidation of compound 1.....	33
3.2.3.2 Structural elucidation of compound 2.....	34
3.2.3.3 Structural elucidation of compound 3.....	34
3.2.3.4 Structural elucidation of compound 4.....	38
3.2.3.5 Structural elucidation of compound 5.....	40
3.2.3.6 Structural elucidation of compound 6.....	42
3.2.3.7 Structural elucidation of compound 7.....	44
3.2.3.8 Structural elucidation of compound 8.....	45

3.2.3.9 Structural elucidation of compound 9	49
3.2.3.10 Structural elucidation of compound 10.....	49
3.2.3.11 Structural elucidation of compound 11	50
3.3 Biological activities of isolated compounds from the stem of <i>K.angustifolia</i>	53
3.3.1 Anti-tyrosinase	53
3.3.2 α -Glucosidase inhibitory activity.....	55
Chapter 4 Conclusions	60
4.1 Chemical constituent of <i>K. angustifolia</i> stems	60
4.2 Biological activities	61
4.3 Suggestions for future work.....	62
APPENDIX.....	63
REFERENCES	83
VITA.....	88

LIST OF TABLES

	Page
Table 1.1 Uses of <i>Knema</i> genus plants in traditional medicine.....	3
Table 1.2 Bioactivities of some <i>Knema</i> genus substances	8
Table 1.3 Antibacterial activity of <i>K. angustifolia</i> extracts.....	11
Table 1.4 Antioxidant activity of the <i>K. angustifolia</i> extracts.....	12
Table 3.1 Anti-tyrosinase activity of <i>K. angustifolia</i> extracts.....	25
Table 3.2 The separation of <i>n</i> -hexane extract of <i>K. angustifolia</i> stems.....	26
Table 3.3 The separation of HS.....	28
Table 3.4 The separation of HS3	29
Table 3.5 The separation of Ea extract of <i>K.angustifolia</i> stems.....	29
Table 3.6 The separation of E2	30
Table 3.7 The separation of E3	31
Table 3.8 The separation of E3.5.....	32
Table 3.9 The tentative ¹ H and ¹³ C NMR chemical shift assignments of 1 , 2 , and 3 ..	37
Table 3.10 The ¹ H and ¹³ C NMR chemical shift assignments of 4 compared with those of quercetin.....	39
Table 3.11 The ¹ H and ¹³ C NMR chemical shift assignments of 5 compared with those of kaempferol	41
Table 3.12 The ¹ H and ¹³ C NMR chemical shift assignments of 6 compared with those of bergenin	43

Table 3.13 The ^1H and ^{13}C NMR chemical shift assignments of 7 compared with those of 11- <i>O</i> -acetyl bergenin	47
Table 3.14 The ^1H and ^{13}C NMR chemical shift assignments of 8 compared with those of catechin.....	48
Table 3.15 The ^1H and ^{13}C NMR chemical shift assignments of 9 compared with those of isovanillic acid.....	51
Table 3.16 The comparative ^1H and ^{13}C NMR chemical shift assignments of 10 and protocatechuic acid	52
Table 3.17 The comparative ^1H and ^{13}C NMR chemical shift assignments of 11 and gallic acid.....	52
Table 3.18 Anti-tyrosinase activity of isolated compounds from <i>K.angustifolia</i>	54
Table 3.19 α -glucosidase inhibitory activity of <i>K. angustifolia</i> extracts	56
Table 3.20 α -glucosidase inhibitory activity of isolated compounds from <i>K. angustifolia</i>	57



LIST OF FIGURES

	Page
Figure 1.1 Twelve species of <i>Knema</i> genus in Thailand	2
Figure 1.2 Chemical constituents from <i>Knema</i> genus	6
Figure 1.3 Stems (A), leaves (B), male flowers (C) and fruits (D) of <i>K. angustifolia</i>	10
Figure 1.4 Production pathways of melanin biosynthesis.....	13
Figure 1.5 Structures of α -glucosidase inhibitor.....	14
Figure 2.1 The stems of <i>Knema angustifolia</i>	16
Figure 3.2 Key HMBC correlation of 3	36
Figure A.1 HR-ESI-MS spectrum of 1 (pos).....	64
Figure A.2 The ^1H NMR (400 MHz) spectrum of 1 (DMSO- d_6).....	65
Figure A.3 The ^{13}C NMR (100 MHz) spectrum of 1 (DMSO- d_6).....	65
Figure A.4 HR-ESI-MS spectrum of 2 (pos).....	66
Figure A.5 The ^1H NMR (400 MHz) spectrum of 2 (DMSO- d_6).....	67
Figure A.6 The ^1H NMR (400 MHz) spectrum of 2 (DMSO- d_6).....	67
Figure A.7 HR-ESI-MS spectrum of 3 (neg).....	68
Figure A.8 The ^1H NMR (500 MHz) spectrum of 3 (CDCl $_3$).....	69
Figure A.9 The ^{13}C NMR (JMOD, 125 MHz) spectrum of 3 (CDCl $_3$).....	69
Figure A.10 The HSQC spectrum of 3 (CDCl $_3$).....	70
Figure A.11 The HMBC spectrum of 3 (CDCl $_3$).....	70
Figure A.12 The ^1H NMR (400 MHz) spectrum of 4 (acetone- d_6).....	71
Figure A.13 The ^{13}C NMR (100 MHz) spectrum of 4 (acetone- d_6).....	71

Figure A.14	The HSQC spectrum of 4 (acetone- d_6).....	72
Figure A.15	The HMBC spectrum of 4 (acetone- d_6)	72
Figure A.16	The ^1H NMR (400 MHz) spectrum of 5 (DMSO- d_6).....	73
Figure A.17	The ^{13}C NMR (100 MHz) spectrum of 5 (DMSO- d_6).....	73
Figure A.18	The ^1H NMR (400 MHz) spectrum of 6 (DMSO- d_6).....	74
Figure A.19	The ^{13}C NMR (100 MHz) spectrum of 6 (DMSO- d_6).....	74
Figure A.20	The HSQC spectrum of 6 (DMSO- d_6).....	75
Figure A.21	The HMBC spectrum of 6 (DMSO- d_6)	75
Figure A.22	The ^1H NMR (400 MHz) spectrum 7 (CD_3OD).....	76
Figure A.23	The ^{13}C NMR (100 MHz) spectrum of 7 (CD_3OD).....	76
Figure A.24	The HSQC spectrum of 7 (CD_3OD).....	77
Figure A.25	The HMBC spectrum of 7 (CD_3OD)	77
Figure A.26	The ^1H NMR (400 MHz) spectrum of 8 (acetone- d_6).....	78
Figure A.27	The ^{13}C NMR (100 MHz) spectrum of 8 (acetone- d_6).....	78
Figure A.28	The HMBC spectrum of 8 (acetone- d_6)	79
Figure A.29	The ^1H NMR (400 MHz) spectrum of 9 (acetone- d_6).....	80
Figure A.30	The ^{13}C NMR (100 MHz) spectrum of 9 (acetone- d_6).....	80
Figure A.31	The ^1H NMR (400 MHz) spectrum of 10 (acetone- d_6).....	81
Figure A.32	The ^{13}C NMR (100 MHz) spectrum of 10 (acetone- d_6)	81
Figure A.33	The ^1H NMR (400 MHz) spectrum of 11 (acetone- d_6).....	82
Figure A.34	The ^{13}C NMR (100 MHz) spectrum of 11 (acetone- d_6)	82

LIST OF SCHEMES

	Page
Scheme 2.1 The extraction of <i>Knema angustifolia</i> stems	18
Scheme 2.2 Procedure for the separation of <i>n</i> -hexane fraction of <i>K.angustifolia</i>	20
Scheme 2.3 Procedure for the separation of Ea fraction of <i>K.angustifolia</i>	21
Scheme 2.4 Hydrolysis of p-nitrophenyl- α -D-glucopyranoside by α -glucosidase	23
Scheme 3.1 Fractionation of fraction H5	27
Scheme 3.2 Fractionation and isolation of HS	27
Scheme 3.3 Fractionation and isolation of HS3	28
Scheme 3.4 Fractionation and isolation of E2	30
Scheme 3.5 Fractionation and isolation of E3.4	32

LIST OF ABBREVIATIONS

1D	One dimensional
2D	Two dimensional
Ac	Acetone
AcOH	Acetic acid
calcd	Calculated
CDCl ₃	Deuterated chloroform
CC	Column chromatography
CH ₂ Cl ₂	Dichloromethane
d	Doublet
dd	Doublet of doublets
ddd	Doublet of doublet of doublets
DMSO-d ₆	Deuterated dimethyl sulfoxide
EtOAc	Ethyl acetate
EtOH	Ethanol
HMBC	Heteronuclear multiple bond correlation
HR-ESI-MS	High resolution electrospray ionization mass
	Spectroscopy
HSQC	Heteronuclear single quantum correlation
m	Multiplet
MHz	Mega Hertz

MeOH	Methanol
NMR	Nuclear magnetic resonance
ppm	Parts per million (chemical shift value)
s	Singlet
t	Triplet
TLC	Thin-layer chromatography
μL	Microliter (s)
μM	Micromolar



Chapter 1

Introduction

For centuries, natural products and their derivatives have been considered to possess an essential role in medicinal chemistry. Bioactive compounds isolated from a rich diversity of plants, animals and microorganisms have been at the very core of many pharmaceutical drugs. Such a significant example is given by the antibiotics filtrate “penicillin” from *Penicillium notatum*, discovered by Fleming in 1928 thereby creating a massive milestone in the discovery of an efficient method to cure deadly infectious diseases¹. Notably, pharmaceutical drugs derived from natural products have illustrated more desirable interactions with human cells, albeit with fewer side effects relative to synthetically made pharmaceutical drugs². Moreover, the abundance of a diverse pool of natural chemical skeletons could be useful for scientists in order to improve the drawback of the known products and to pursue novel drug candidates.

Thailand located in Southeast Asia, is known as a tropical country with a variety of plant species, particularly herbs which were utilized in traditional medicine for the prevention or treatment of various diseases³. Therefore, these herbal plants could serve as a promising source, and further scientific study should be carried out to aid a medicinal chemistry advance. Specifically, the extracts of *Knema angustifolia* stems collected at Nongkhai province of Thailand, possessed intense cytotoxic activity, coupled with high antioxidant activity – collaborated with the investigation of

Phadungkit and co-workers in 2010⁴. In addition, until the present, there has been no report regarding the chemical constituents. Therefore, it is interesting to establish this plant as a source of bioactive compounds with potential uses in medication. Through the separation and purification process of plant material, the chemical components of *K. angustifolia* will be assessed, as well as their biological activities – for example, enzyme inhibitory activities – will be elucidated.

1.1 Characteristics and traditional usage of plants in *Knema* genus

The *Knema* genus belongs to Myristicaceae family and are widely distributed in tropical habitats situated in Asia, Africa and Australia. In Thailand, at least 12 different species have been identified (Figure 1.1)⁵.

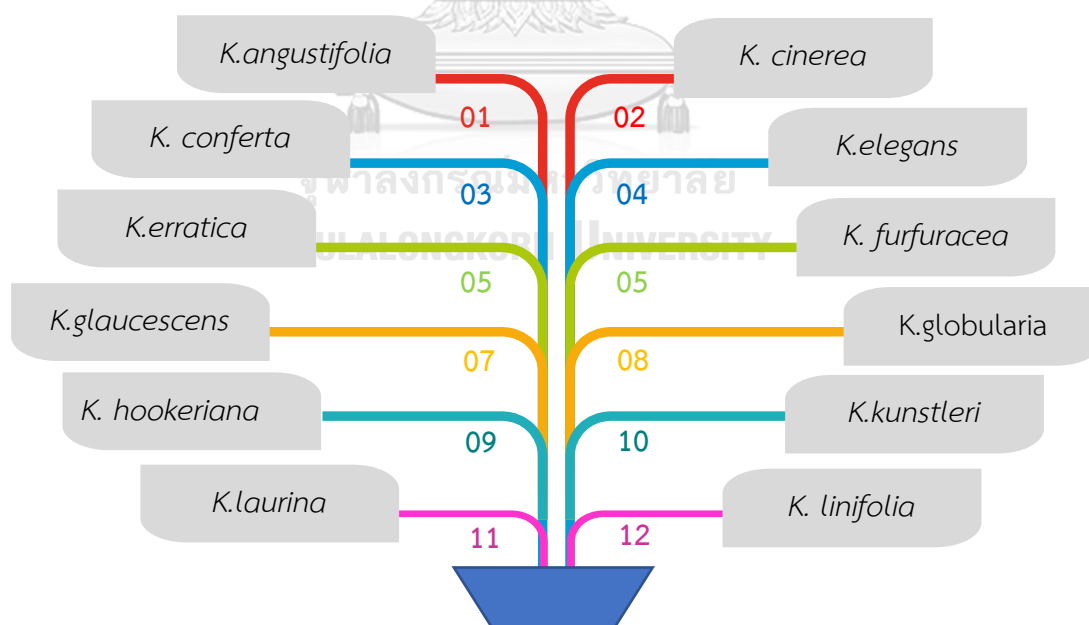


Figure 1.1 Twelve species of *Knema* genus in Thailand

Plants in *Knema* genus have been popularly used as folk medicine in the culture of various countries, especially in the Asian region. For instance, the mixture of *K. globularia* seeds and ointment has been traditionally used for centuries by the indigenous people of Indonesia and China to cure skin diseases, particularly scabies and to apply in the medicinal soap field. In the Philippines, an infusion of the barks of *K. heterophylla* was prepared and considered as a gargle for sore mouth and throat. Other contributions of *Knema* plants in traditional medication were reported in **Table 1.1**.

Table 1.1 Uses of *Knema* genus plants in traditional medicine

Plant	Plant part	Country	Uses or treatment	References
<i>K. angustifolia</i>	Stems	Thailand	Blood tonic or body tonic mediator	6
<i>K. attenuata</i>	-	India	Spleen and breathing disorders.	7
<i>K. furfuraceae</i>	Barks	Thailand	Remedy for sores, pimples, and cancers	8
<i>K. glaucescens</i>	Barks	Indonesia	Abdominal illnesses	9
<i>K. laurina</i>	-	Malaysia	Digestive and inflammatory diseases	10
<i>K. tenuinervia</i>	Barks	Thailand	Therapy for cancer	11

1.2 Chemical constituents of *Knema* genus

The previous investigation on chemical constituents of this genus illustrated the presence of several useful skeletons such as stilbenes, flavonoids, lignans, anacardic acid, alkyl/acyl resorcinol, and other compounds.

Twelve compounds: desoxyrhapontigenin (1), 3,4'-dimethoxy-5-hydroxystilbene (2), 1-(2-methoxy-4-hydroxy-phenyl)-3-(3-hydroxy-4-methoxyphenyl)propane (3), 1-(2,6-dihydroxyphenyl)-tetradecan-1-one (4), malabaricone A (5), (*Z*)-1-(2,6-dihydroxy phenyl)-tetradec-(?)-en-1-one (6), 1-(2,4,6-trihydroxyphenyl)-tetradecan-1-one (7), 1-(2,4,6-trihydroxyphenyl)-9-phenylnonan-1-one (8), (*Z*)-1-(2,4,6-trihydroxyphenyl) tetradec-(?)-en-1-one (9), (+)-episesamin (10), (+)-xanthoxylol (11), and (\pm)-7,4'-di-hydroxy-3'-methoxyflavan (12) were isolated from the woods of *K. austrosiamensis* (Figure 1.2)¹².

In 1993, from the leaves of *K. furfuracea*, Zahir and coworkers discovered two new phenylacylphenols: knerachelins A (13) and B (14) (Figure 1.2)¹³.

In addition, in 2009, Rangkaew and coworkers isolated a new acyclic diterpene acid: glaucaic acid (15), together with seven known compounds: 1-(2,6-dihydroxy-phenyl)tetradecan-1-one (4), malabaricone A (5), 1-(2,4,6-trihydroxyphenyl)-9-phenyl-nonan-1-one (8), dodecanoylphloroglucinol (16), sesamin (17), asarinin (18), myristinin D (19) from the fruits of *K. glauca*. Besides, two compounds: (\pm)-7,4'-dihydroxy-3'-methoxyflavan (12) and myristinin A (20) were found from the leaves and stems, respectively (Figure 1.2)¹⁴.

From the stem barks of *K. glomerata*, Zeng and coworkers reported the presence of three new compounds: kneglomeratanol (**21**), kneglomeratanones A (**22**) and B (**23**), along with ten known compounds: 3-(12'-phenyldodecyl)phenol (**24**), 3-(10'-phenyldecyl)phenol (**25**), 5-pentadecylresorcinol (**26**), 5-(10'-phenyldecyl)-resorcinol (**27**), 5-(12'-phenyldodecyl)resorcinol (**28**), 2,4-dihydroxy-6-(10'-phenyldecyl)-aceto-phenone (**29**), 2-hydroxy-6-(12'-phenyldodecyl)benzoic acid (**30**), formononetin (**31**), biochanin A (**32**), and 8-*O*-methylretusin (**33**) (**Figure 1.2**)¹⁵.

In 2011, Akhtar and coworkers isolated five derivatives of alkenyl phenol and salicylic acid (**Figure 1.1**) from the stem barks of *K. laurina*, including (+)-2-hydroxy-6-(10'-hydroxypentadec-8'(E)-enyl)benzoic acid (**34**) and 3-pentadec-10'(Z)-enylphenol (**35**), 3-heptadec-10'(Z)-enylphenol (**36**), 2-hydroxy-6-(pentadec-10'(Z)-enyl)benzoic acid (**37**), and 2-hydroxy-6-(10'(Z)-heptadecenyl)benzoic acid (**38**) (**Figure 1.2**)¹⁶.

From *K. globularia*, the investigation of Wenli and coworkers showed the existence of kaempferol-3-*O*- β -D-glucopyranoside (**39**), quercetin-3-*O*- β -D-glucopyranoside (**40**) in 2000¹⁷ and eight compounds, named taxifolin (**41**), luteolin (**42**), catechin (**43**), 3',4',6' trihydroxyaurone (**44**), 7-megastigmene-3,6,9 triol (**45**), β -sitosterol (**46**), and daucosterol (**47**) in 2002 (**Figure 1.2**)¹⁸.

In 2019, from the EtOAc fraction of *K. pachycarpa* stems, Giap and coworkers discovered two new acetophenone derivatives: knepachycarpanone A (**48**) and knepachycarpanone B (**49**) and a new cardanol derivative knepachycarpanol C (**50**)¹⁹. In the same year, from the *n*-hexane extract, five new compounds, named

knepachycarpic acid A (51), B (52), knepachycarpanol A (53), B (54), and knepachycarpasinol (55)²⁰ were isolated (Figure 1.2).

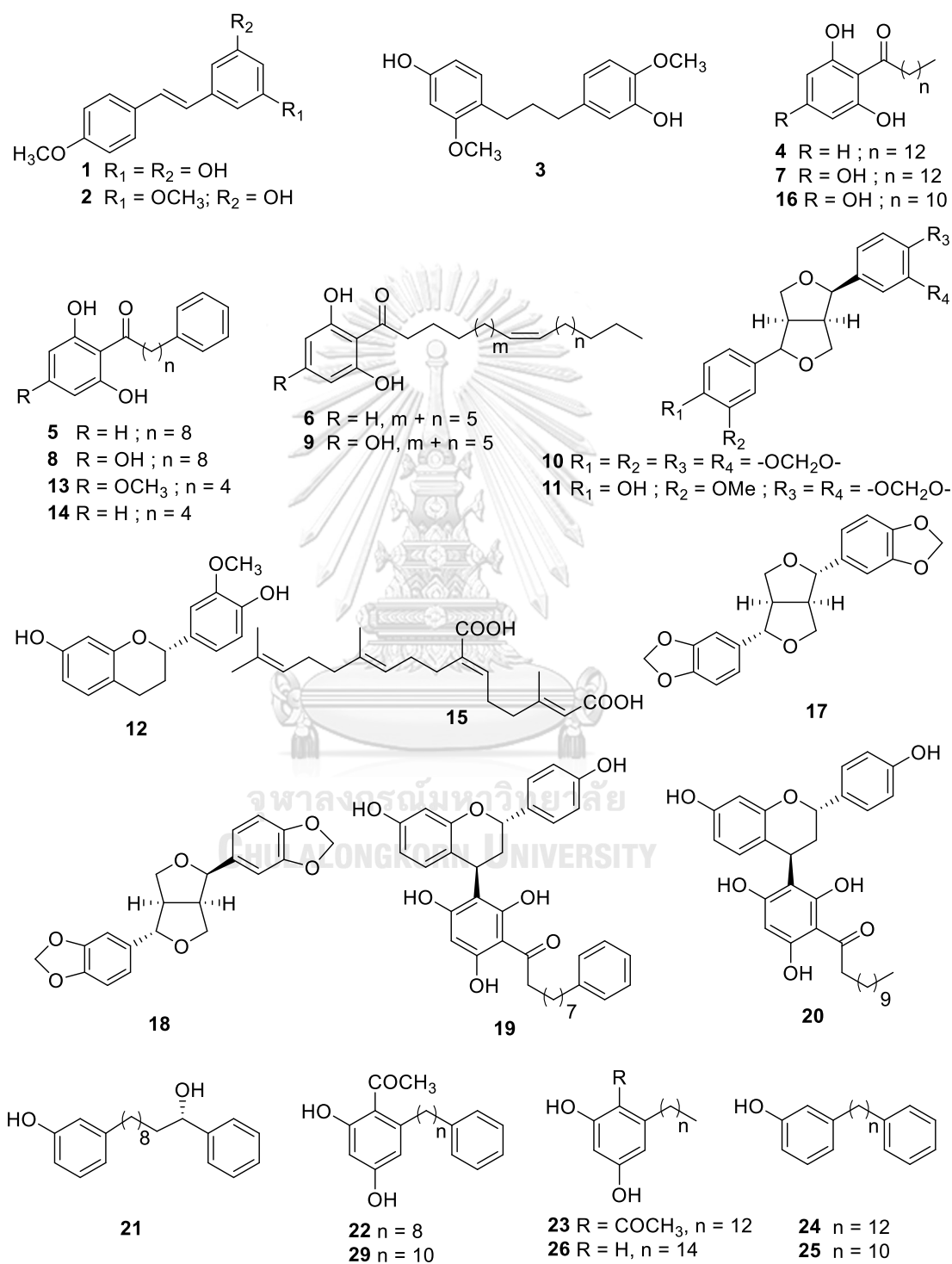


Figure 1.2 Chemical constituents from *Knema* genus

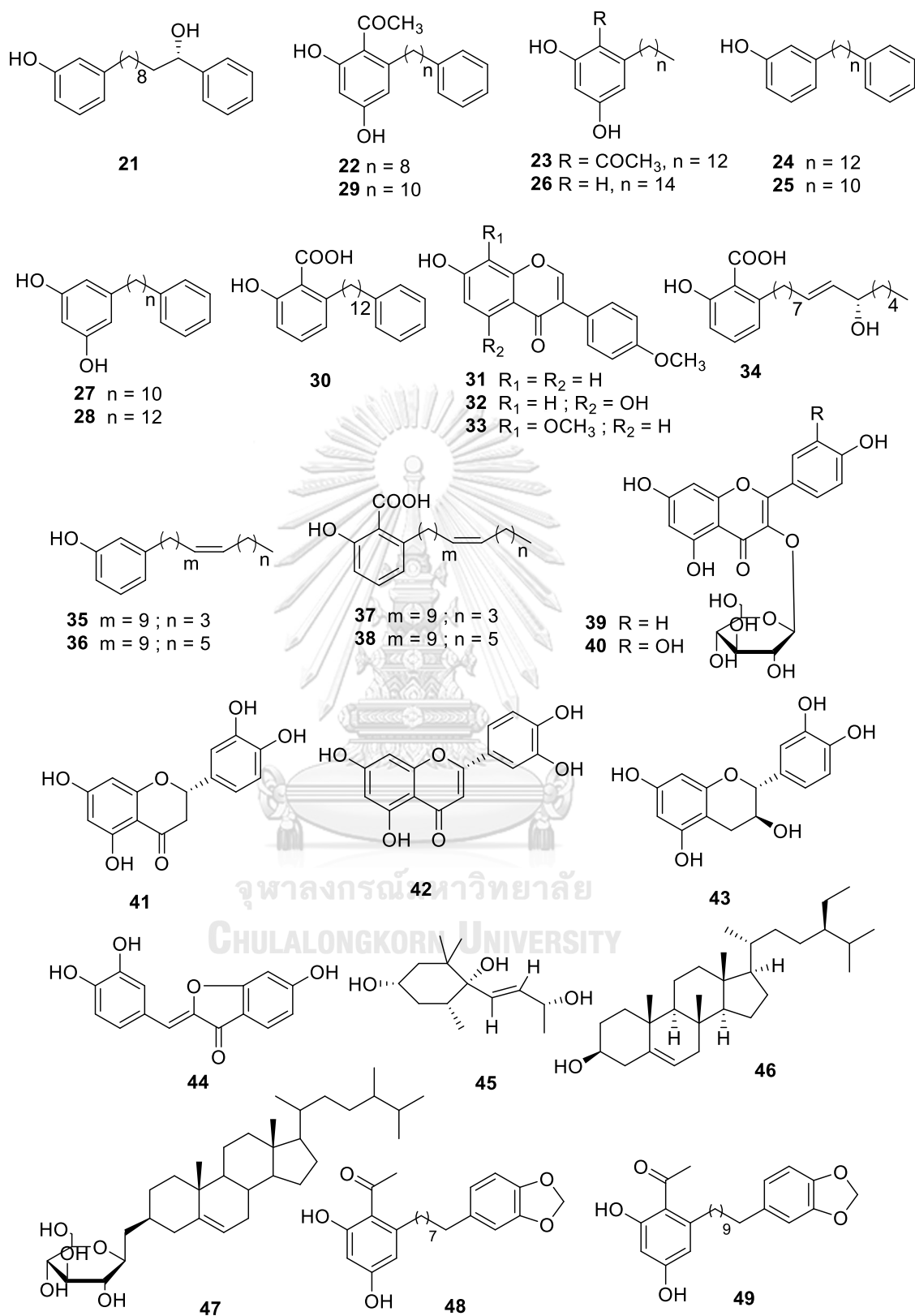


Figure 1.2 Chemical constituents from *Knema* genus (continued)

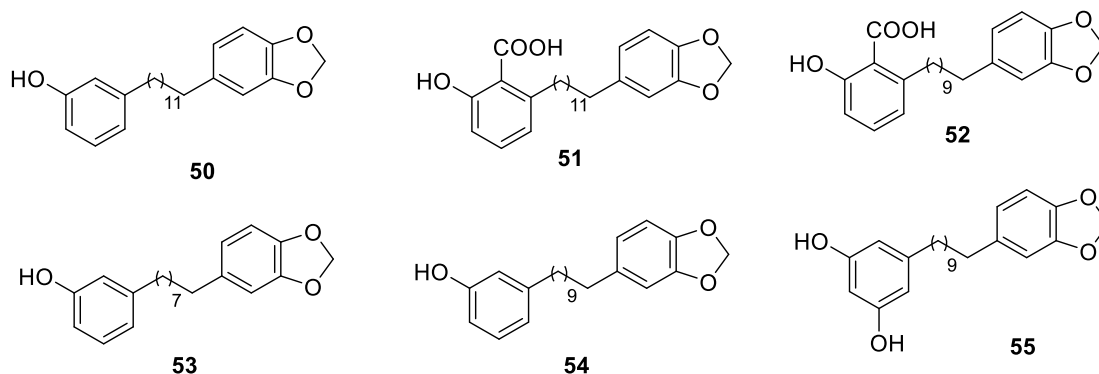


Figure 1.2 Chemical constituents from *Knema* genus (continued)

1.3 Bioactive compounds from *Knema* genus

The isolated compounds from this genus exhibited various pharmacological effects, including antibacterial, antiviral, antimalarial, cytotoxicity and anti-acetylcholinesterase activities. A brief outline of their biological activities were illustrated in Table 1.2

Table 1.2 Bioactivities of some *Knema* genus substances

Antibacterial activity		
Compounds	Organism	References
Knerachelins A (13) and B (14)	- <i>Staphylococcus aureus</i> with MIC values 8 and 4 $\mu\text{g/mL}$ for 13 and 14, respectively - <i>Streptococcus pneumoniae</i> , with MIC value 8 $\mu\text{g/mL}$ for both compounds	13

Antiviral activity		
Compounds	Organism	References
Malabaricone A (5)	Malarial parasite <i>Plasmodium falciparum</i> (IC ₅₀ 2.78 µg/mL)	14
Dodecanoylphloroglucinol (16)	Herpes simplex virus type 1 (IC ₅₀ 3.05 µg/mL)	
Enzyme inhibition activity		
2-hydroxy-6-(10'(Z)-heptadecenyl)benzoic acid (38)	Acetylcholinesterase with IC ₅₀ value of 0.57 µM.	16
Knepachycarpanol A (53) and knepachycarpasinol (55)	Acetylcholinesterase with IC ₅₀ values of 2.60 and 2.46 mM, respectively	
Cytotoxicity		
Kneglomeratanone B (23)	MCF-7 (IC ₅₀ 1.12 µg/mL)	15
3-(12'-phenyldodecyl)phenol (24)	A-549 (IC ₅₀ 1.85 µg/mL) and HT-29 (IC ₅₀ 2.62 µg/mL)	

1.4 Botanical aspects and traditional usage of *Knema angustifolia*

K. angustifolia (Roxb.) Warb. has been known as “Kamlang Leuat Ma” in Thailand⁶. Besides that, the indigenous people of Thai still called this plant with other names, such as Mamuang Leaut Noi, Phadong Leaut, Phadong Fai or Leaut Kway. It is a medium-sized tree containing the red resin in its bark, usually used by a word meaning “horse blood” in their local names, and the details of botanical characteristics were described below²¹:

Trees: evergreen tree growing 10-20 m tall with twigs slender.

Leaves: simple with the nerves in a fishbone arrangement.

Flowers: the individual plant has either male inflorescences or female inflorescences. While male inflorescences contain 7-8 flowered, female inflorescences have only 1-2 flowered. Its flowers covered with brown woolly hairs outside and cream or yellowish inside.

Fruits: globose, orange with crusty red granules and covered initially with brownish hairs. Fruit stalk 0.5–1.2 cm long and 0.2–0.4 cm broad.



Figure 1.3 Stems (A), leaves (B), male flowers (C) and fruits (D) of *K. angustifolia*

The stems have traditionally been used as whole-body tonic or blood tonic agent. It can be used as an herbal drink for many purposes such as nourish and create blood, cure lymphatic wounds, abscesses, rashes. Moreover, this plant can mix with other herbal plants to make ginseng with various benefits for health.

1.5 Previous study on *K. angustifolia*

Although the plants in *Knema* genus were previously investigated by many scientists; only one paper in 2010 was described the phytochemical screening and biological activities of *K. angustifolia*⁴. In that study, both EtOH and dichloromethane extracts possessed moderate antibacterial activity against *S. aureus* (Table 1.3). Moreover, the EtOH extracts showed the modest antioxidant activity compared to ascorbic acid (Table 1.4) and high cytotoxicity against lung cancer cell line (NCI-H187) with IC₅₀ value of 4.55 µg/mL. The dichloromethane extract showed less potent candidate for both activities.

Table 1.3 Antibacterial activity of *K. angustifolia* extracts

	Zone of inhibition, nm		
	<i>S. aureus</i> ATTC 25923	<i>E. Coli</i> ATTC 25922	<i>P. aeruginosa</i> ATTC 27853
dichloromethane extract	7.56±0.40		
EtOH extract	10.67±0.57		
amoxycillin 10 µg/disk	10.67±0.57	11.83±0.76	6.67±0.57

Table 1.4 Antioxidant activity of the *K. angustifolia* extracts

	EC ₅₀ , µg/mL
dichloromethane extract	42.25±3.66
EtOH extract	13.90±1.35
ascorbic acid	4.86±0.89

To determine what compounds responsible for their biological activities, based on preliminary testing, the existence of condensed tannins, phenolic compounds, and triterpenes in both extracts were reported. According to this result, *K. angustifolia* was considered not only as a plenty source of bioactive compounds but also as a hopeful plant for in-depth investigation.

1.6 Biological activity

1.6.1 Anti-tyrosinase activity²²

Tyrosinase is a vital multifunctional enzyme containing copper on the active site that plays a vital role in the biosynthesis of melanin (**Figure 1.4**) by accelerating the hydroxylation reaction. In this process, two types of melanin, including pheomelanin which takes responsibility for the skin's brown/black color and eumelanin which imparts a pink or red color to the skin, were formed. Melanin is considered as the perfect protection against the damage made by the ultraviolet radiation. Less or excess melanin can cause many skin disorders and aesthetic

problems such as dark circles and freckles. Therefore, by controlling the level of melanin, tyrosinase can indirectly avoid some skin's diseases.

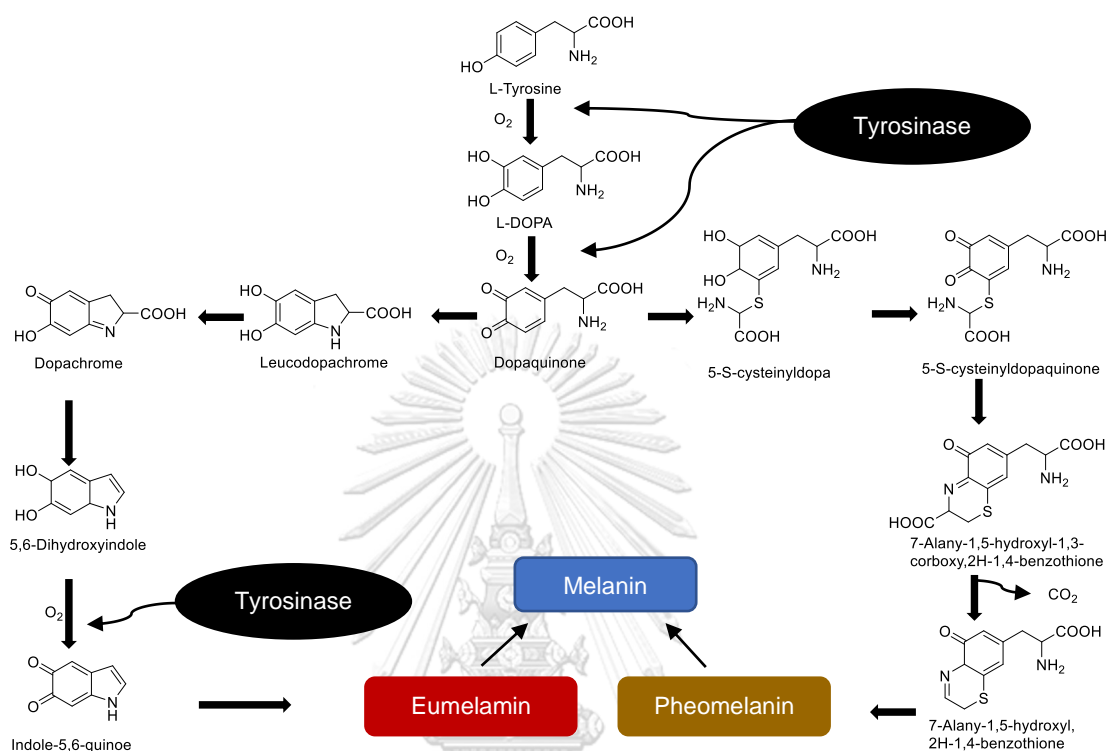


Figure 1.4 Production pathways of melanin biosynthesis

1.6.2 α -glucosidase inhibitory activity

Diabetes has become one of the biggest epidemics of the 21st century. According to the International Diabetes Federation, the number of people affected by diabetes reaches 425 million in 2017, and this figure is expected to rise over the next decades²³.

α -glucosidase inhibitors (AGIs) prevent the fast breakdown of sugars in the blood and convert carbohydrates into monosaccharides. Therefore, it can reduce postprandial blood glucose and also insulin levels²⁴. Acarbose, voglibose, and

miglitol are the available oral antidiabetic drugs in the market (**Figure 1.5**). However, they have been associated with some severe side effects related to gastrointestinal²⁵. Thus, there is a tremendous interest in finding alternatives antidiabetic agents.

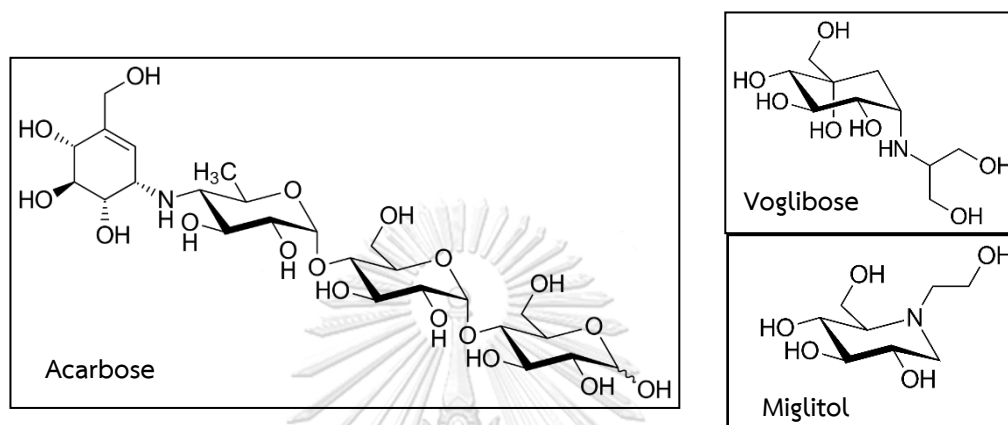


Figure 1.5 Structures of α -glucosidase inhibitor

1.7 The goal of this research

At present, the discovery of new medicine is considered as an essential part of the research. Natural products have played a key role in pharma research, as many medicines are either natural products or derivatives thereof. Thailand has a diverse pool of plant species, particularly herb which can be used for the treatment of various diseases. Among them, the stems of *K. angustifolia* have traditionally been used as whole body tonic or blood tonic agent. Moreover, in 2010, the preliminary biological tests demonstrated that the ethanolic extract of this plant possessed strong cytotoxic activity against the lung cancer cell line and had high antioxidant activity. Therefore, the target of this research is summarized that follows:

- To isolate and elucidate the structures of chemical constituents from *Knema angustifolia* stems.
- To evaluate the biological activities of isolated compounds, such as anti-tyrosinase and α -glucosidase inhibitory activities.



Chapter 2

Experimental

2.1 Plant material

The stems of *Knema angustifolia* (Roxb.) Warb. were collected from Amnat Charoen province, Thailand in 2017 (**Figure 2.1**). The botanical identification was confirmed and a voucher specimen was deposited in the herbarium of Department of Botany, Faculty of Science, Chulalongkorn University.



Figure 2.1 The stems of *Knema angustifolia*

2.2 Chemical and enzymes

Most solvents [acetone, dichloromethane (CH_2Cl_2), methanol (MeOH), ethanol (EtOH), ethyl acetate (EtOAc) and acetic acid (AcOH)] were purchased from the suppliers and used without further purification, except for *n*-hexane. The chemicals were used as follows: *p*-nitrophenyl- α -D-glucopyranoside (pNPG). Enzyme α -glucosidase from *Saccharomyces cerevisiae* E.C 3.2.1.20.

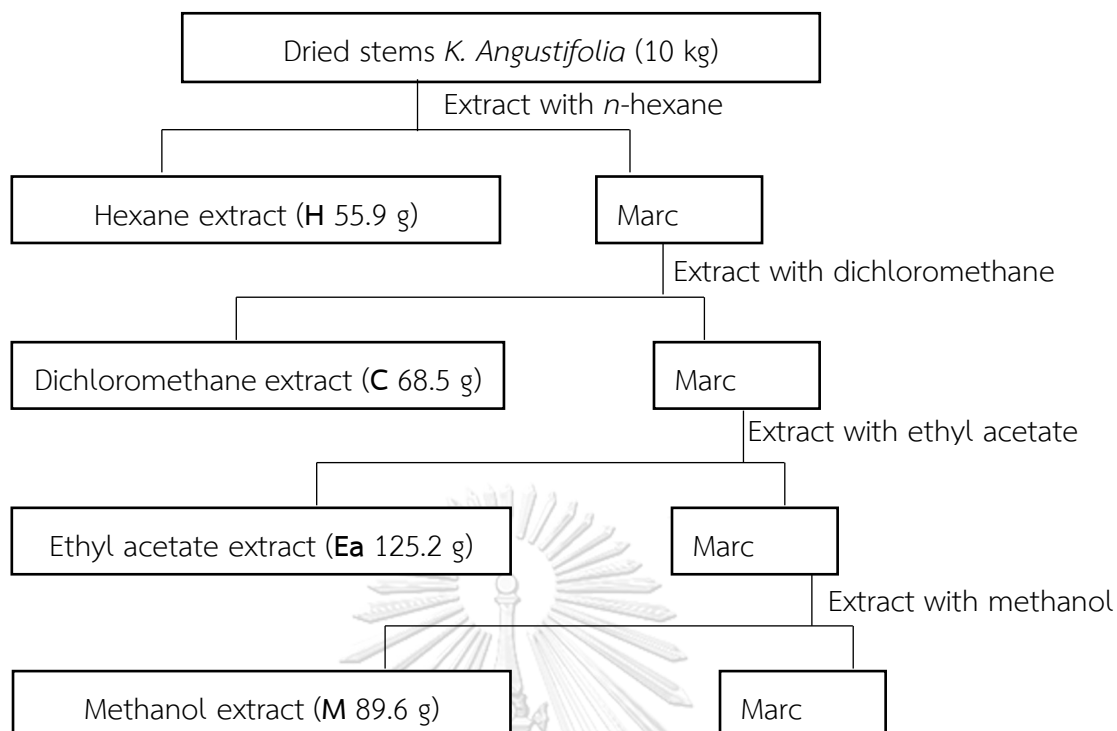
2.3 Instruments and equipment

Thin layer chromatography (TLC) analyses were carried out on pre-coated silica gel Merck Kieselgel (60 F₂₅₄), and spots were analyzed by UV light or visualized by spraying with a solution of 5% vanillin in acidic ethanolic solution followed by heating. The open column was performed using normal phase silica gel (No. 7734, and 9385, Merck) and Sephadex LH-20.

The solvent was evaporated in vacuum using rotatory evaporator Buchi-111. 1D and 2D NMR spectra were acquired on Bruker Advance 500 MHz and 400 MHz spectrometers. Chemical shifts in ppm were referenced to the corresponding residual solvent signal (CDCl₃: δ_{H} = 7.26, δ_{C} = 77.2 ppm, acetone-d₆: δ_{H} = 2.05, δ_{C} = 29.8 ppm, CD₃OD: δ_{H} = 4.87, δ_{C} = 40.0 ppm, DMSO-d₆: δ_{H} = 2.50, δ_{C} = 39.5 ppm). The HR-ESI-MS data were recorded on a Bruker microTOF Q-II mass spectrometer.

2.4 Extraction procedure of the *Knema angustifolia* stems

The dried stems of *K. angustifolia* (10 kg) were ground and extracted by maceration with *n*-hexane, CH₂Cl₂, EtOAc and MeOH, sequentially. Then, the solvent was evaporated in vacuum using rotatory evaporator to obtain the *n*-hexane (**H** 55.9 g, 0.56% w/w); CH₂Cl₂ (**C** 68.5 g, 0.69% w/w); EtOAc (**Ea** 125.2 g, 1.25% w/w) and MeOH (**M** 89.6 g, 0.90% w/w) extracts (**Scheme 2.1**).

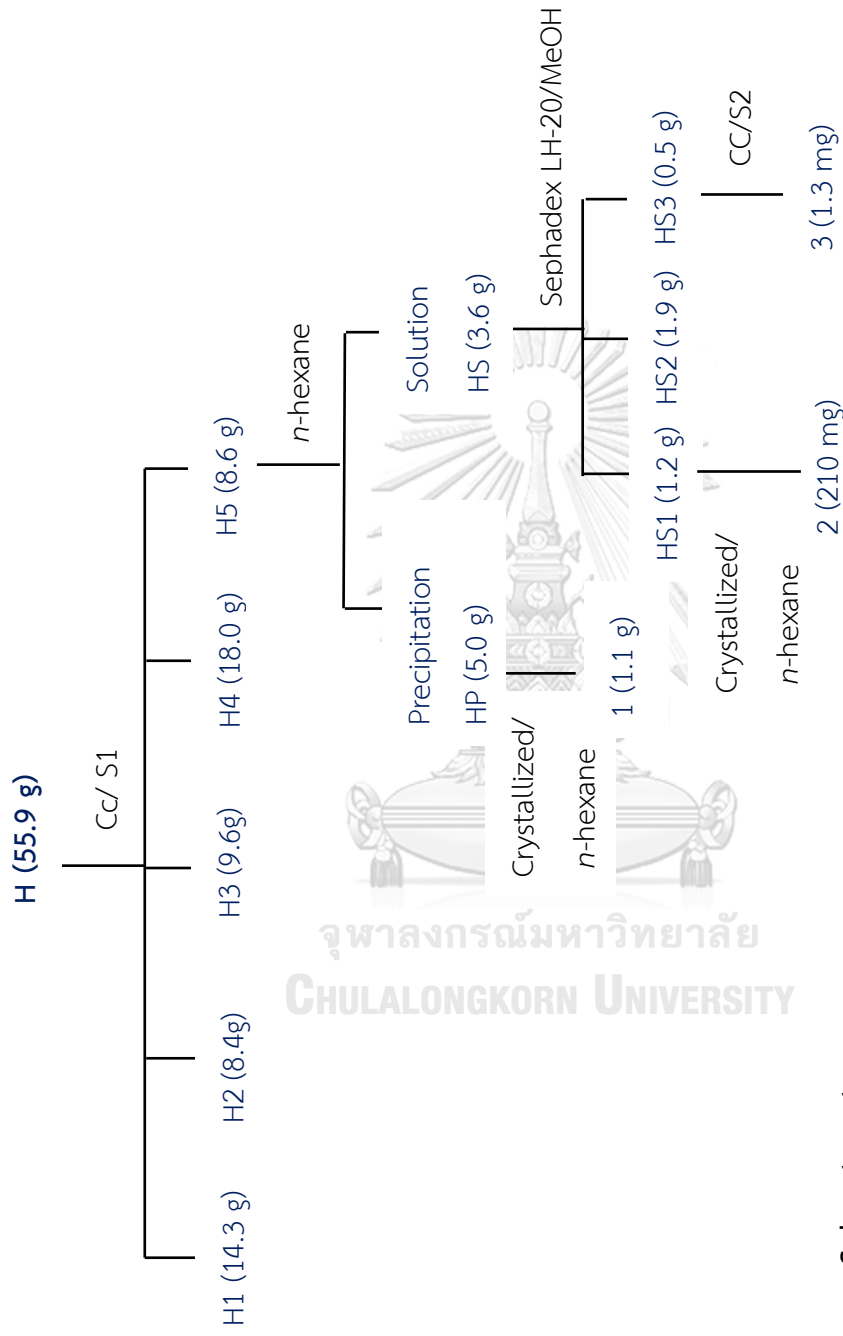


Scheme 2.1 The extraction of *Knema angustifolia* stems

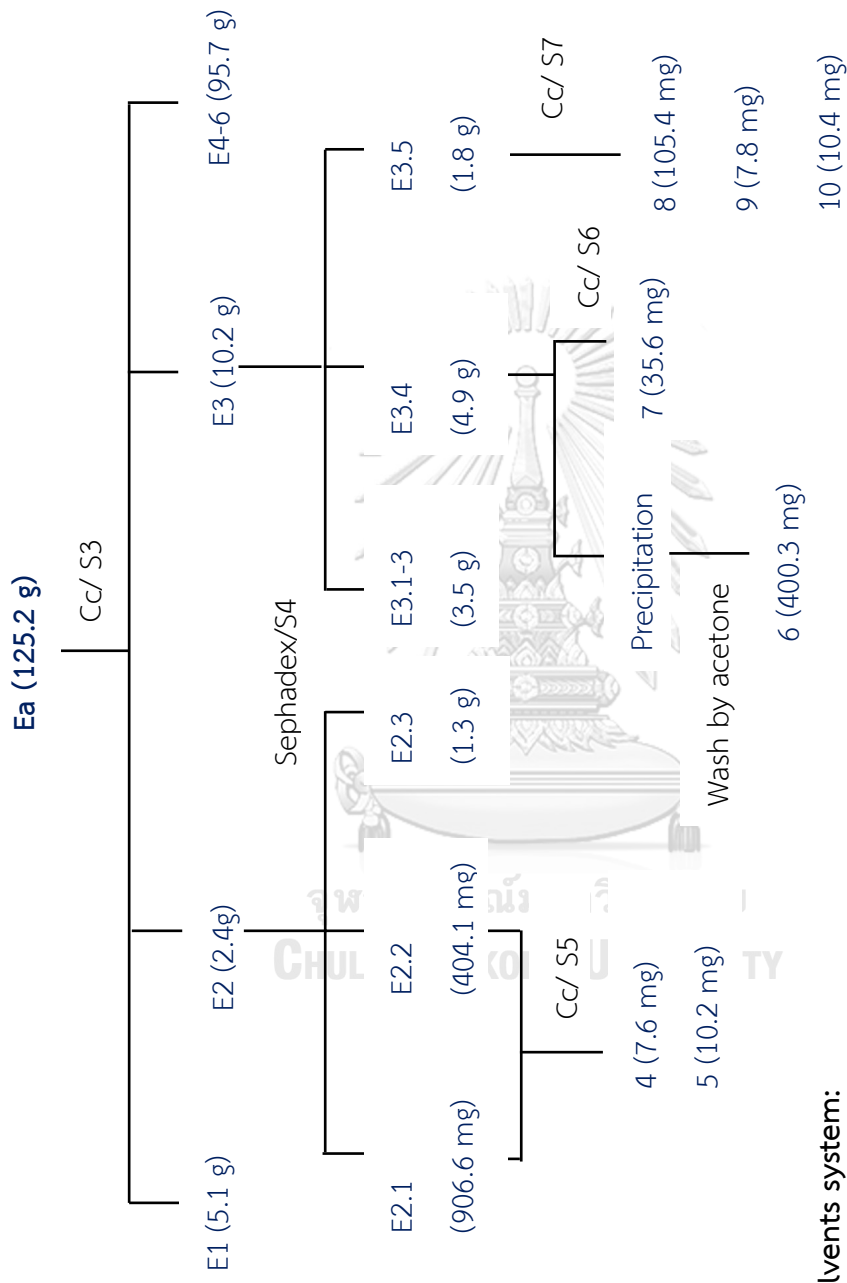
The *n*-hexane (H) extract was applied to normal phase silica gel column chromatography (CC), eluted with the gradient of *n*-hexane:EtOAc:acetone (15:1:1 to 5:1:1) to obtain five fractions **H1-5**. Fraction **H5** (8.6 g) was dissolved in *n*-hexane to afford the precipitate **HP** (5.0 g) and the left solution **HS** (3.6 g). The former was crystallized with *n*-hexane to afford **1** (1.1 g). The latter was subjected to Sephadex LH-20, eluted with MeOH to obtain three fractions **HS1-3**. **HS1** (1.2 g) was crystallized with *n*-hexane to afford **2** (210 mg). **HS3** (0.5 g) was rechromatographed by CC, eluted with the solvent system of *n*-hexane:CH₂Cl₂:MeOH:H₂O (10:10:0.4:0.01, v/v/v/v) to give three subfractions **HS3.1-3.3**. **HS3.1** (35 mg) was purified by preparative thin-layer chromatography, eluted with *n*-hexane:CH₂Cl₂:EtOAc:acetone:AcOH

(30:10:4:2.5:0.5, v/v/v/v/v) to afford **3** (1.3 mg). The summary of the separation of *n*-hexane extract can be depicted as shown in **Scheme 2.2**.

The ethyl acetate (**Ea**) extract was subjected to silica gel column chromatograph eluting with CH₂Cl₂:EtOAc:acetone:AcOH (10:4:2.5:1, v/v/v/v), giving six fractions **E1-E6**. **E2** (2.4 g) and **E3** (10.2 g) were selected for rechromatography on Sephadex LH-20, eluted with MeOH:CH₂Cl₂ (1:1), to afford five fractions **E2.1-E2.5** for the former, and five fractions **E3.1-E3.5** for the latter. Further purification of **E2.1** (906.6 mg) using an isocratic mobile phase consisting of a hexane/CH₂Cl₂/EtOH/H₂O (9:10:2:0.05, v/v/v/v) led to the isolation of **4** (7.6 mg) and **5** (4.2 mg). The precipitation occurred in **E3.4** which was subsequently washed many times with acetone to give the pure compound **6** (400.3 mg). Fraction **E3.4** was subjected to silica gel column eluting with hexane/CH₂Cl₂/EtOAc/AcOH (2:1:3:0.1, v/v/v/v) to obtain **7** (35.6 mg). **E3.5** (1.8 g) was subjected to silica gel column, using isocratic hexane/CH₂Cl₂/EtOAc/EtOH/H₂O solvent system (10:15:9:25:0.1, v/v/v/v/v) to grant three subfractions **E3.5.1-E3.5.3**. **E3.5.1** was then purified by column chromatograph with solvent system hexane/acetone/AcOH (4:3:0.06, v/v/v) to obtain **8** (105.4 mg), **9** (7.8 mg), **10** (10.4 mg) and **11** (20.5 mg). The summary of the separation of **Ea** extract is shown in **Scheme 2.3**.



Scheme 2.2 Procedure for the separation of *n*-hexane fraction of *K. angustifolia*



Solvents system:

- S3: CH₂Cl₂: EtOAc: acetone: HOAc (10:4:2.5:1)
- S4: MeOH:CH₂Cl₂ (1:1)
- S5: hexane/CH₂Cl₂/EtOH/H₂O (9:10:2:0.05)
- S6: hexane/CH₂Cl₂/EtOAc/HOAc (2:1:3:0.1)
- S7: hexane/acetone/HOAc (4:3:0.06)

Scheme 2.3 Procedure for the separation of Ea fraction of *K.angustifolia*

2.5 Bioassay Procedures

2.5.1 Anti-tyrosinase activity

The tyrosinase inhibitory activity was performed following the previous method with some modifications²⁸. The extracts and isolated compounds were dissolved in the solution comprised of 10% DMSO in buffer, in which two-fold dilution was completed to obtain various concentrations. Briefly, 50 μ L of each sample solution in buffer and 50 μ L tyrosinase enzyme from a mushroom (250 U/mL) were placed in a 96 well plate. After pre-incubation in 5 minutes, 50 μ L of L-tyrosine (5 mM) was later added as a substrate into the mixture and then incubated further for 30 minutes. After that, the absorbance of dopachrome was measured at 490 nm by a micro plate reader. Kojic acid was used as a positive control. The amount of inhibition was expressed as the percentage of concentration necessary to achieve 50% inhibition (IC_{50}). The IC_{50} values were determined by the data analysis.

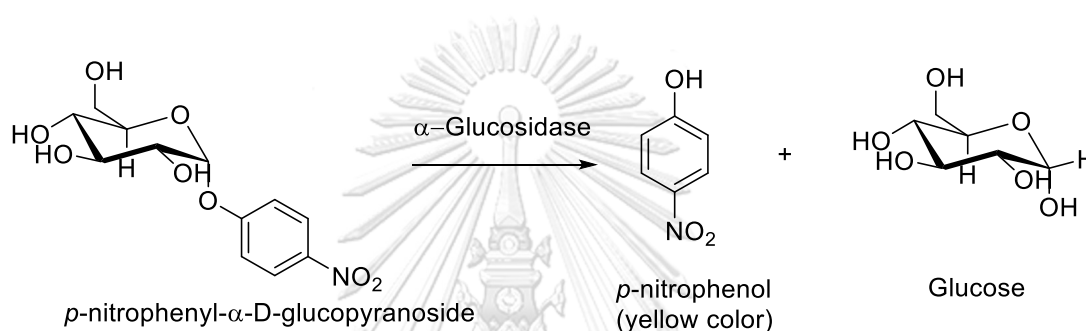
The percent of tyrosinase inhibition was calculated from the following formula:

$$\% \text{ inhibition} = \left(\frac{A_{\text{control}} - A_{\text{sample}}}{A_{\text{control}}} \right) \times 100 \quad (1)$$

Where A_{control} was the absorbance value at 490 nm of the mixture without the tested sample, and A_{sample} was the absorbance value of mixture contained the tested sample.

2.5.2 α -glucosidase inhibitory activity

The α -glucosidase inhibitory was measured using spectrophotometric method²⁹. The amount of product (*p*-nitrophenol) released from the substrate *p*-nitrophenyl- α -D-glucopyranoside (pNPG) determined the hydrolytic activity of α -glucosidase (Scheme 2.4).



Scheme 2.4 Hydrolysis of *p*-nitrophenyl- α -D-glucopyranoside by α -glucosidase

Enzyme α -glucosidase from *Saccharomyces cerevisiae* E.C 3.2.1.20 (0.1 U/mL) and pNPG (1mM) as substrate were dissolved in 0.1 mM phosphate buffer (pH 6.9). In the 96-well plates, 10 μ L of samples in DMSO or positive control was added with 40 μ L of enzyme then incubated at 37 $^{\circ}$ C for 10 min. Afterward, 50 μ L substrate was added into the mixture. The reaction was carried out at 37 $^{\circ}$ C in 20 minutes, and then 100 μ L of 1 M Na_2CO_3 was used to terminate the reaction. Enzymatic activity was quantified by measuring the absorbance at 405 nm (ALLSHENG micro plate reader AMR-100). Acarbose® was used as a standard control and all samples were analyzed in triplicate at different concentrations to obtain the IC_{50} value of compounds. Percentage inhibition was calculated by the equation described below:

$$\% \text{ inhibition} = \left(\frac{A_{\text{control}} - A_{\text{sample}}}{A_{\text{control}}} \right) \times 100 \quad (2)$$

A_{control} is the absorbance of control without tested solution. A_{sample} is the absorbance of control with tested solution



Chapter 3

Results and discussion

The medicinal plant *Knema angustifolia* has been used in Thai folk medicine for the treatment of a wide range of diseases; however chemical data on this plant are scarce. The preliminary screening tests revealed that *K. angustifolia* stems were potential sources for further investigation. Therefore, the main aim of this research was to isolate and elucidate the structures of chemical constituents. The biological activities such as anti-tyrosinase and α -glucosidase were in addition evaluated.

3.1 Preliminary study of crude extracts

According to the procedure shown in **Scheme 2.1**, four extracts including *n*-hexane, CH₂Cl₂, EtOAc, MeOH extracts were gained. They were further applied for preliminary anti-tyrosinase activity. The results are demonstrated in **Table 3.1**.

Table 3.1 Anti-tyrosinase activity of *K. angustifolia* extracts

Extracts	IC ₅₀ (μg/mL)
<i>n</i> -hexane	50.2±0.7
CH ₂ Cl ₂	118.9±1.8
EtOAc	51.6±1.3
MeOH	115.9±0.8

Based on this result, intense anti-tyrosinase activity belongs to *n*-hexane and EtOAc extracts with IC₅₀ value of 50.2 and 51.6 μg/mL, respectively. Thus, these

extracts were chosen as the probable foundation to discover bioactive compounds from this plant.

3.2 Chemical constituents from *K.angustifolia* stems

3.2.1 Separation of *n*-hexane extract

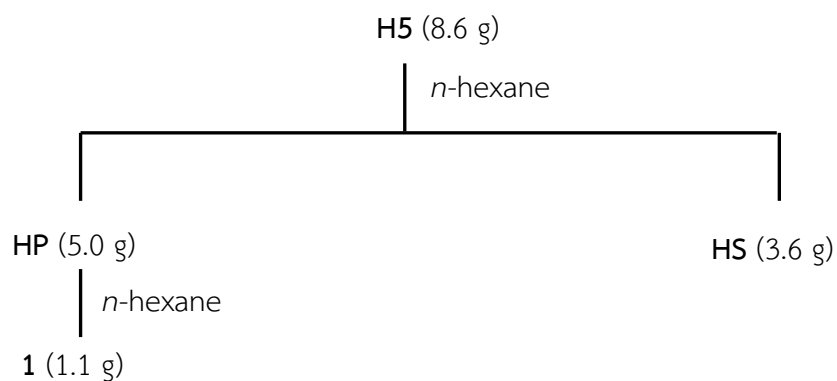
The *n*-hexane extract (55.9 g) as yellow material was applied to normal phase silica gel column, eluted with the gradient of hexane:EtOAc:acetone (15:1:1 to 5:1:1) to obtain five fractions **H1-5**. The results of separation are demonstrated in **Table 3.2**.

Table 3.2 The separation of *n*-hexane extract of *K. angustifolia* stems

Solvent system	Fraction	Weight (g)	Remarks
hexane:EtOAc:acetone (15:1:1 to 5:1:1)	H1	5.8	yellow oil
	H2	12.9	brownish-yellow
	H3	15.2	brownish-yellow
	H4	10.3	dark brown
	H5	8.6	brownish-yellow

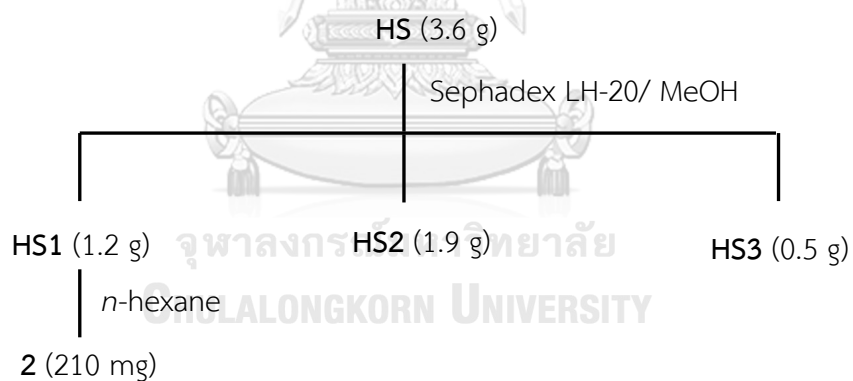
3.2.1.1 Separation of fraction **H5**

H5 (8.6 g) was dissolved in *n*-hexane to afford the precipitate **HP** (5.0 g) and the solution **HS** (3.6 g). The former was crystallized in warming *n*-hexane many times to afford **1** (1.1 g). The detailed separation is shown in **Scheme 3.1**.



Scheme 3.1 Fractionation of fraction H5

HS (3.6 g) was subjected to Sephadex LH-20 column, eluted with MeOH to obtain three fractions **HS1-3**. **HS1** (1.2 g) was recrystallized with *n*-hexane to afford **2** (210 mg). The separation is described in **Scheme 3.2** and **Table 3.3**.



Scheme 3.2 Fractionation and isolation of HS

Table 3.3 The separation of **HS**

Solvent system	Fraction	Weight (g)	Remarks
MeOH 100% (Sephadex)	HS1	1.2	yellow oil
	HS2	1.9	brownish-yellow
	HS3	0.5	brownish-yellow

HS3 (0.5 g) was rechromatographed by CC, eluted with the solvent system of *n*-hexane:CH₂Cl₂:MeOH:H₂O (10:10:0.4:0.01, v/v/v/v) to give three subfractions **HS3.1-3.3**. **HS3.1** (35 mg) was purified by preparative thin-layer chromatography, eluted with *n*-hexane:CH₂Cl₂:EtOAc:acetone:AcOH (30:10:4:2.5:0.5, v/v/v/v/v) to afford **3** (1.3 mg). The summary of the separation of *n*-hexane extract can be depicted as shown in **Scheme 3.3** and **Table 3.4**.

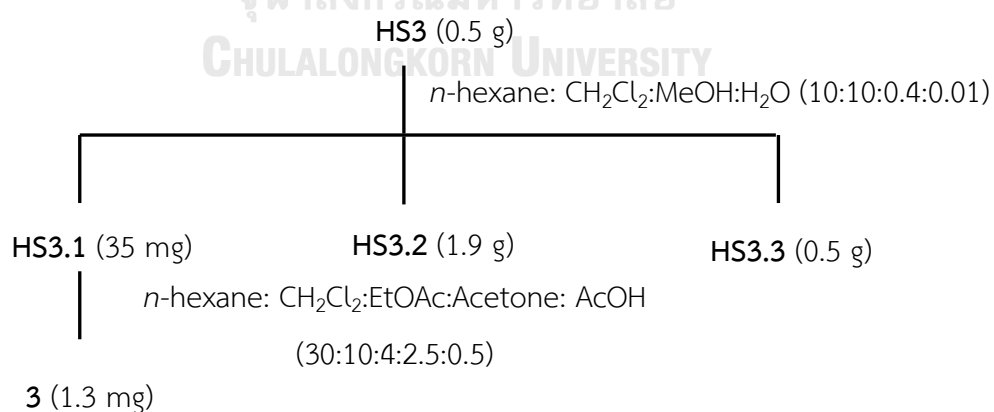
**Scheme 3.3** Fractionation and isolation of **HS3**

Table 3.4 The separation of **HS3**

Solvent system	Fraction	Weight (mg)	Remarks
MeOH 100% (Sephadex)	HS3.1	35	yellow oil
	HS3.2	167	brownish-yellow
	HS3.3	285	brownish-yellow

3.2.2 Separation of ethyl acetate extract

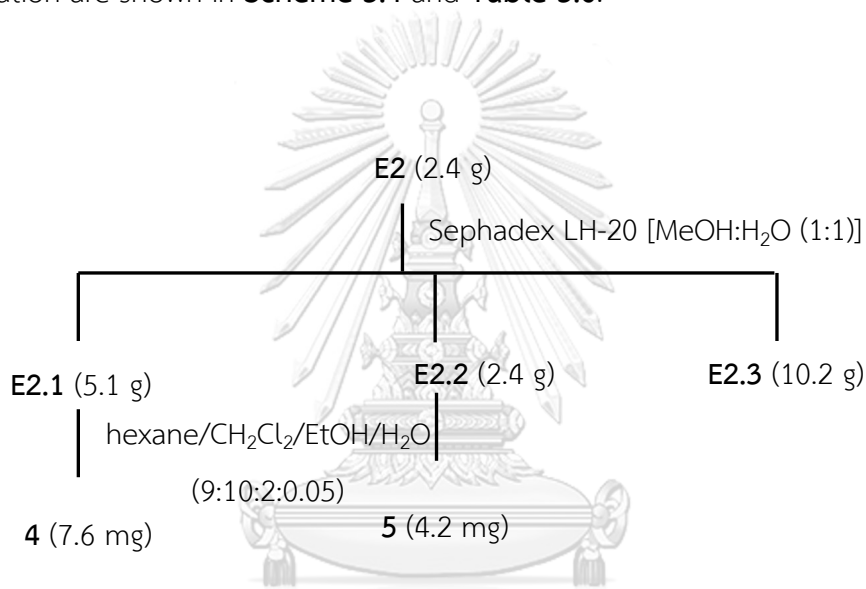
The Ea extract (125.2 g) as a brownish yellow syrup was applied to normal phase silica gel column and eluted with a solvent system of $\text{CH}_2\text{Cl}_2/\text{EtOAc}/\text{acetone}/\text{AcOH}$ (10:4:2.5:0.5) to afford six fractions **E1-E6**. The results of separation are shown in **Table 3.5**.

Table 3.5 The separation of Ea extract of *K.angustifolia* stems

Solvent system	Fraction	Weight (g)	Remarks
$\text{CH}_2\text{Cl}_2/\text{EtOAc}/\text{acetone}/\text{AcOH}$ (10:4:2.5:0.5)	E1	5.1	yellow oil
	E2	2.4	yellow syrup
	E3	10.2	brownish-yellow
	E4	27.3	red-brown
	E5	63.7	dark brown
	E6	11.8	dark brown

3.2.2.1 Separation of fraction **E2**

E2 (2.4 g) was subjected to Sephadex LH-20 and eluted the column with [MeOH: CH₂Cl₂ (1:1)] to give three fractions **E2.1-E2.3**. After that, fractions **E2.1** and **E2.2** were applied to silica gel CC using hexane/CH₂Cl₂/EtOH/H₂O solvent system (9:10:2:0.05) led to the isolation of **4** (7.6 mg) and **5** (4.2 mg). The results of separation are shown in **Scheme 3.4** and **Table 3.6**.



Scheme 3.4 Fractionation and isolation of **E2**

Table 3.6 The separation of **E2**

Solvent system	Fraction	Weight (g)	Remarks
MeOH: H ₂ O (1:1) (Sephadex)	E2.1	5.1	yellow syrup
	E2.2	2.4	brownish-yellow
	E2.3	10.2	dark brown

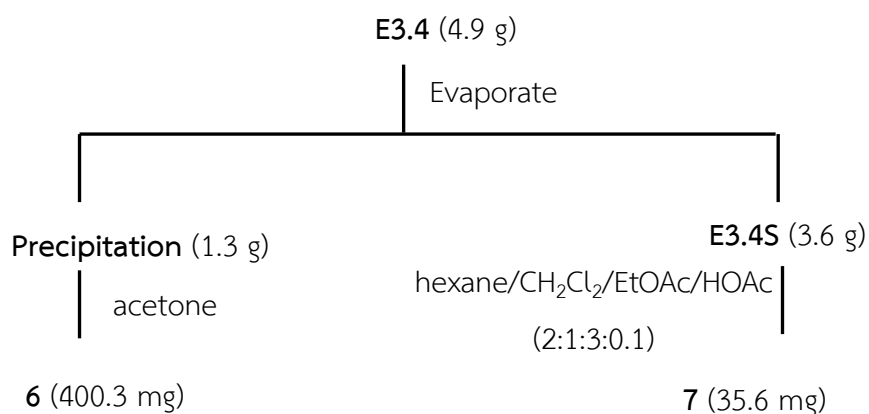
3.2.2.2 Separation of fraction **E3**

E3 (10.2 g) was subjected to Sephadex L-20 and eluted the column with [MeOH: CH₂Cl₂ (1: 1)] to give five fractions **E3.1-E3.5** as described in **Table 3.7**.

Table 3.7 The separation of **E3**

Solvent system	Fraction	Weight (g)	Remarks
MeOH: H ₂ O (1:1) (Sephadex)	E3.1	1.1	brown oil
	E3.2	1.5	brownish-yellow
	E3.3	0.9	brownish-yellow
	E3.4	4.9	dark brown
	E3.5	1.8	dark brown

During the evaporating solvent to a small volume, **E3.4** gave some white precipitation. Further washing the precipitation with acetone, the pure compound **6** was obtained. The leftover designated as **E3.4S** was subjected to silica gel column eluting with hexane/CH₂Cl₂/EtOAc/AcOH (2:1:3:0.1) to obtain **7** (35.6 mg). The separation is shown in **Scheme 3.5**.



Scheme 3.5 Fractionation and isolation of **E3.4**

E3.5 (1.8 g) was subjected to silica gel column eluted with isocratic hexane/CH₂Cl₂/EtOAc/EtOH/H₂O solvent system (10:15:9:25:0.1, v/v/v/v) to grant three subfractions **E3.5.1-E3.5.3** as described in **Table 3.8**.

Table 3.8 The separation of **E3.5**

Solvent system	Fraction	Weight (mg)	Remarks
hexane/CH ₂ Cl ₂ /EtOAc/EtOH/H ₂ O (10:15:9:25:0.1)	E3.5.1	874	white solid
	E3.5.2	403	white solid
	E3.5.3	591	brownish-yellow

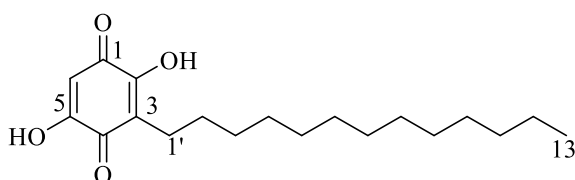
Fraction **E3.5.1** was then purified by column chromatography with hexane/acetone/AcOH (4:3:0.06, v/v/v) to obtain **8** (105.4 mg), **9** (7.8 mg), **10** (10.4 mg) and **11** (20.5 mg).

3.2.3 Structural elucidation of isolated compounds

3.2.3.1 Structural elucidation of compound **1**

1 (1.1 g, 1.97% yield based on *n*-hexane extract), orange plates, had the molecular formula of $C_{19}H_{30}O_4$ based on an $[M+Na_2-H]$ ion peak at m/z 367.1851 (calcd. for $C_{19}H_{29}Na_2O_4$, 367.1855) (**Figure A.1**) with five double-bond equivalents.

The 1H NMR spectrum of **1** (**Figure A.2**) revealed the signal of one singlet olefinic methine (δ_H 5.77), two methylene groups [$(\delta_H$ 2.27, t, $J = 7.5$ Hz), $(\delta_H$ 1.34, m)] and one methyl (δ_H 0.84, t, $J = 6.0$ Hz). Owing to molecular formula requirements and eight protons being evident from 1H NMR analysis, twenty protons detected at δ_H 1.25-1.30 were considered as ten aliphatic methylene groups. The ^{13}C NMR of **1** (**Figure A.3**) presented two quaternary carbons (δ_C 117.4 and 103.8) and twelve methylene carbons in the linker (δ_C 22.0, 31.3) along with one methyl carbon δ_C 13.9). All reported data of **1** were similar to those of rapanone³⁰. Notably, the signal of two carbonyl groups (C-1, C4) and two oxygenated quaternary carbons (C-2 and C-5) not appeared due to the fluxional effect. Thus, **1**, namely rapanone was determined.

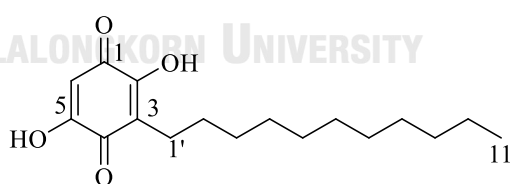


Compound **1**: Rapanone

3.2.3.2 Structural elucidation of compound **2**

2 (210 mg, 0.38% yield based on *n*-hexane extract), isolated as an orange powder, gave a molecular formula of $C_{17}H_{26}O_4$ based on its positive-ion HR-ESI-MS data, which showed $[M+Na_2-H]$ peak at m/z 339.1543 (calcd. for $C_{17}H_{25}Na_2O_4$, 339.1543) (**Figure A.4**).

The 1H NMR and ^{13}C NMR data of **2** (**Figures A.5 and A.6**) demonstrated significant similarity with those of **1**, except for the appearance of 16 protons of long-chain methylene groups at δ_H 1.25-1.30 instead of 20, indicating the presence of two fewer methylene groups than rapanone in the side chain. The number of carbon in this moiety further determined based on the mass analysis with the molecular formula $C_{17}H_{26}O_4$. Moreover, all signals in the NMR data of **2** were in agreement with literature reported of embelin by Mahendran (2014)³¹. The structure of embelin **2** was established as shown as follows:



Compound **2**: Embelin

3.2.3.3 Structural elucidation of compound **3**

3 (1.3 mg, 0.002% yield based on *n*-hexane extract) was obtained as yellow amorphous powder. Its HR-ESI-MS peak at m/z 361.2397 ($[M-H]^-$, calcd. for 361.2384) and m/z 723.4864 ($[2M-H]^-$, calcd. for 723.4841) (**Figure A.7**) suggested a molecular formula of $C_{22}H_{34}O_4$ with six indices of hydrogen deficiency.

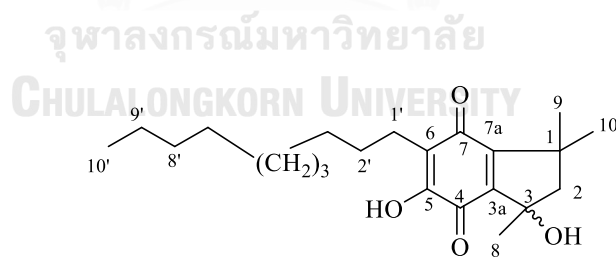
The ^1H NMR spectrum of **3** (Figure A.8), in accordance with the HSQC spectrum (Figure A.10) indicated the presence of two hydroxy groups (δ_{H} 8.11 and 7.36), four methyls (δ_{H} 1.78, 1.33, 1.17 and 0.87), one diastereotopic methylene group [δ_{H} 2.75 (1H, d, $J = 3.0, 15.0$ Hz) and 1.84 (1H, d, $J = 15.0$ Hz, H-2b)] and the signals of an aliphatic long chain connecting of δ_{H} 2.40, (2H, t, $J = 7.5$ Hz, H-1'), 1.45 (2H, m), and the consisting of broad signal in the range of 1.20-1.30 ppm]. The ^{13}C NMR spectrum (Figure A.9) revealed the existence of two conjugated ketone carbons (δ_{C} 182.2 and 181.8), six quaternary carbons (δ_{C} 151.4, 120.3, 117.7, 115.1, 79.8, 29.6), one olefin methine (δ_{C} 125.2), four methyls (δ_{C} 28.4, 14.1, 14.1, 14.0), and one methylene (δ_{C} 47.3) and the methylenes of a long chain in the range of 22 to 30 ppm.

These above chemical features indicated that **3** was a derivative of embelin/rapanone, co-occurred in the same source with the differences at C-3a and C-7a. The location of the aliphatic long-chain was defined at C-6 based on the downfield chemical shift of the methylene δ_{H} 2.40 (H₂-1', t, $J = 7.5$ Hz) and its HMBC (Figure A.11) cross peaks to C-5 (δ_{C} 151.4), C-6 (δ_{C} 117.7), and C-7 (δ_{C} 181.8). The HMBC cross peaks of the 5-OH group (δ_{H} 7.36) to C-6 and C-4 (δ_{C} 182.2) indicated its adjacent position toward the aliphatic chain. The spectroscopic data were highly reminiscent of those of embelin/rapanone^{30, 32}.

The second spin system through C-8-C-3-C-2-C-1-C-9/10 could be deduced based on HMBC correlations. Indeed, all three methyl groups at δ_{H} 1.78 (H₃-8), δ_{H}

1.33 (H₃-9), and δ_{H} 1.17 (H₃-10) gave HMBC correlations to C-2 (δ_{C} 47.3) while proton H₂-2 (2.75 & 1.80) gave the HMBC correlations to C-1, C-3, C-8 and C-9/10, confirming the previous statement. The HMBC correlations of H₃-8 (δ_{H} 1.78) to both carbons C-2 (δ_{C} 47.3) and C-3 (δ_{C} 79.8) and the downfield chemical shift of C-3 (δ_{C} 79.8) defined the location of 3-OH group. Lastly, HMBC correlations of H₃-9/10 and H₂-2 to C-7a (δ_{C} 120.3) and of both H₂-2 and H₃-8 of C-3a (δ_{C} 115.1) determined the linkages between C-1/C-7a and C-3/C-3a. Altogether, the planar structure of **3**, namely angustiquinone was identified. Unfortunately, the only stereocenter C-3 could not be defined due to the limit amount of **3**.

To the best of our knowledge, angustiquinone represented the first 1,1,3-trimethyl-2,3-dihydro-1H-indene-4,7-dione scaffold bearing a long chain. The key HMBC and chemical shift assignments of **3** were described in **Figure 3.1** and **Table 3.9**.



Compound **3**: Angustiquinone

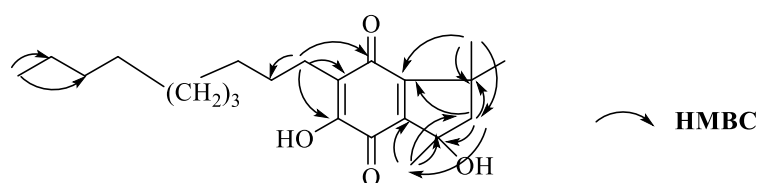


Figure 3.2 Key HMBC correlation of **3**

Table 3.9 The tentative ^1H and ^{13}C NMR chemical shift assignments of **1**, **2**, and **3**

Position	1 ^a (DMSO- <i>d</i> ₆)		2 ^a (DMSO- <i>d</i> ₆)		3 ^b (CDCl ₃)	
	δ_{H} , <i>J</i> (Hz)	δ_{C}	δ_{H} , <i>J</i> (Hz)	δ_{C}	δ_{H} , <i>J</i> (Hz)	δ_{C}
1		na		na		29.6
2		na		na	2.75, d, 15 1.84, d, 15	47.3
3		117.4		117.4		79.8
4		na		na		182.2
5		na		na	6.51, s	151.4
6	5.77, s	103.8	5.77 s	103.8		117.7
7						181.8
8					1.78, s	28.4
9					1.33, s	14.1
10					1.17, s	14.1
3a						115.1
7a						120.3
1'	2.27, t, (7.2)		2.27, t, (7.2)		2.40, t, (7.5)	22.7
2'	1.34, m		1.34, m			
2'-9'					1.25- 1.33, m	
3'-10'			1.25 – 1.30, m	22.0 to 31.3		
3'-12'	1.25 – 1.30, m	22.0 to 31.3				
10'			0.84, t, (6.0)	13.9	0.87, t, (6.5)	14.0
11'						
13'	0.84, t, (6.0)	13.9				

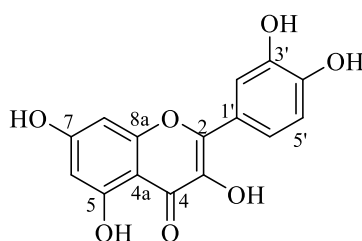
^aRecorded at 400 MHz, ^bRecorded at 500 MHz.

^{na}Carbon peaks not appeared due to fluxional effect

3.2.3.4 Structural elucidation of compound **4**

4 (7.6 mg, 0.006% yield based on EtOAc extract) was obtained as a yellow amorphous powder. The ^1H NMR spectrum (**Figure A.12**) revealed one hydrogen-bonded hydroxyl group at δ_{H} 12.10 (OH-5), two *meta*-coupled aromatic protons at δ_{H} 6.21 (1H, d, $J = 2.0$ Hz, H-6) and 6.47 (1H, d, $J = 1.6$ Hz, H-8) on ring A, an ABX proton system at δ_{H} 7.76 (1H, d, $J = 2.0$ Hz, H-2'), 7.65 (1H, dd, $J = 8.4, 2.0$ Hz, H-6'), 6.93 (1H, d, $J = 8.4$ Hz, H-5'), due to a 3', 4'-disubstitution on ring B. The ^{13}C NMR spectrum (**Figure A.13**) showed the occurrence of fifteen carbon signals, including one carbonyl group (δ_{C} 176.6), five aromatic methine carbons (δ_{C} 121.5, 116.2, 115.8, 99.2 and 94.5), five aromatic tertiary carbons (all being immediately identified as oxygenated at δ_{C} 165.1, 162.3, 157.8, 148.4 and 145.9), two aromatic quaternary carbons (δ_{C} 123.8 and 104.1), and two oxygenated alkenes (δ_{C} 147.0, 136.8). All NMR data suggested that the structure of **4** could be completed into a flavonol skeleton.

Comparing the ^1H and ^{13}C NMR spectra of **4** with those of quercetin³³, **4** was clearly elucidated as quercetin.



Compound **4**: Quercetin

Table 3.10 The ^1H and ^{13}C NMR chemical shift assignments of **4** compared with those of quercetin

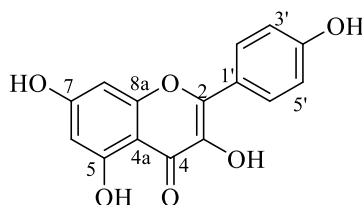
Position	4 ^a (acetone- d_6)		Quercetin ^a (CD_3OD)	
	δ_{H} , mult J , (Hz)	δ_{C}	δ_{H} , mult J , (Hz)	δ_{C}
2		147.0		148.0
3		136.8		137.2
4		176.6		177.3
5		162.4		162.5
6	6.21, d, (2.0)	99.2	6.20, d, (2.0)	99.3
7		165.1		165.6
8	6.47, d, (1.6)	94.5	6.40, d, (2.0)	94.4
4a		104.2		104.5
8a		157.8		158.3
1'		123.8		124.2
2'	7.76, d, (2.0)	115.8	7.75, d, (2.0)	116.0
3'		145.9		146.2
4'		148.4		148.8
5'	6.93, d, (8.4)	116.3	6.90, d, (8.5)	116.3
6'	7.65, dd, (8.4, 2.0)	121.5	7.65, dd, (8.5, 2.0)	121.7
5-OH	12.12, s			

^aRecorded at 400 MHz

3.2.3.5 Structural elucidation of compound **5**

5 (10.2 mg, 0.008% yield based on EtOAc extract) was isolated as yellow amorphous powder. The ^1H NMR spectral data of **5** (Figure A.16) revealed four phenolic groups (δ_{H} 12.5, 10.81, 20.12, 9.38), an AA'BB' spin system comprising two pairs of two protons doublets at δ_{H} 8.04 (2H, d, $J = 8.8$ Hz) and 6.93 (2H, d, $J = 8.8$ Hz), an AX spin system comprising two doublets protons at δ_{H} 6.44 (1H, d, $J = 2.0$ Hz) and 6.20 (1H, d, $J = 2.0$ Hz). The ^{13}C NMR spectrum (Figure A.17) indicated the presence of a carbonyl (δ_{C} 175.9), six aromatic methine (δ_{C} 129.5, 115.5, each two carbons and 98.2, 93.5), four tertiary carbons (all oxygenated carbons at δ_{C} 163.9, 160.7, 159.2 and 156.2), two aromatic quaternary carbons (δ_{C} 121.7 and 103.1), and two oxygenated alkene (δ_{C} 146.9 and 135.7).

The ^1H and ^{13}C NMR spectral data of **5** was similar to those of **4**, with an addition of one aromatic proton on B-ring. These results when compared to literature data of kaempferol³⁴, is suggestive that **5** was kaempferol.



Compound **5**: Kaempferol

Table 3.11 The ^1H and ^{13}C NMR chemical shift assignments of **5** compared with those of kaempferol

Position	5 ^a (DMSO- <i>d</i> ₆)		Kaempferol ^c (DMSO- <i>d</i> ₆)	
	δ_{H} , mult <i>J</i> , (Hz)	δ_{C}	δ_{H} , mult <i>J</i> , (Hz)	δ_{C}
2		146.9		146.8
3		135.7		135.6
4		175.9		175.9
5		156.2		156.2
6	6.20, d, (2.0)	98.2	6.19, d, (1.8)	98.2
7		163.9		163.9
8	6.45, d, (2.0)	93.5	6.44, d, (1.8)	93.5
4a		103.1		103.0
8a		160.7		160.7
1'		121.7		121.7
2'/6'	8.00, d, (8.8)	129.5	8.04, d, (9.0)	129.5
3'/5'	6.93, d, (8.8)	115.5	6.92, d, (9.0)	115.4
4'		159.2		159.2
5-OH	12.48, s			

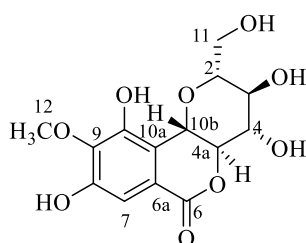
^aRecorded at 400 MHz, ^cRecorded at 600 MHz

3.2.3.6 Structural elucidation of compound **6**

6 (400.3 mg, 0.32% yield based on EtOAc extract) was isolated as white crystal. The ^1H NMR spectrum of **6** (Figure A.18), in combination with the HSQC spectrum, exhibited a signal for five hydroxyl groups (δ_{H} 9.76, 8.44, 5.64, 5.43 and 4.92), one aromatic proton at δ_{H} 6.99 (1H, s), one methoxy group at δ_{H} 3.76 (3H, s), five bergenin type oxymethine signals at δ_{H} 4.96 (1H, d, $J = 10.4$ Hz), 4.00 (1H, dd, $J = 10.0, 9.6$ Hz), 3.65 (1H, ddd, $J = 9.2, 8.8, 4.4$), 3.57 (1H, m), 3.21 (1H, m), and one oxygenated methylene group at δ_{H} 3.84 (1H, d, $J = 11.6$ Hz), 3.45 (1H, m).

The ^{13}C NMR (Figure A.19) revealed the existence of fourteen carbon signals, comprising of one ester carbonyl carbon (δ_{C} 163.4), five quaternary carbons (δ_{C} 150.9, 148.1, 140.7, 118.1, 116.0), one methoxyl carbon (δ_{C} 59.9), five oxymethine carbons (δ_{C} 81.7, 79.8, 73.7, 72.2, 70.7), one aromatic methine (δ_{C} 109.5) and one methylene (δ_{C} 61.1). The position of aromatic proton at δ_{H} 6.99 at C-7 was confirmed from its HMBC correlation to C-6 (Figure A.21).

From all above information, both ^1H and ^{13}C NMR chemical shift values of **6** were consistent with those reported by De Abreu *et al.* (2008)³⁵ and Khan *et al.* (2016)³⁶, therefore **6** was identified as bergenin.



Compound **6**: Bergenin

Table 3.12 The ^1H and ^{13}C NMR chemical shift assignments of **6** compared with those of bergenin

Position	4^a (DMSO- d_6)		Bergenin ^a (DMSO- d_6)	
	δ_{H} , mult J , (Hz)	δ_{C}	δ_{H} , mult J , (Hz)	δ_{C}
2	3.57, m	81.7	3.58, ddd, (7.6, 3.2, 1.9)	81.7
3	3.21, m	70.7	3.20, ddd, (8.8, 7.6, 5.0)	70.7
4	3.65, ddd, (9.2, 8.8, 4.4)	73.7	3.65, ddd, (9.5, 8.8, 5.3)	73.7
6		163.4		163.4
7	6.99, s	109.5	6.98, s	109.5
8		150.9		150.9
9		140.7		140.7
10		148.1		148.1
11	3.45, m 3.84, d, (11.6)	61.1	3.44, ddd, (10.9, 8.1, 1.9) 3.85, dd, (10.9, 3.2)	61.1
12	3.76, s	59.9	3.78, s	59.8
4a	4.00, dd, (10.0, 9.6)	79.8	4.00, dd, (10.4, 9.5)	79.8
6a		118.1		118.1
10a		116.0		116.0
10b	4.96, d, (10.4)	72.2	4.96, d, (10.4)	72.1
3-OH	5.43, d, (5.6)		5.42, d, (5.0)	
4-OH	5.64, d, (4.4)		5.64, d, (5.3)	
8-OH	9.76, s		9.76, s	
10-OH	8.44, s		8.45, s	
11-OH	4.92, m		4.91, m	

^aRecorded at 400 MHz

3.2.3.7 Structural elucidation of compound **7**

7 (35.6 mg, 0.03% yield based on EtOAc extract) was isolated as white solid. The ^1H -NMR spectrum (**Figure A.22**) displayed one aromatic methine at δ_{H} 7.11 (1H, s, H-7), five bergenin type oxymethine signals at δ_{H} 4.99 (1H, d, $J = 10.4$ Hz), 4.09 (1H, t, $J = 10.0$ Hz), 3.87 (1H, m), 3.83 (1H, m), 3.46 (1H, m), one methylene [δ_{H} 4.66 (1H, dd, $J = 12.0, 5.1$ Hz) and 4.23 (1H, dd, $J = 12.0, 5.1$ Hz)], and one methyl at δ_{H} 2.13 (1H, s). The ^{13}C NMR spectrum (**Figure A.23**) showed the presence of sixteen carbon signals, including two carbonyl groups (δ_{C} 172.6 and 165.7), six methines (δ_{C} 111.2, 81.3, 80.4, 75.4, 74.3 and 71.9), one oxygenated methylene (δ_{C} 64.7), one methyl (δ_{C} 20.6), one methoxy (δ_{C} 60.9) and five quaternary carbons, three of which was oxygenated (δ_{C} 152.4, 149.3 and 142.5).

The comparison in the ^1H and ^{13}C NMR spectra between **7** and **6** pointed out the similarity in the chemical structures of two compounds, excepted for the appearance of an acetyl group at δ_{H} 2.13 (3H, s, H-2') in **7**. This acetyl group could be located at C-11 based on the HMBC correlations observed from the methyl proton at δ_{H} 2.13 (H3-2') to δ_{C} 64.7 (C-11) (**Figure A.23**).

The structure was supported by the analysis of the NMR data with those in previous studies^{37, 38}. Thus, the structure of 11-*O*-acetyl bergenin (**7**) was established.

8a, respectively, and the typical catechol B-ring signal at δ_c 145.6(x2) for C-3' and C-4' also confirmed the catechin nature of the core of this molecule.

The spectral data of **8** were compared with the literature³⁹ and confirmed that the structure of **8** was catechin.

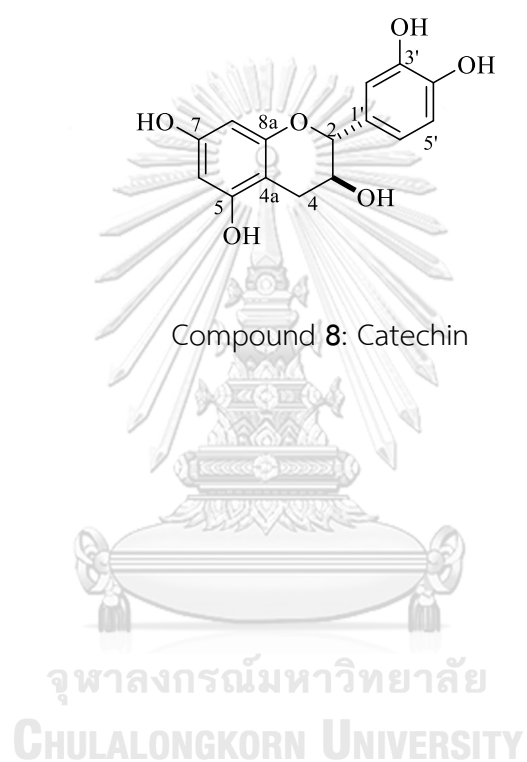


Table 3.13 The ^1H and ^{13}C NMR chemical shift assignments of **7** compared with those of 11-*O*-acetyl bergenin

Position	7 ^a (CD ₃ OD)		11- <i>O</i> -acetyl bergenin ^a (CD ₃ OD)	
	δ_{H} , mult <i>J</i> , (Hz)	δ_{C}	δ_{H} , mult <i>J</i> , (Hz)	δ_{C}
2	3.83, m	80.4	3.81, m	80.3
3	3.46, m	71.9	3.46, m	71.8
4	3.87, m	75.4	3.85, m	75.6
6		165.7		165.8
7	7.11, s	111.2	7.09, s	111.3
8		152.4		152.7
9		142.5		142.4
10		149.3		149.3
11	4.66, dd, (12.0, 5.1)	64.7	4.65, m	64.6
	4.23, dd, (12.0, 5.1)		4.23, m	
12	3.92, s	60.9	3.90, s	60.9
4a	4.09, t, (10.0)	81.3	4.07, dd, (9.6, 10.4)	81.3
6a		119.5		119.4
10a		117.0		117.2
10b	4.99, d, (10.4)	74.3	4.99, d, (10.4)	74.3
1'		172.7		172.6
2'	2.13, s	20.6	2.11	20.6

^aRecorded at 400 MHz

Table 3.14 The ^1H and ^{13}C NMR chemical shift assignments of **8** compared with those of catechin

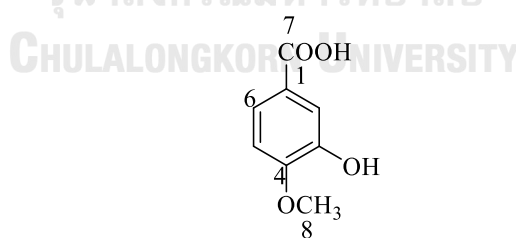
Position	8 ^a (acetone- <i>d</i> ₆)		Catechin ^a (acetone- <i>d</i> ₆)	
	δ_{H} , mult <i>J</i> , (Hz)	δ_{C}	δ_{H} , mult <i>J</i> , (Hz)	δ_{C}
2	4.56, d, (8.0)	82.5	4.55, d, (7.5)	82.8
3	4.00, m	68.3	3.98, ddd, (8.0, 7.5, 5.5)	68.3
4	2.90, dd, (16.0, 5.6) 2.53, dd, (16.0, 8.4)	28.7	2.91, dd, (16.0, 5.5) 2.52, dd, (16.0, 8.0)	28.8
5		157.1		157.2
6	6.02, d, (2.0)	95.4	6.02, d, (2.0)	96.1
7		157.6		157.7
8	5.88, d, (2.0)	96.1	5.87, d, (2.0)	95.3
4a		100.6		100.6
8a		156.8		156.9
1'		132.0		131.8
2'	6.90, d, (1.6)	115.2	6.88, d, (2.0)	115.2
3'		145.6		146.1
4'		145.6		146.0
5'	6.79, d, (8.4)	115.7	6.77, d, (8.0)	115.7
6'	6.74, dd, (8.0, 2.0)	120.0	6.73, dd, (8.1, 2.0)	118.8

^aRecorded at 400 MHz

3.2.3.9 Structural elucidation of compound **9**

9 (7.8 mg, 0.006% yield based on EtOAc extract) was obtained as white amorphous powder showing the violet spot under the UV light. The ^1H NMR spectrum (**Figure A.29**) showed signals of three aromatic protons [δ_{H} 7.58 (1H, dd, $J = 8.4, 2.0$ Hz, H-6), 7.55 (1H, d, $J = 2.0$ Hz, H-2) and 6.90 (1H, d, $J = 8.4$ Hz, H-5)], indicating the presence of 1,3,4-trisubstitution system in the aromatic ring, and one oxygenated methyl group at δ_{H} 3.90 (3H, H-8). The ^{13}C NMR spectrum (**Figure A.30**) confirmed the existence of one carbonyl group at δ_{C} 167.7, C-7, one methoxyl group at δ_{C} 56.4, C-8, three aromatic methine (δ_{C} 124.9, 115.6 and 113.6), and three quaternary aromatic carbons (δ_{C} 152.1, 148.1 and 123.0).

These spectroscopic data were compatible with isovanillic acid⁴⁰; therefore **9** was isovanillic acid.



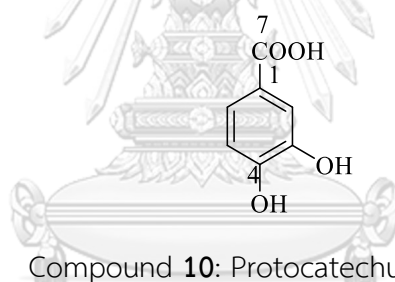
Compound **9**: Isovanillic acid

3.2.3.10 Structural elucidation of compound **10**

10 (10.4 mg, 0.008% yield based on EtOAc extract) was obtained as white amorphous powder showing the violet spot under the UV light. The ^1H NMR

spectrum (**Figure A.31**) revealed three aromatic protons in an ABX system at δ_{H} 7.45 (1H, dd, $J = 8.4, 2.0$ Hz, H-6), 7.52 (1H, d, $J = 2.0$ Hz, H-2) and 6.89 (1H, d, $J = 8.4$ Hz, H-5). The ^{13}C NMR spectrum (**Figure A.32**) showed the presence of one carbonyl group at δ_{C} 167.7, C-7), three aromatic methine (δ_{C} 123.6, 117.5 and 115.7), and three quaternary aromatic carbons (δ_{C} 150.8, 145.6 and 123.6).

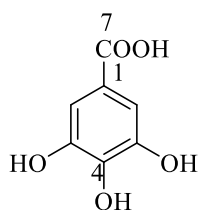
After comparing the NMR data of **10** with those of **9**, the difference two compounds were the loss of methoxyl group at position 4 in case of **10**. Moreover, this NMR spectrum was similar to that of protocatechuic acid⁴¹, as detailed in **Table 3.17**. **10** was thus elucidated as protocatechuic acid.



3.2.3.11 Structural elucidation of compound **11**

11 (20.5 mg, 0.016% yield based on EtOAc extract) was isolated as white amorphous powder. The ^1H NMR spectrum (**Figure A.33**) showed the existence of only two symmetric aromatic protons at δ_{H} 7.15 (2H, s, H-2, H-6). The ^{13}C NMR (**Figure A.34**) indicated one carbonyl group at δ_{C} 167.9, C-7), two aromatic methines at δ_{C} 110.2 (x2), C-2, C-6, and four quaternary aromatic carbons (δ_{C} 146.0 x 2, 138.7 and 122.1).

According to all NMR data, it is suggested that the structure of **11** be gallic acid⁴².



Compound **11**: Gallic acid

Table 3.15 The ¹H and ¹³C NMR chemical shift assignments of **9** compared with those of isovanillic acid

Position	9 ^a (acetone- <i>d</i> ₆)		Isovanillic acid ^a (acetone- <i>d</i> ₆)	
	δ_{H} , mult <i>J</i> , (Hz)	δ_{C}	δ_{H} , mult <i>J</i> , (Hz)	δ_{C}
1		123.0		122.9
2	7.55, d, (2.0)	115.6	7.58, d, (1.6)	115.5
3		148.1		148.1
4		152.1		152.0
5	6.90, d, (8.4)	113.6	6.92, d, (8.4)	113.5
6	7.58, dd, (8.4, 2.0)	124.9	7.61, dd, (8.4, 1.6)	124.8
7		167.7		167.8
8	3.90, s	56.4	3.93, s	56.3

^aRecorded at 400 MHz

Table 3.16 The comparative ^1H and ^{13}C NMR chemical shift assignments of **10** and protocatechuic acid

Position	10 ^a (acetone- <i>d</i> ₆)		Protocatechuic acid ^c (acetone- <i>d</i> ₆)	
	δ_{H} , mult <i>J</i> , (Hz)	δ_{C}	δ_{H} , mult <i>J</i> , (Hz)	δ_{C}
1		123.2		123.2
2	7.52, d, (2.0)	117.5	7.53, d, (2.0)	117.6
3		145.6		145.5
4		150.8		150.6
5	6.89, d, (8.4)	115.7	6.90, d, (8.3)	115.8
6	7.45, dd, (8.4, 2.0)	123.6	7.48, dd, (8.3, 2.0)	123.7
7		167.7		167.7

^aRecorded at 400 MHz, ^cRecorded at 600 MHz

Table 3.17 The comparative ^1H and ^{13}C NMR chemical shift assignments of **11** and gallic acid

Position	11 ^a (acetone- <i>d</i> ₆)		Gallic acid ^a (CDCl ₃)	
	δ_{H} , mult <i>J</i> , (Hz)	δ_{C}	δ_{H} , mult <i>J</i> , (Hz)	δ_{C}
1		122.1		120.5
2/6	7.15, s	110.2	6.9, s	108.8
3/5		146.0		145.5
4		138.7		138.1
7		167.9		167.6

^aRecorded at 400 MHz

3.3 Biological activities of isolated compounds from the stem of *K.angustifolia*

The separation of *K. angustifolia* stems led to the isolation of eleven compounds. These compounds were further evaluated for the biological activities including anti-tyrosinase and α -glucosidase inhibition activity.

3.3.1 Anti-tyrosinase

The tyrosinase assay was performed by the method of Larik *et al.* (2017) with slight adjustments. Kojic acid was used as a standard positive control.

The results of *K. angustifolia* extracts for anti-tyrosinase activity were mentioned in the first part of the preliminary biological activity test, both *n*-hexane and EtOAc extracts exhibited as the potent tyrosinase inhibitory sources. Thus, the isolated compounds were chosen to evaluate for that of activity as presented in

Table 3.18.

Due to a shortage of material, angustiquinone (**3**) could not be assayed for the activity of mushroom tyrosinase. Rapanone (**1**) and embelin (**2**), contained the long-chain saturated carbons in their molecules, possessed the value of IC_{50} more than 200 μ M. This might be implied that the steric effect of the long chain reduced the activity.

Table 3.18 Anti-tyrosinase activity of isolated compounds from *K. angustifolia*

Compounds	IC ₅₀ (μM)
Rapanone (1)	> 200
Embelin (2)	> 200
Angustiquinone (3)	NT
Quercetin (4)	43.3±0.26
Kaempferol (5)	156.5±0.34
Bergenin (6)	NA
11-O-acetyl bergenin (7)	NA
Catechin (8)	> 200
Isovanillic acid (9)	> 200
Protocatechuic acid (10)	> 200
Gallic acid (11)	> 200
Kojic acid	36.1±1.07

NT: not tested, NA: not active

From the literature review for flavonoids, it has been demonstrated that 3-hydroxyl-4-ketone moiety, which makes the chelate with copper, was the key to determine the inhibitory activity, and the loss of one factor will complete abolishing the activity. This hypothesis was confirmed in our research. While quercetin (4) and kaempferol (5) exhibited moderate activity with IC₅₀ value 43.3±0.26 and 156.5±0.34 μM, respectively, catechin (8) displayed IC₅₀ more than 200 μM. In addition, 4 was

found to be 3.6-fold more active than **5**. The only difference between these two compounds is that **4** has an extra hydroxyl group at C-3', which is consist of with the literature findings⁴³.

Bergenin (**6**) and its derivative 11-*O*-acetyl bergenin (**7**) were inactive toward mushroom tyrosinase. It could be indicated that the bulky glycosides moiety in the structures of **6** and **7** effected on the active site of the enzyme by preventing the inhibitor.

For the monophenolic compounds, isovanillic acid (**9**), protocatechuic acid (**10**), and gallic acid (**11**) revealed weak inhibitors against mushrooms tyrosinase with IC₅₀ value more than 200 μM.

3.3.2 α-Glucosidase inhibitory activity

α-Glucosidase inhibitory assay of extracts and isolated compounds from *K. angustifolia* stems was evaluated using Ramadhan's method with slight modification²⁹. Acarbose, an oral anti-diabetes drug, was used as a positive control. The lower IC₅₀ values demonstrated the stronger enzymatic inhibition. The results are demonstrated in **Tables 3.19** and **3.20**.

Table 3.19 α -glucosidase inhibitory activity of *K. angustifolia* extracts

Extracts	IC ₅₀ ($\mu\text{g/mL}$)
<i>n</i> -hexane	20.91 \pm 0.40
CH ₂ Cl ₂	10.10 \pm 0.32
EtOAc	< 2
MeOH	< 2

In general, all herbal extracts showed potential activity. Notably, the higher α -glucosidase inhibitory activity was detected from both EtOAc and MeOH extracts. Previous studies have illustrated that the strong α -glucosidase inhibitors were the essential sources for the treatment of diabetes mellitus type 2. Therefore, the discovery of the bioactive compounds from *K. angustifolia* may warrant further investigation for its ability to promote good health.

Table 3.20 α -glucosidase inhibitory activity of isolated compounds from *K. angustifolia*

Compounds	IC ₅₀ (μ M)
Rapanone (1)	9.25 \pm 0.26
Embelin (2)	1.30 \pm 0.17
Angustiquinone (3)	NT
Quercetin (4)	71.20 \pm 1.04
Kaempferol (5)	23.15 \pm 1.25
Bergenin (6)	NA
11-O-acetyl bergenin (7)	87.70 \pm 1.01
Catechin (8)	151.60 \pm 1.88
Isovanillic acid (9)	> 200
Protocatechuic acid (10)	> 200
Gallic acid (11)	> 200
Acarbose	93.63 \pm 0.49

NT: not tested, NA: not active

According to the results in **Table 3.20**, rapanone (1) and embelin (2), *p*-benzoquinone derivatives from *K. angustifolia*, showed tremendous activity compared to other isolated compounds with IC₅₀ 9.3 \pm 0.26 and 1.3 \pm 0.17 μ M, respectively. The result also displayed that 1 and 2 gave much higher inhibitory activity than commercial α -glucosidase inhibitor acarbose with IC₅₀ 93.6 \pm 0.49 μ M. 2

with better inhibitory effect was reported to possess antidiabetic effect towards induced diabetic rats, which probably explained the excellent activity towards α -glucosidase⁴⁴. The reduction of the alkane chain in **2** led to better inhibitory activity compared to **1**.

The isolated flavonoids including quercetin (**4**), kaempferol (**5**), catechin (**8**) also showed moderate α -glucosidase inhibitor with IC_{50} 71.2 \pm 1.04, 23.2 \pm 1.25 and 151.6 \pm 1.88 μ M. Previous reports illustrated that the activity of some flavonoids showed better activities than commercial diabetic drug acarbose. Various kinetic mechanisms of flavonoids were also established^{25, 45, 46}. The structure-activity relationships (SARs) of these compounds established by Zeng *et al.* suggested that the hydroxyl groups on rings A, B, and C were essential for α -glucosidase inhibition. In detail, 4'-OH substitution on ring B and 3-OH substitution on ring C, which could interact with the positively charged groups on the enzyme, was considered as a crucial role for the activity. Moreover, another study reported that the existence of a hydroxyl group at the C-3 'position of ring B decreased the inhibitory effect on the enzyme⁴⁷. The fact that quercetin (**4**) had a better effect than kaempferol (**5**) was consistent with these SARs.

11-O-acetyl bergenin (**7**) good activity with IC_{50} 87.7 \pm 1.01 μ M compared to bergenin which showed no activity towards α -glucosidase. The acetyl group in 11-O-acetyl bergenin played a vital role in increasing α -glucosidase activity compared to

the hydroxyl group at bergenin itself. It was also reported that the derivatives of bergenin such as 11-*O*-benzoylbergenin, 11-*O*-(3',4'-dimethoxybenzoyl)-bergenin, 11-*O*-vanilloylbergenin and 11-*O*-protocatechuoylbergenin revealed better activity towards α -glucosidase⁴⁸.

Similarly to anti-tyrosinase activity, isovanillic acid (**9**), protocatechuic acid (**10**) and gallic acid (**11**) displayed IC_{50} more than 200 μ M. Unfortunately, the new compound angustiquinone (**3**) was unable to determine for α -glucosidase activity due to the minimum amount of compound. To the best of our knowledge, this is the first report of rapanone (**1**) embelin (**2**), and 11-*O*-acetyl bergenin (**7**) as α -glucosidase inhibitor.

Base on the results, the detected compounds could be responsible for the biological activities of *n*-hexane and EtOAc extracts.

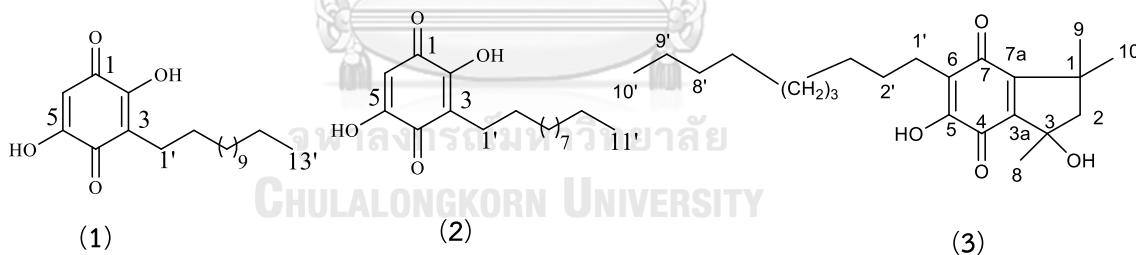
Chapter 4

Conclusions

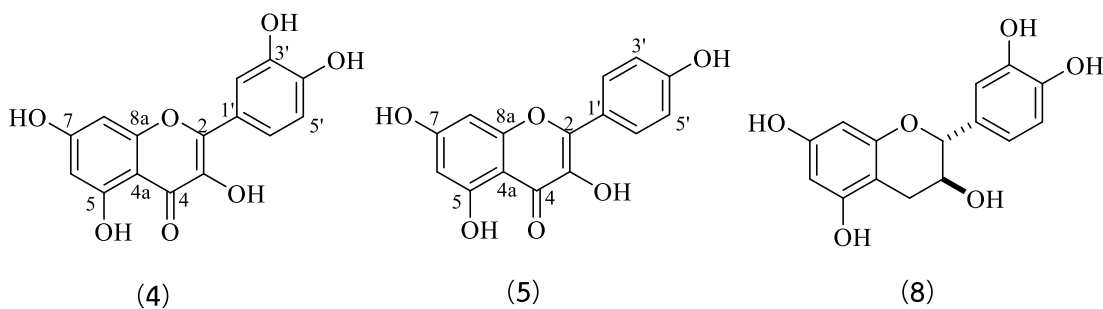
4.1 Chemical constituent of *K. angustifolia* stems

This is the first report on the chemical constituents of *K. angustifolia* plant. Further repeated column chromatography of *n*-hexane and EtOAc extracts led to the isolation of one novel quinone: angustiquinone (3) and ten known compounds: rapanone (1), embelin (2), quercetin (4), kaempferol (5), bergenin (6), 11-*O*-acetyl bergenin (7), catechin (8), isovanillic acid (9), protocatechuic acid (10), gallic acid (11). The structures of isolated compounds are shown in **Figure 4.1**. Each structure was unambiguously elucidated using 1D and 2D NMR analyses, in addition to the use of literature for the comparison of the experimental data acquired.

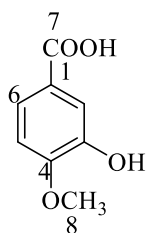
• Para-benzoquinone



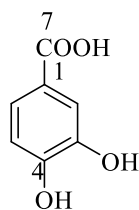
Flavonoids



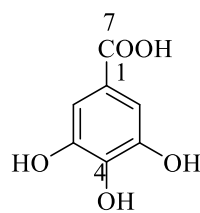
- Monoaromatic ring



(9)

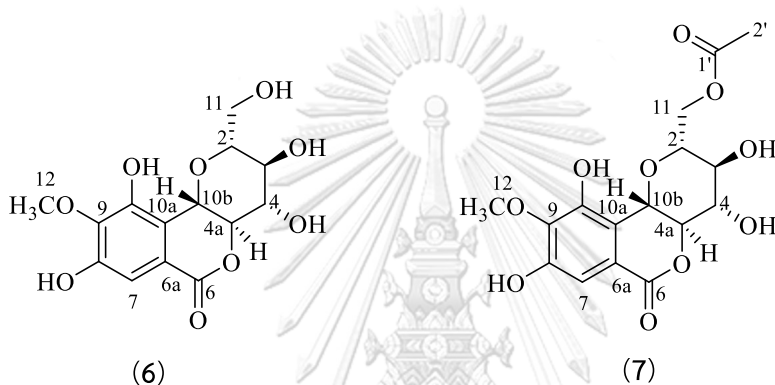


(10)



(11)

- Other skeletons



(6)

(7)

4.2 Biological activities

The isolated substances were evaluated for the biological activities including anti-tyrosinase, α -glucosidase inhibitory activity.

According to the results of anti-tyrosinase activity, quercetin (**4**) showed the highest inhibitory effect with IC_{50} 42.3 ± 0.25 μ M, followed by kaempferol (**5**) with IC_{50} 156.5 ± 0.34 . Interestingly, the activity of both compounds were lower than that of a positive control, kojic acid (IC_{50} 36.1 ± 1.07).

The bright point of this research is the discovery of promising α -glucosidase inhibitors. Most compounds including **1**, **2**, **4**, **5** and **8** showed excellent activity

better than the commercial drug acarbose. Especially, rapanone (1) and embelin (2) exhibited as the best candidates, with 10 and 72-folds, respectively. Therefore, it could serve as auspicious substances for designing new potent α -glucosidase inhibitors.

4.3 Suggestions for future work

This investigation has disclosed that *K. angustifolia* had the potential to provide medicinally beneficial compounds. Therefore, it is necessary to continue to isolate more compounds and evaluate their biological activities for applying on medicinal fields. Notably, rapanone (1) and embelin (2) revealed the potent candidates for α -glucosidase inhibitory activity, thus the further studies such as kinetic mechanism could be investigated. Moreover, synthesis of their derivatives is one of the excellent directions to develop the benefits of natural products.



APPENDIX

จุฬาลงกรณ์มหาวิทยาลัย
CHULALONGKORN UNIVERSITY

Generic Display Report

Analysis Info

Analysis Name D:\Data\Data Service\190813\KAHM1_RC2_01_2900.d
Method nv_pos_6min_profile_wguardcol_190624.m
Sample Name KAHM1
Comment

Acquisition Date 8/13/2019 8:36:51 PM

Operator CU.
Instrument micrOTOF-Q II

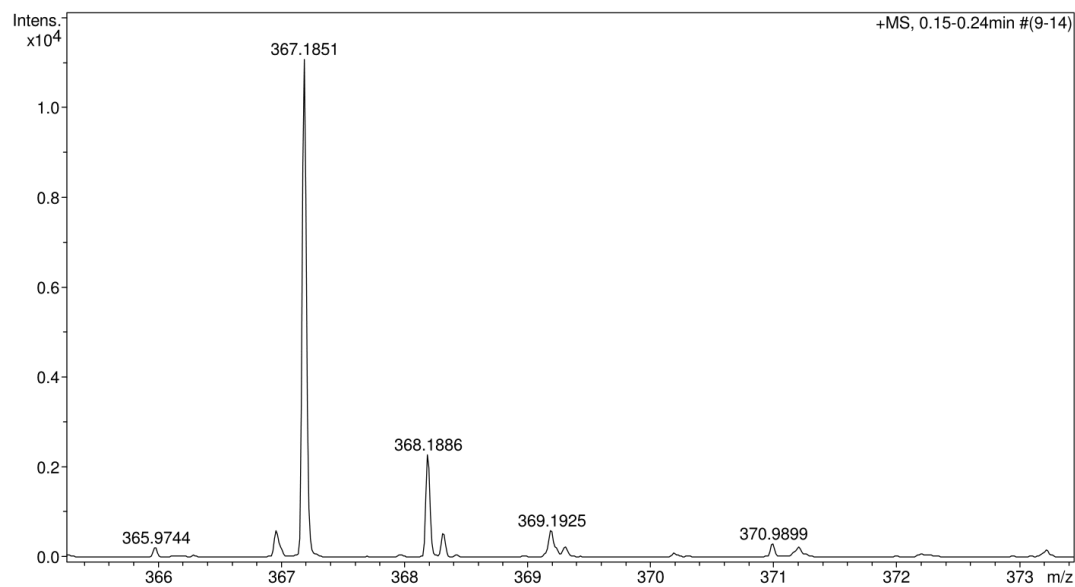
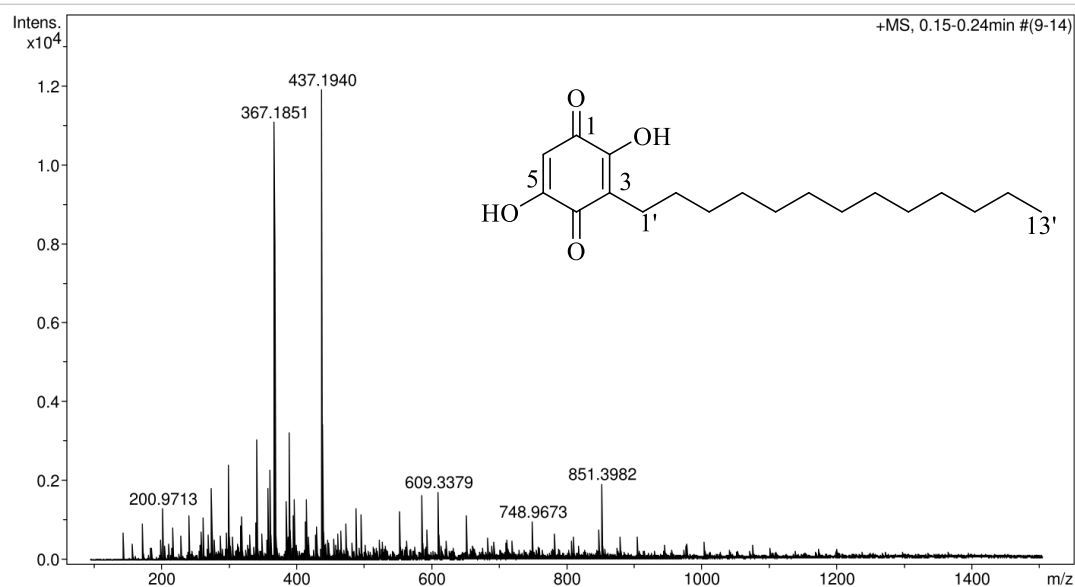


Figure A.1 HR-ESI-MS spectrum of 1 (pos)

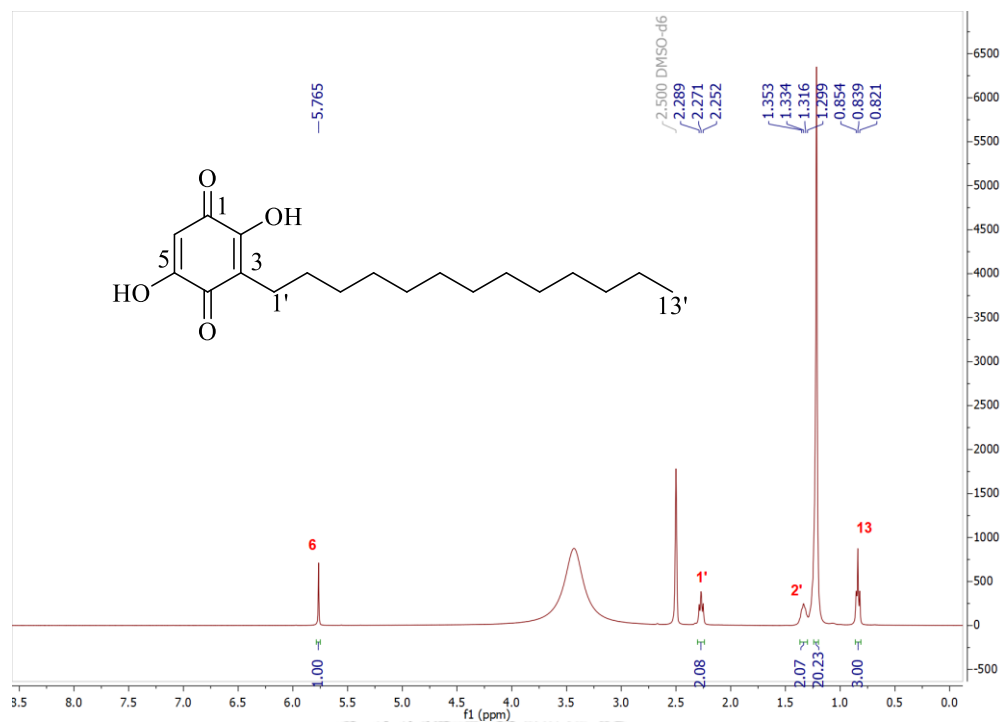


Figure A.2 The ^1H NMR (400 MHz) spectrum of 1 (DMSO- d_6)

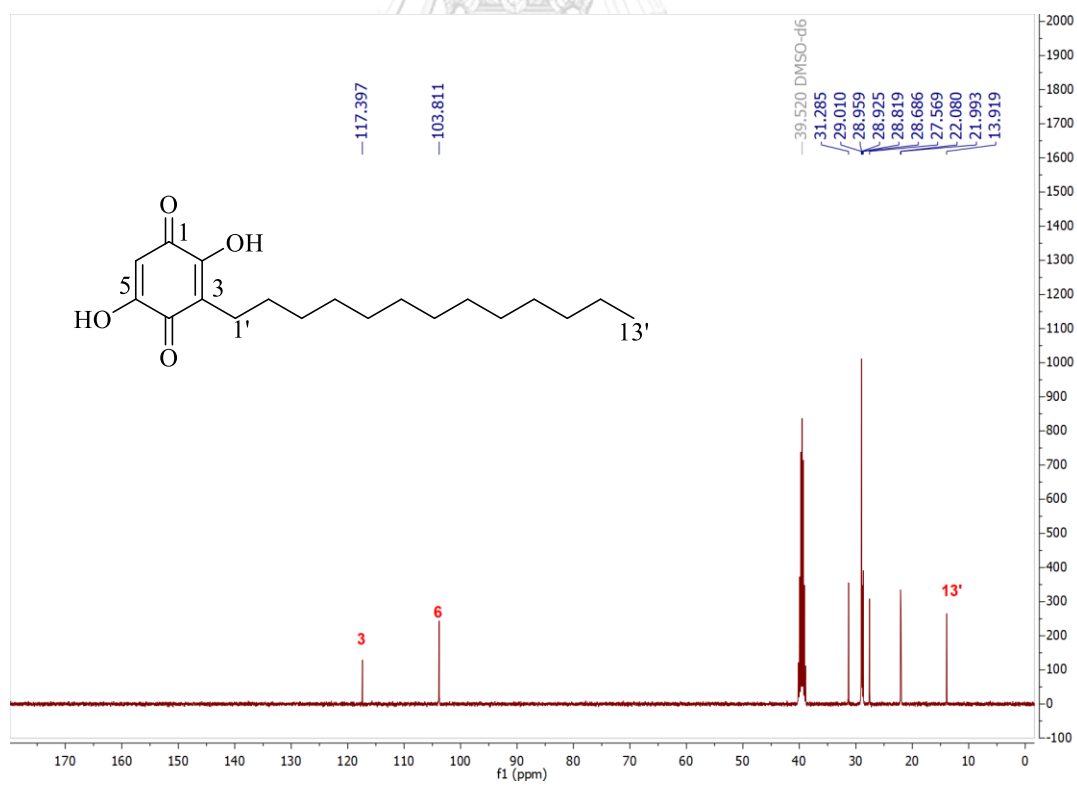


Figure A.3 The ^{13}C NMR (100 MHz) spectrum of 1 (DMSO- d_6)

Generic Display Report

Analysis Info

Analysis Name D:\Data\Data Service\190923\Embelin_RA5_01_3106.d
Method nv_pos_6min_profile_wguardcol_190624.m
Sample Name Embelin
Comment

Acquisition Date 9/23/2019 7:16:36 PM

Operator CU.
Instrument micrOTOF-Q II

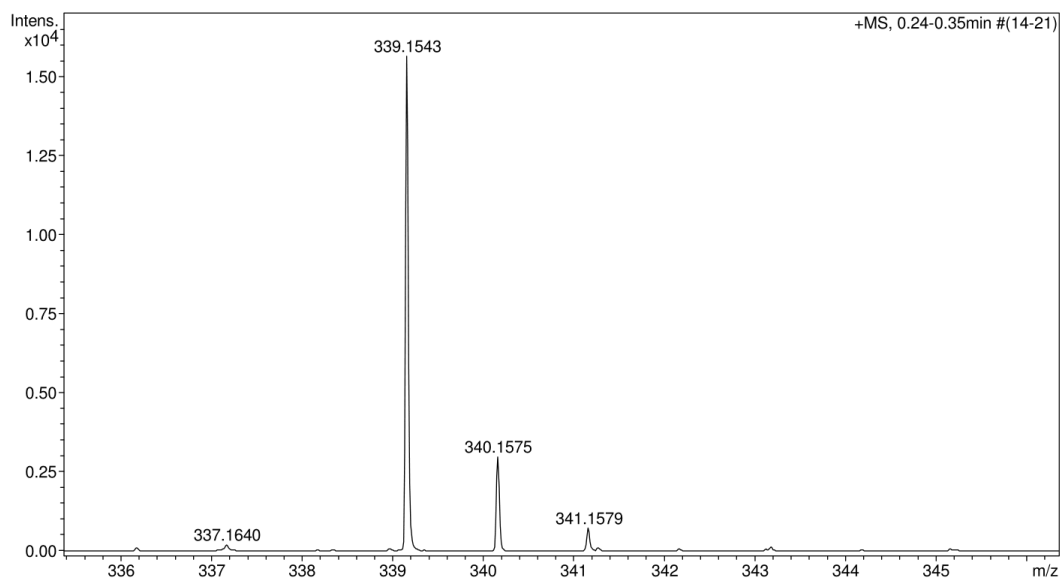
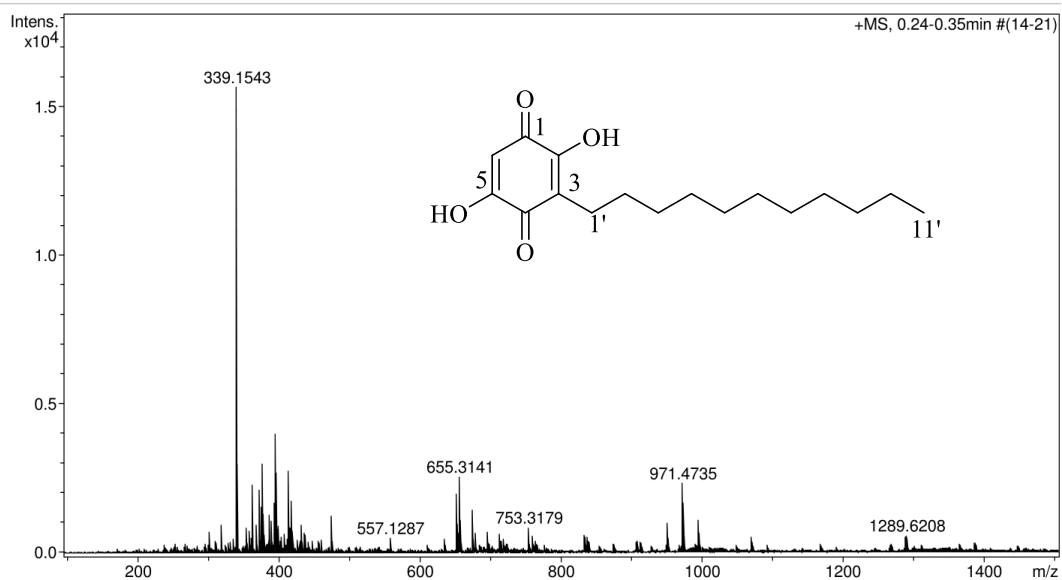


Figure A.4 HR-ESI-MS spectrum of 2 (pos)

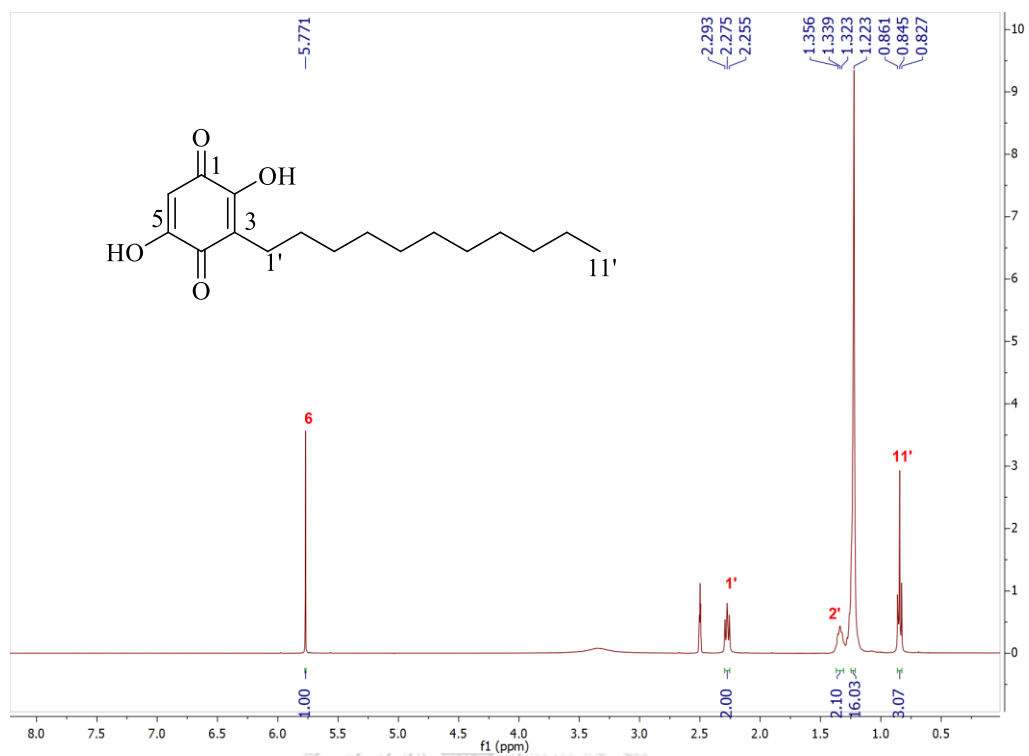


Figure A.5 The ^1H NMR (400 MHz) spectrum of 2 (DMSO- d_6)

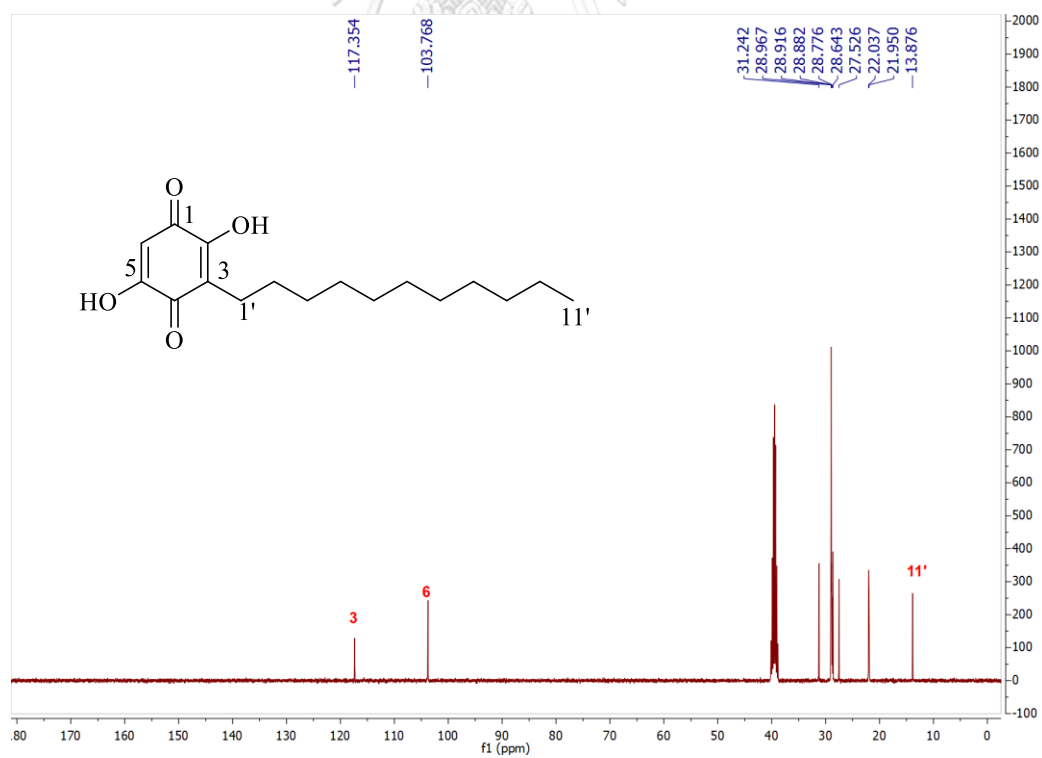


Figure A.6 The ^{13}C NMR (400 MHz) spectrum of 2 (DMSO- d_6)

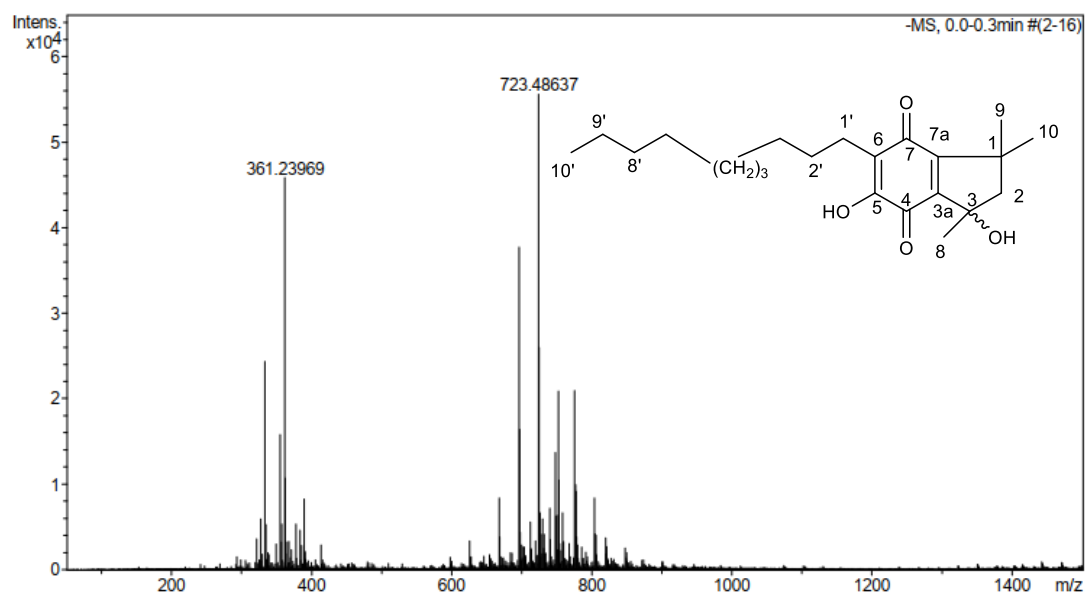


Figure A.7 HR-ESI-MS spectrum of **3** (neg)

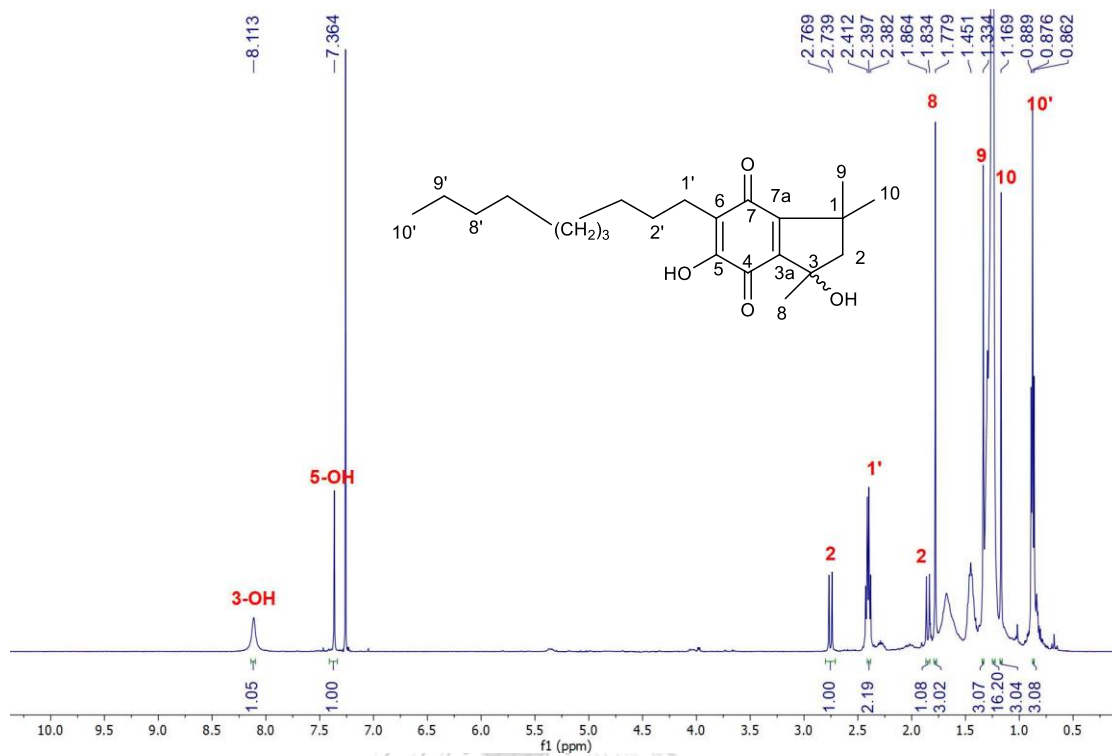


Figure A.8 The ^1H NMR (500 MHz) spectrum of **3** (CDCl_3)

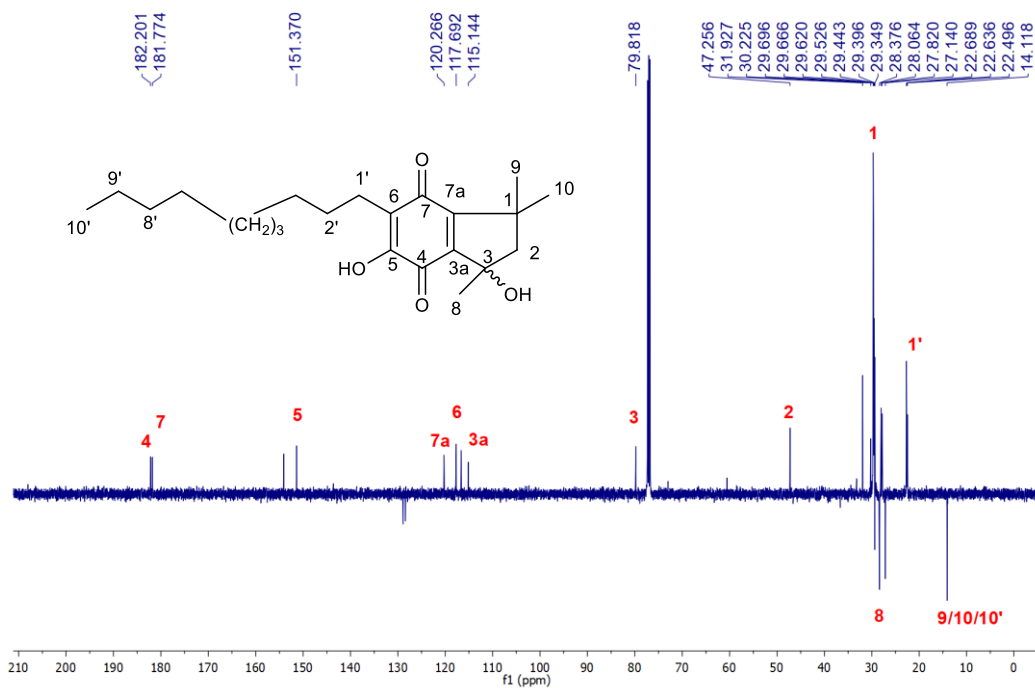
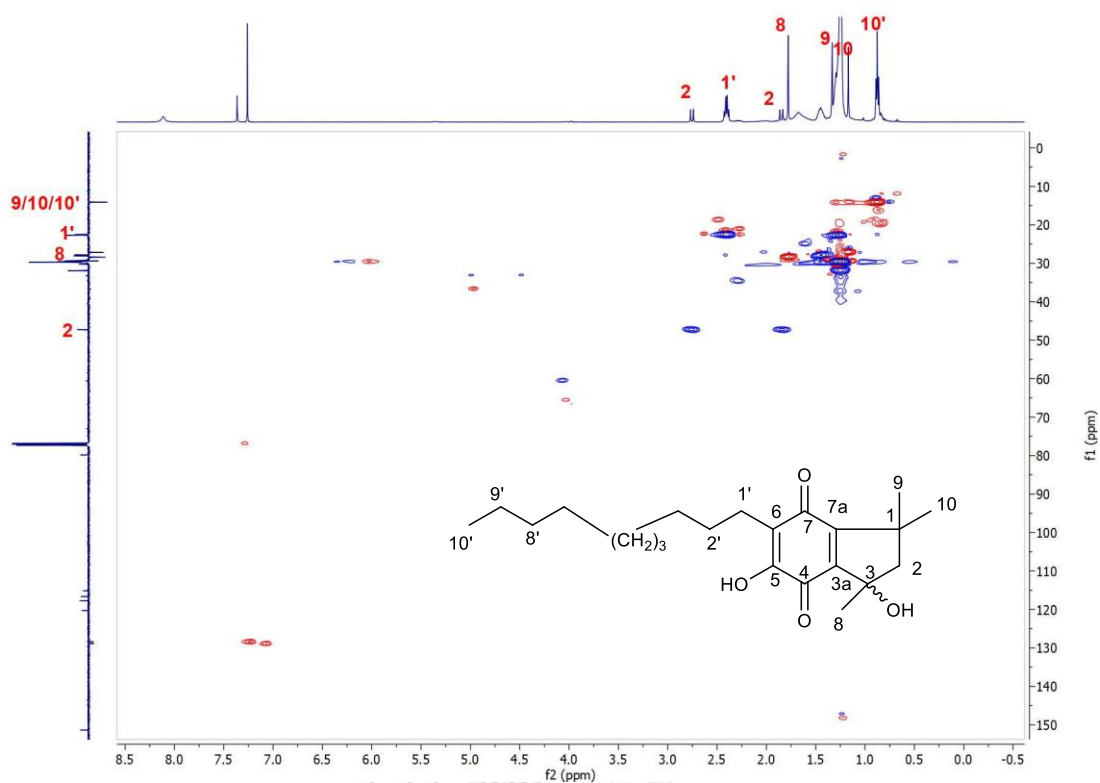
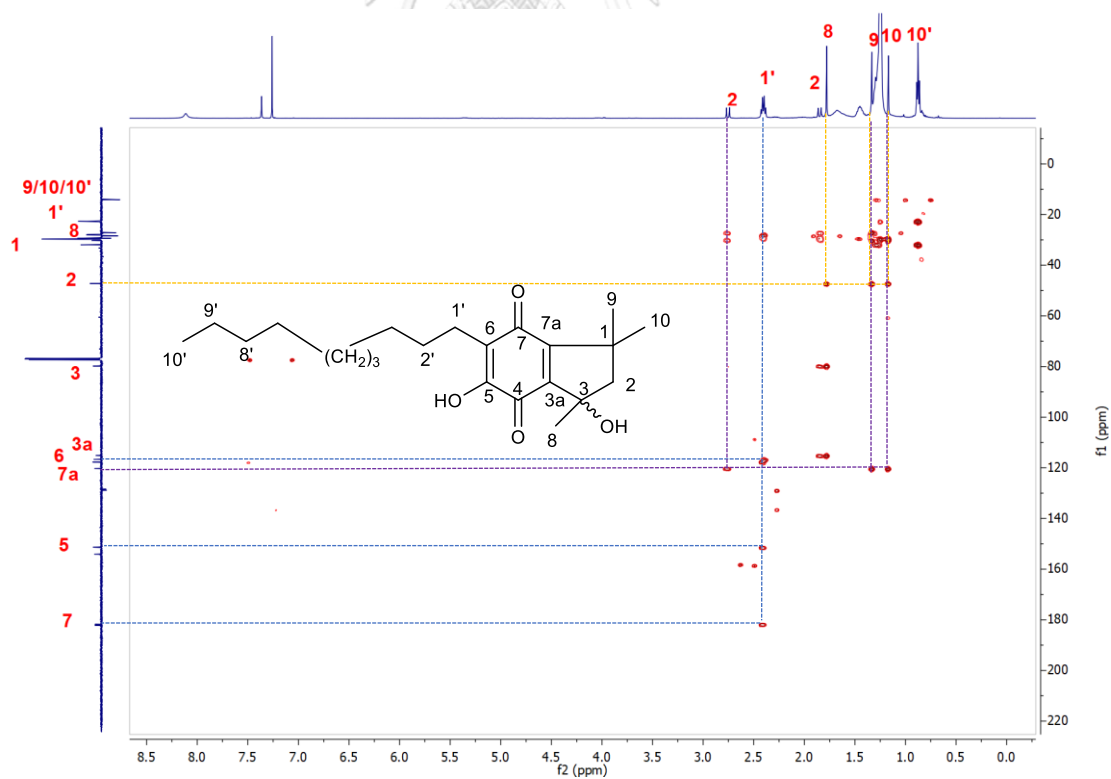


Figure A.9 The ^{13}C NMR (JMOL, 125 MHz) spectrum of **3** (CDCl_3)

Figure A.10 The HSQC spectrum of **3** (CDCl_3)Figure A.11 The HMBC spectrum of **3** (CDCl_3)

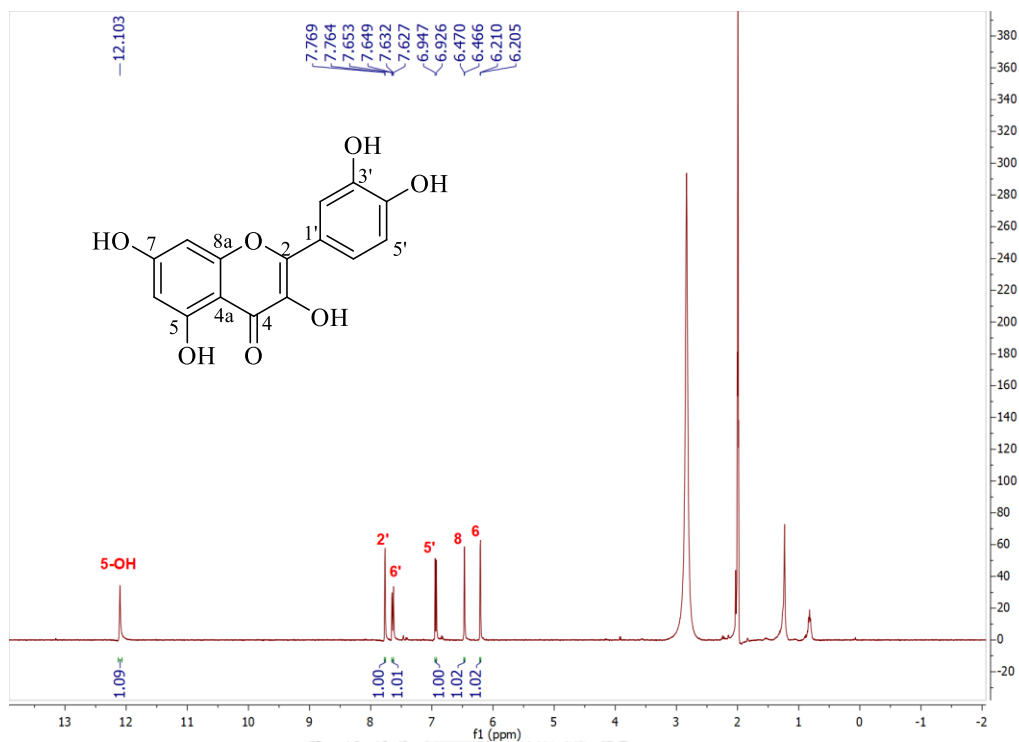


Figure A.12 The ^1H NMR (400 MHz) spectrum of **4** (acetone- d_6)

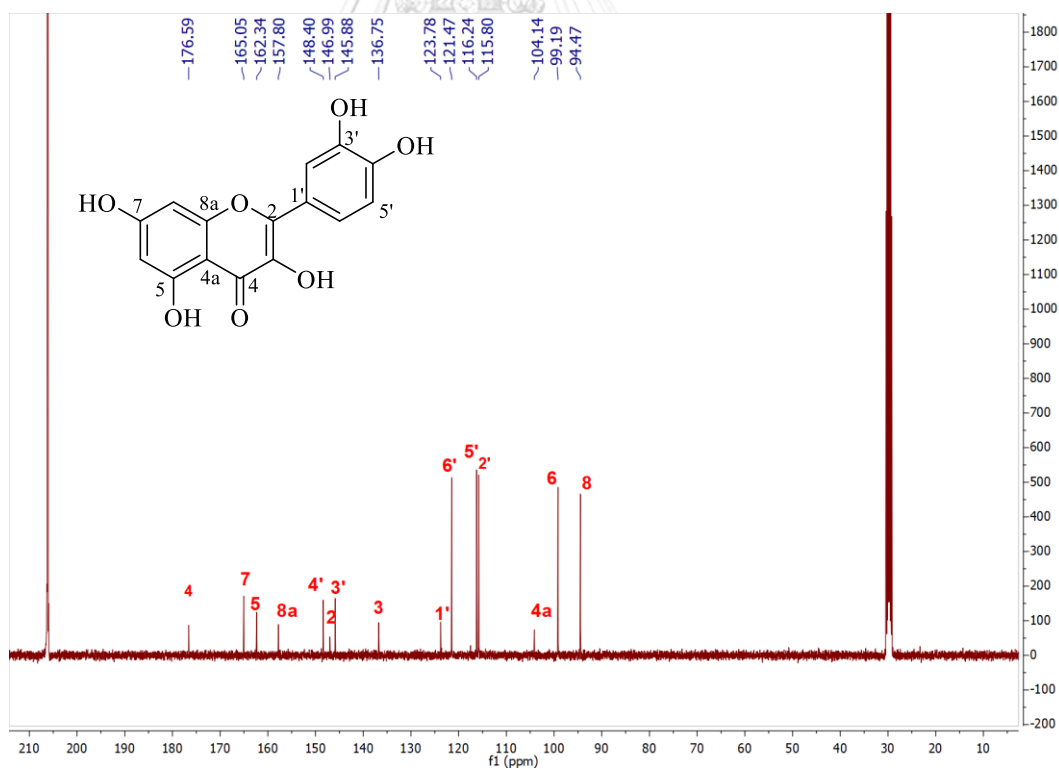
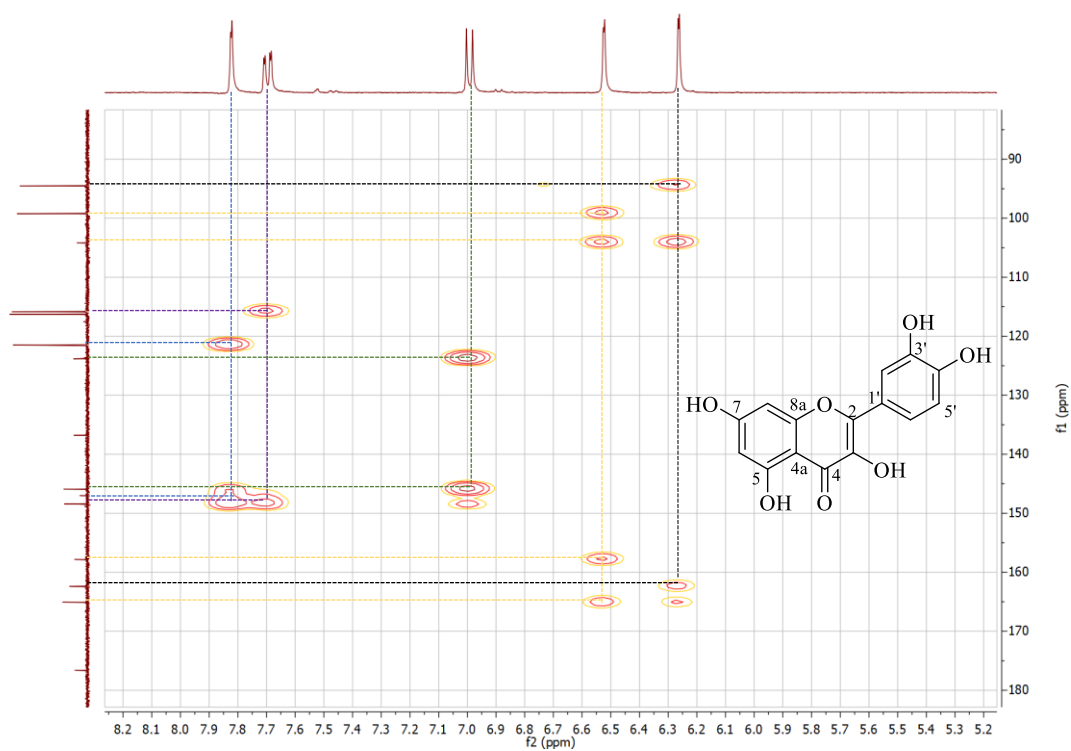
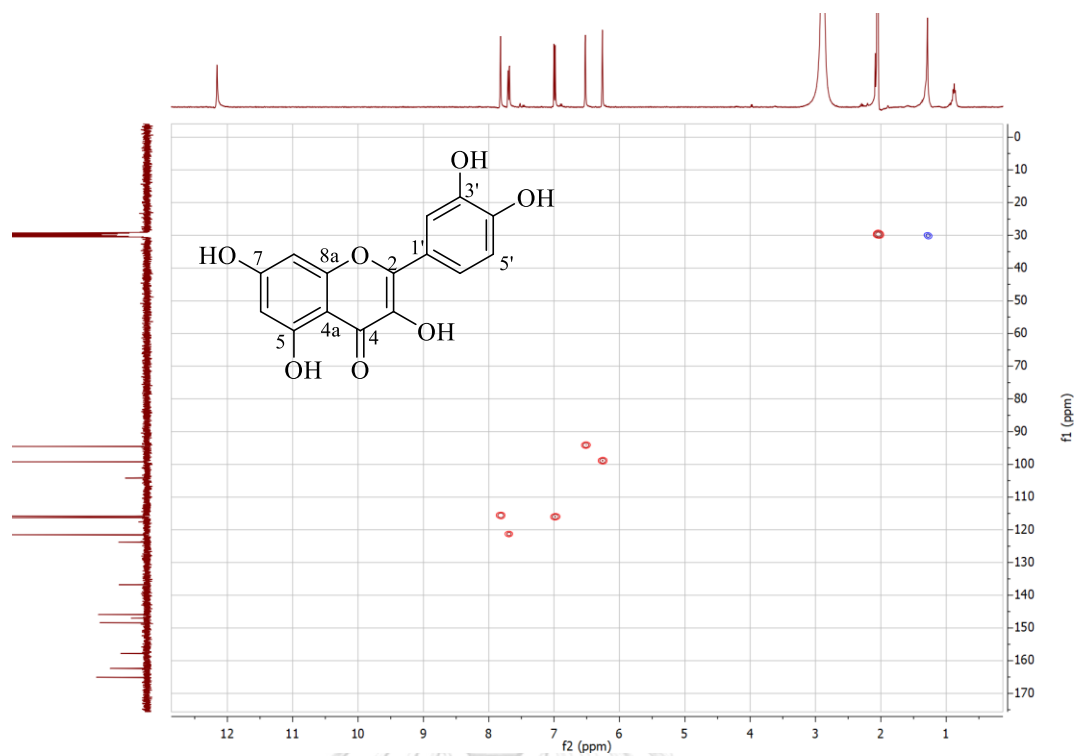


Figure A.13 The ^{13}C NMR (100 MHz) spectrum of **4** (acetone- d_6)



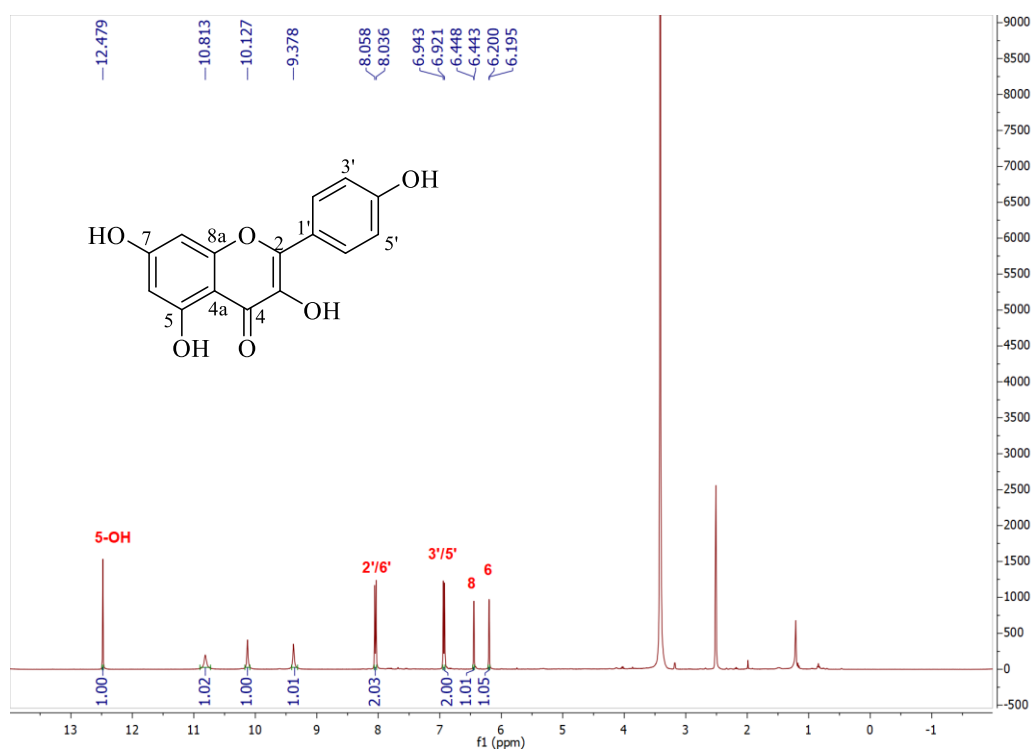


Figure A.16 The ^1H NMR (400 MHz) spectrum of **5** ($\text{DMSO-}d_6$)

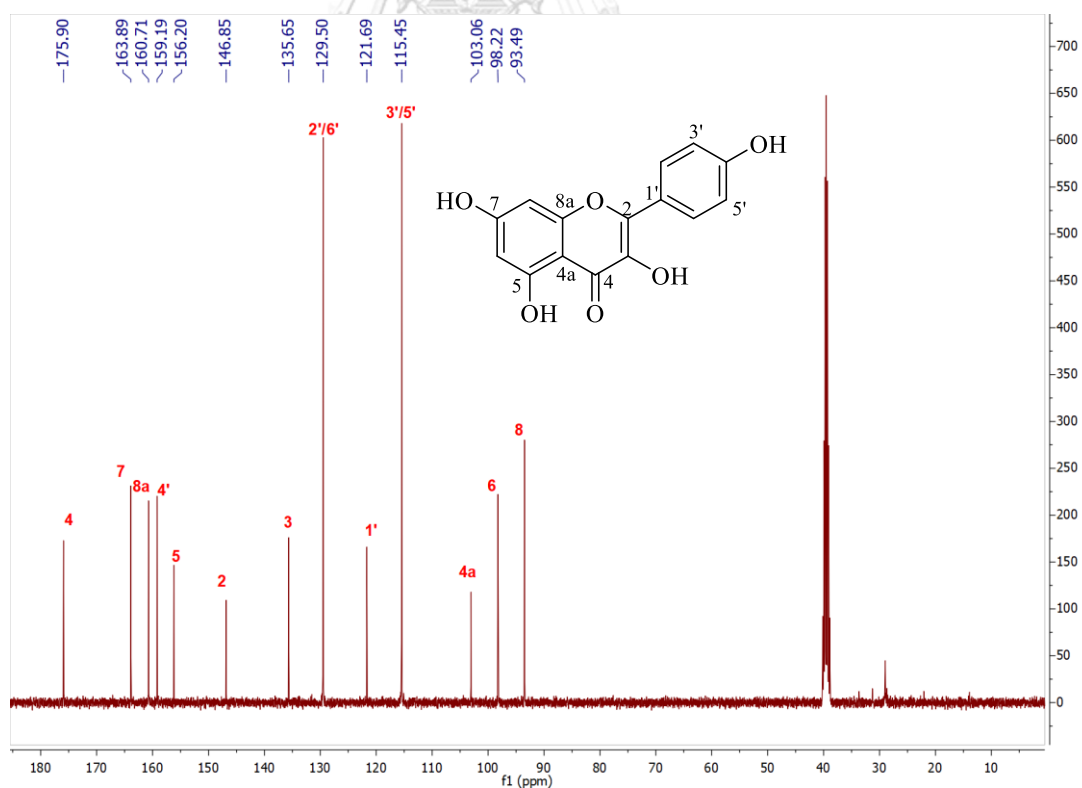


Figure A.17 The ^{13}C NMR (100 MHz) spectrum of **5** ($\text{DMSO-}d_6$)

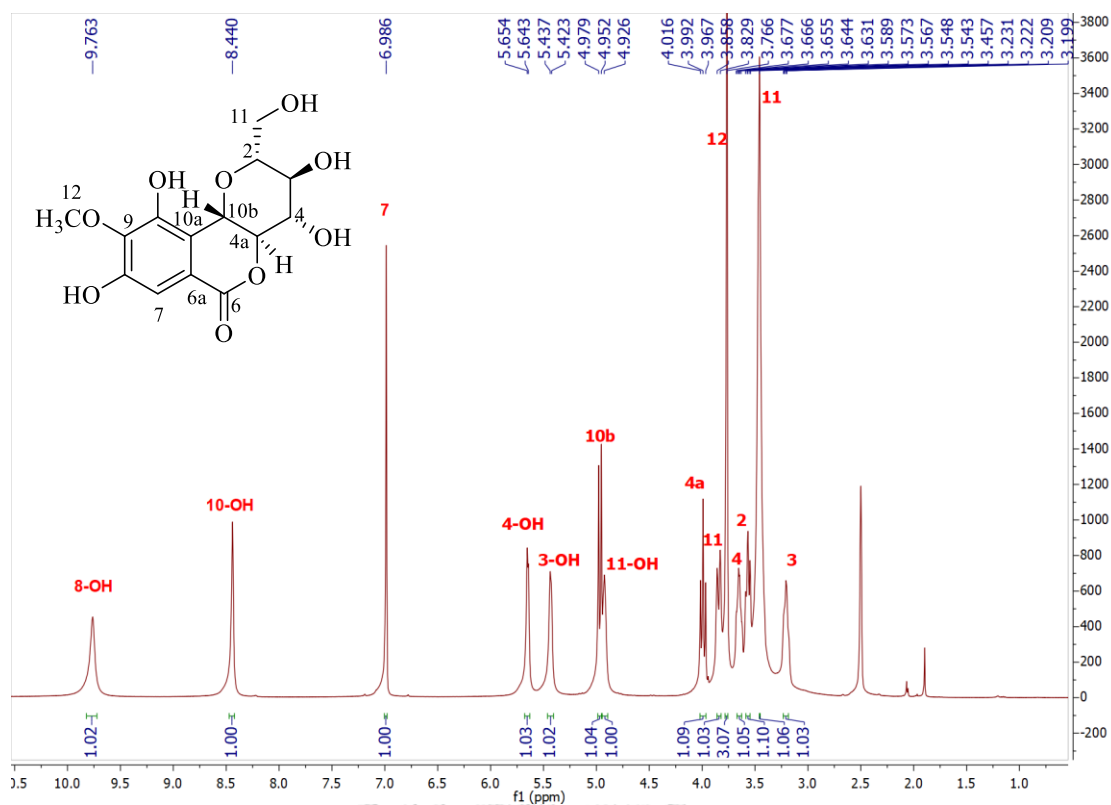


Figure A.18 The ^1H NMR (400 MHz) spectrum of **6** ($\text{DMSO-}d_6$)

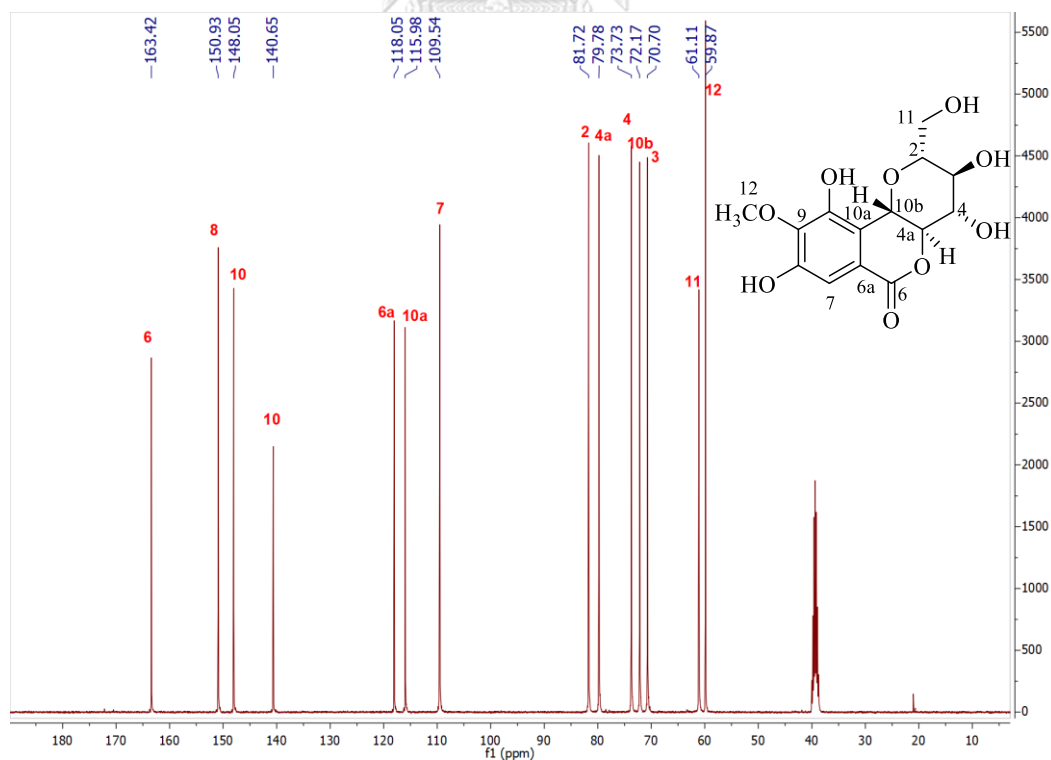


Figure A.19 The ^{13}C NMR (100 MHz) spectrum of **6** ($\text{DMSO-}d_6$)

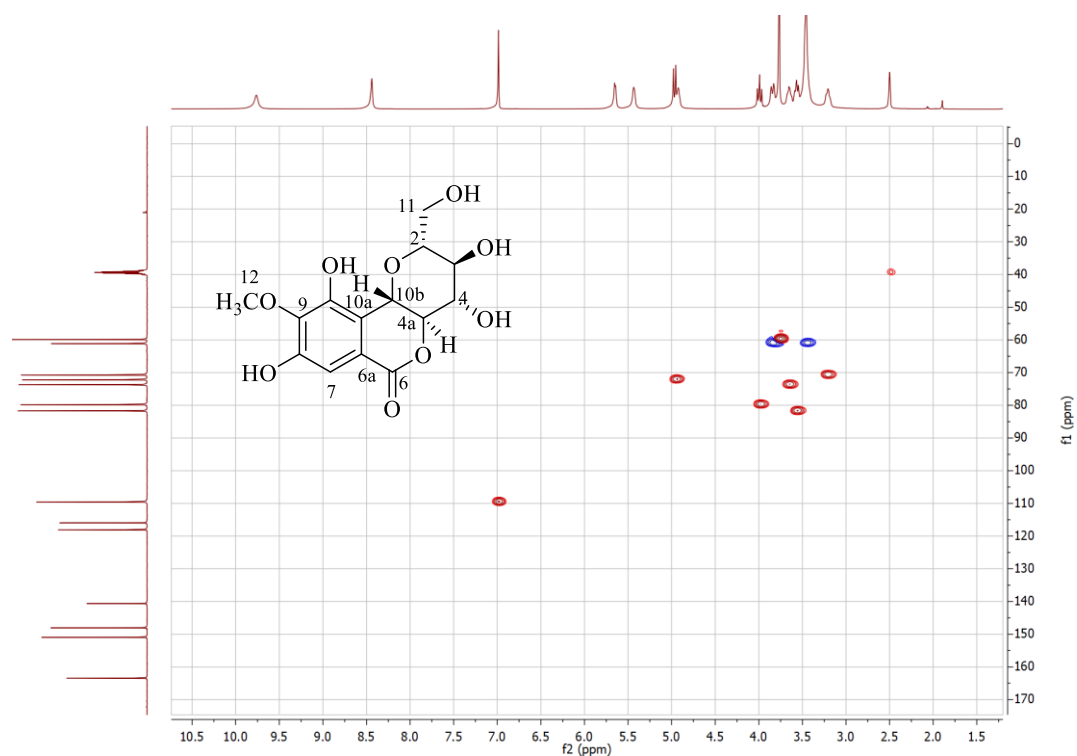


Figure A.20 The HSQC spectrum of **6** (DMSO- d_6)

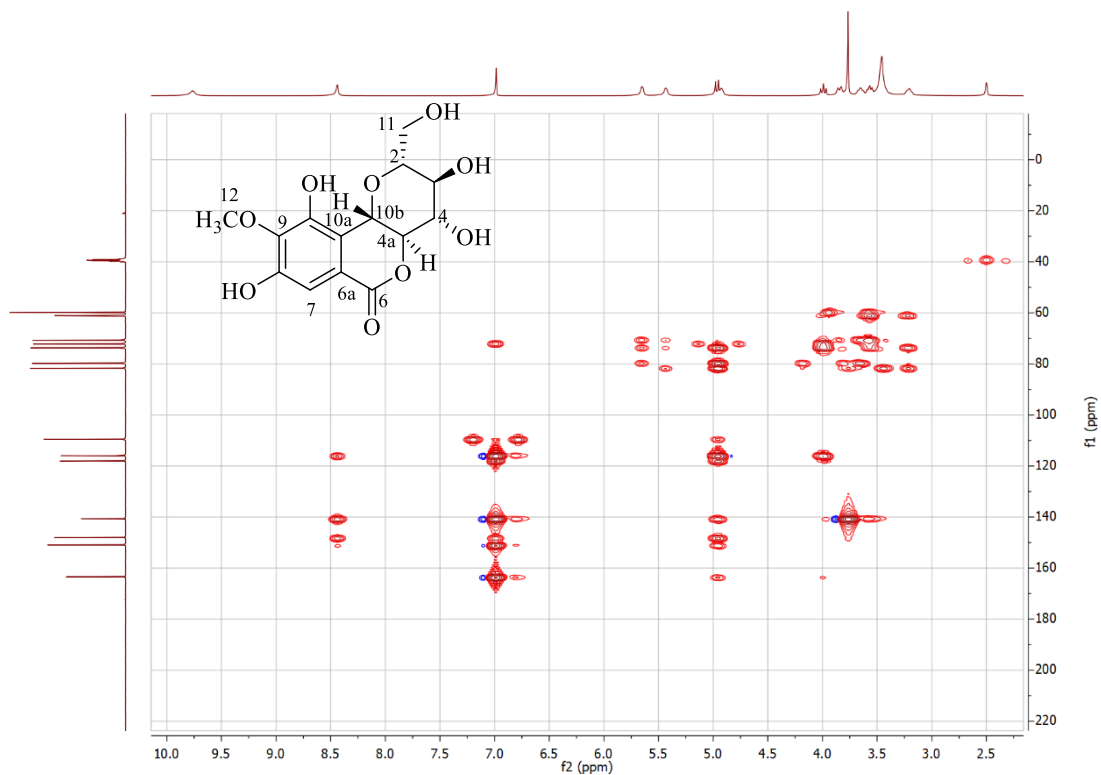


Figure A.21 The HMBC spectrum of **6** (DMSO- d_6)

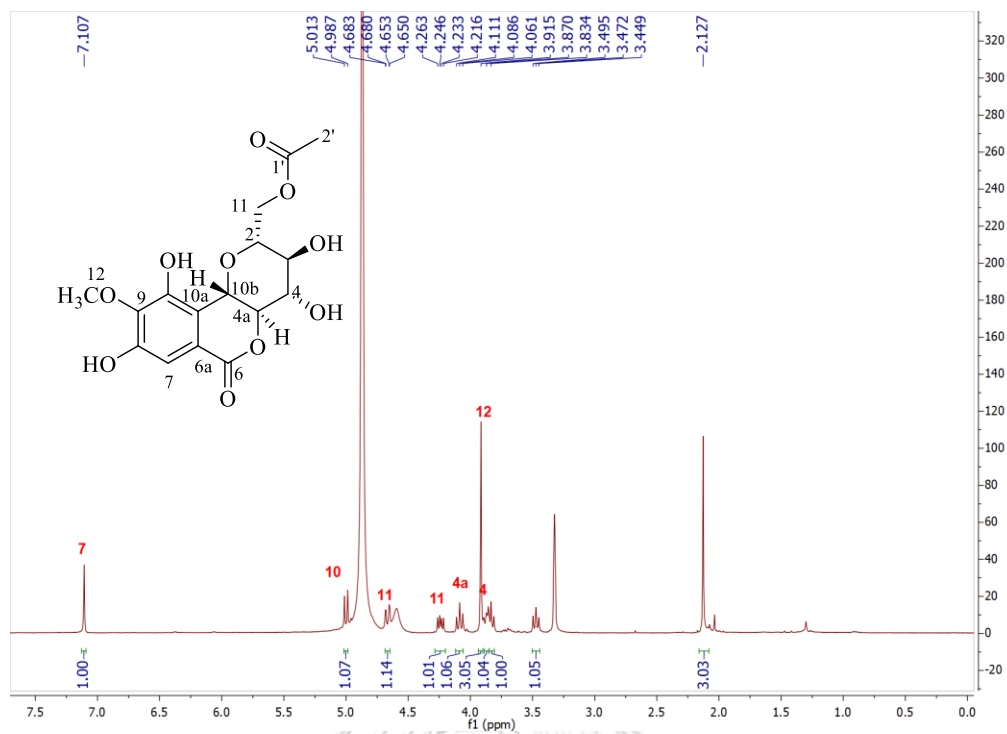


Figure A.22 The ^1H NMR (400 MHz) spectrum of **7** (CD_3OD)

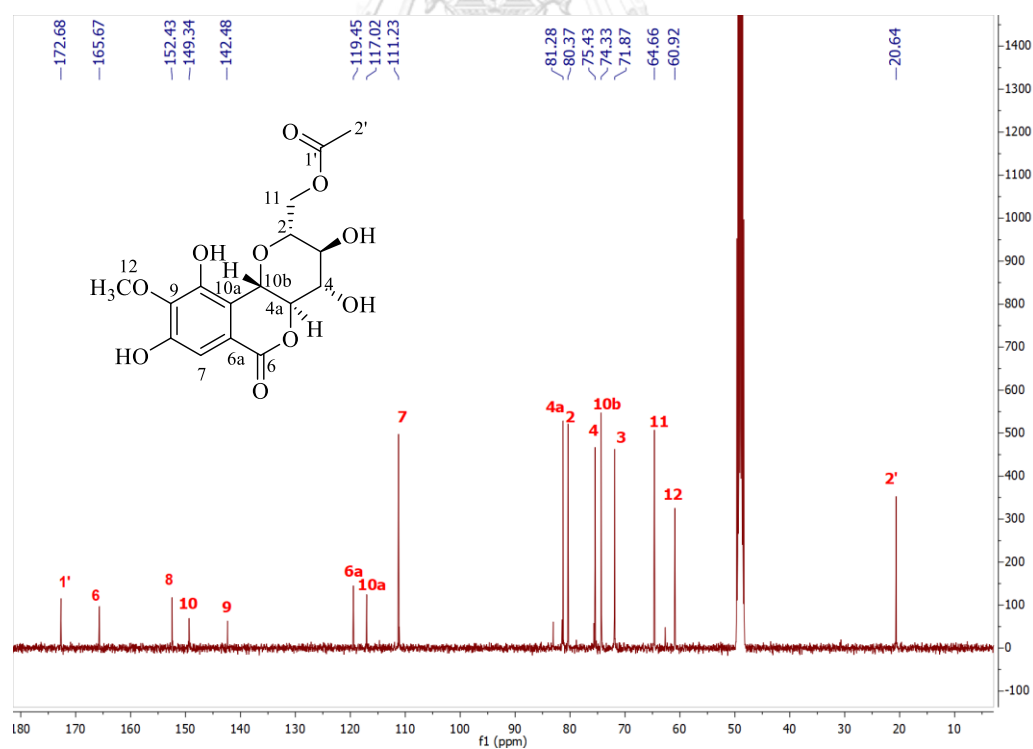
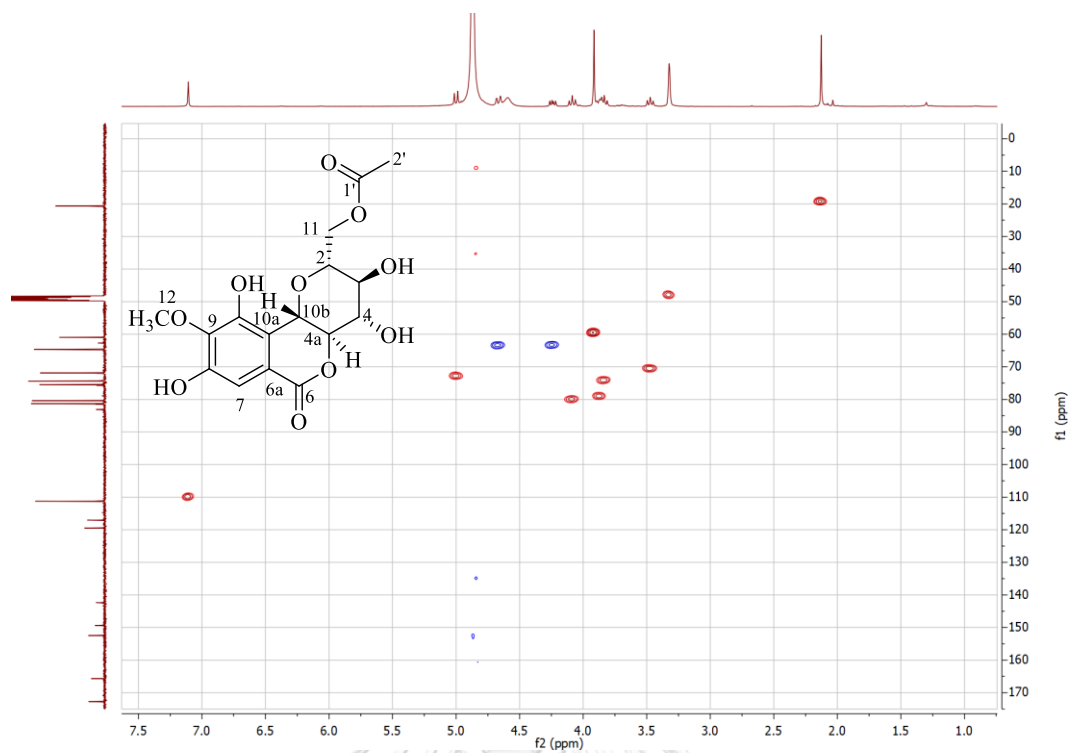
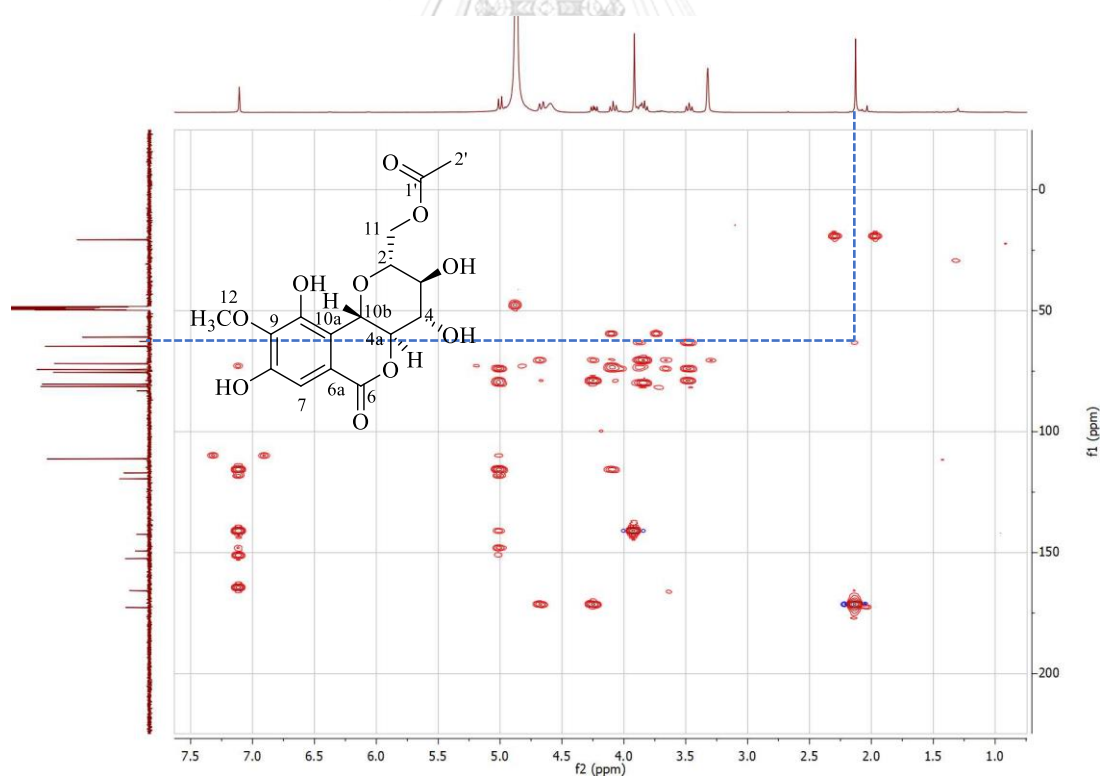


Figure A.23 The ^{13}C NMR (100 MHz) spectrum of **7** (CD_3OD)

Figure A.24 The HSQC spectrum of 7 (CD_3OD)Figure A.25 The HMBC spectrum of 7 (CD_3OD)

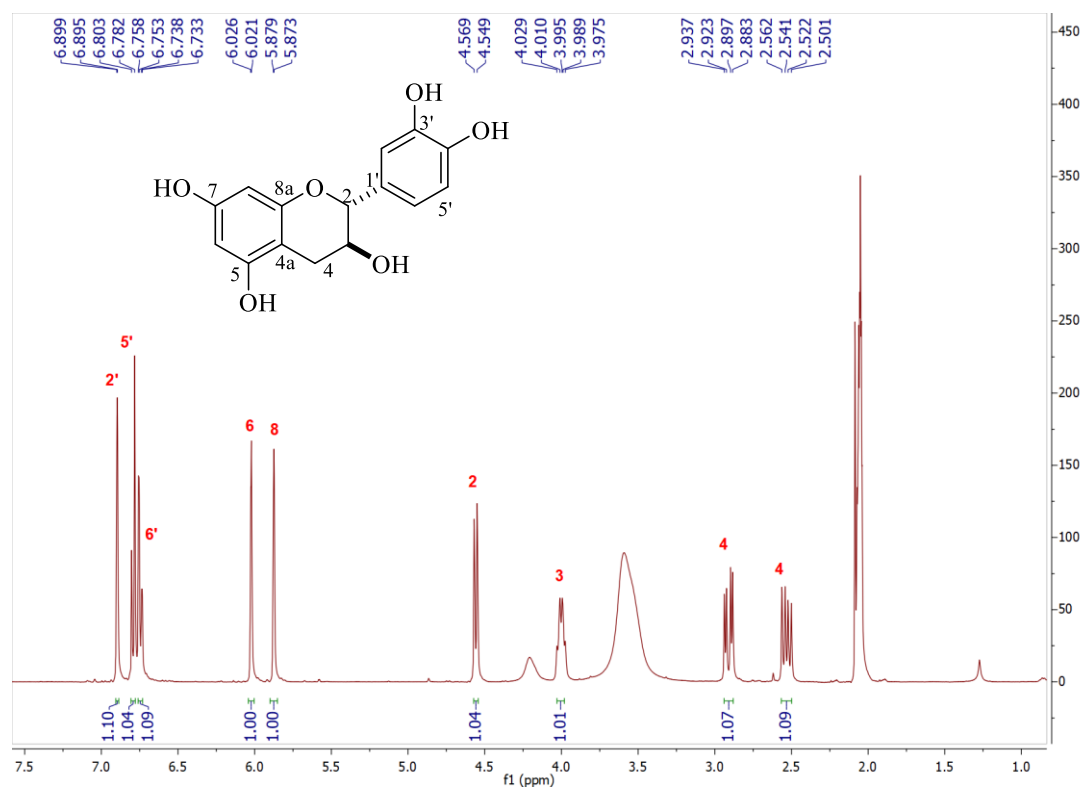


Figure A.26 The ¹H NMR (400 MHz) spectrum of **8** (acetone-*d*₆)

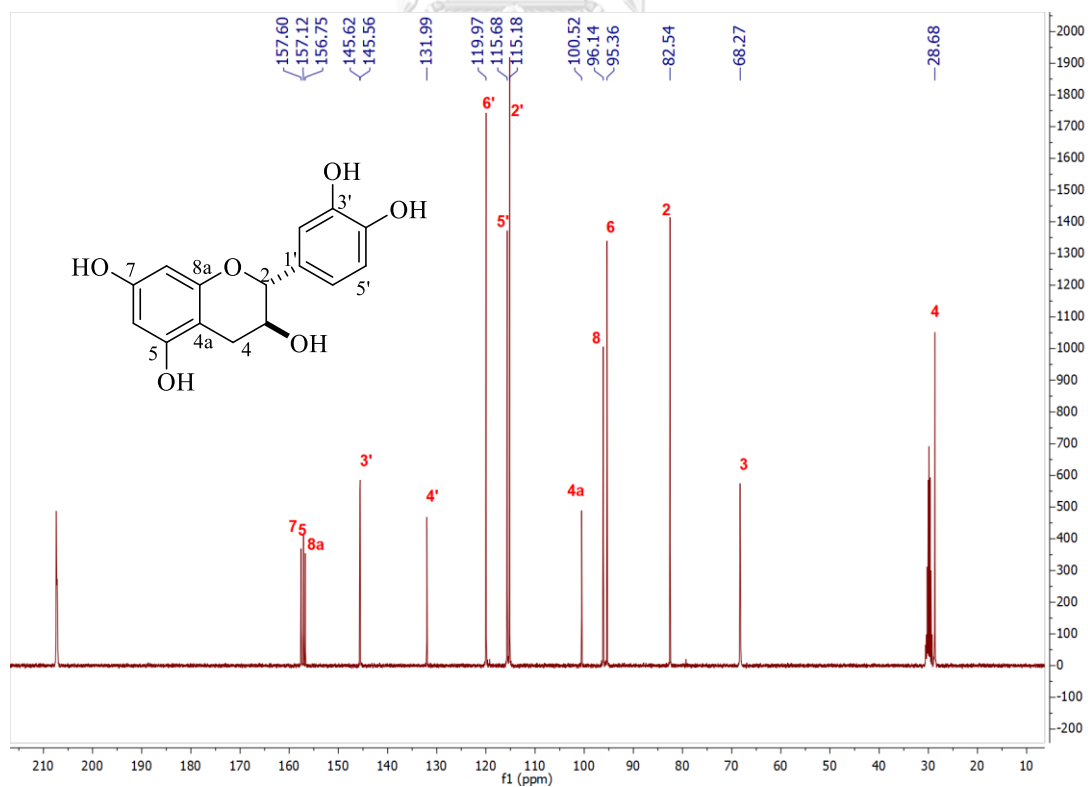


Figure A.27 The ¹³C NMR (100 MHz) spectrum of **8** (acetone-*d*₆)

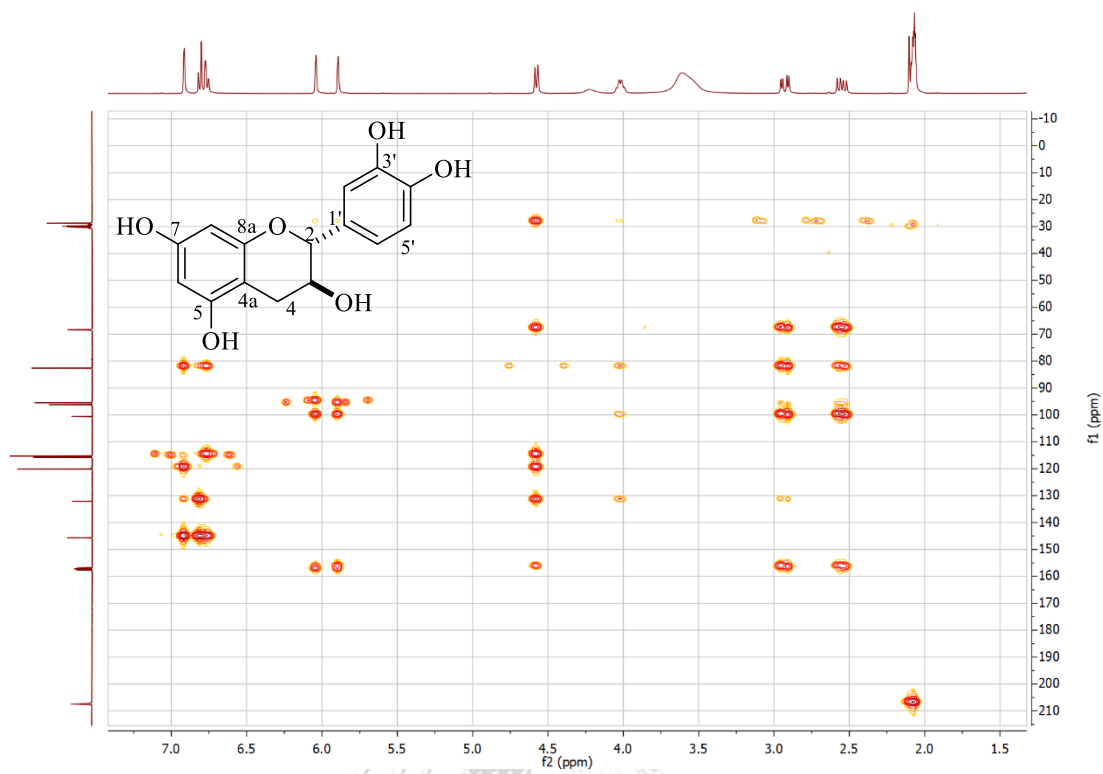
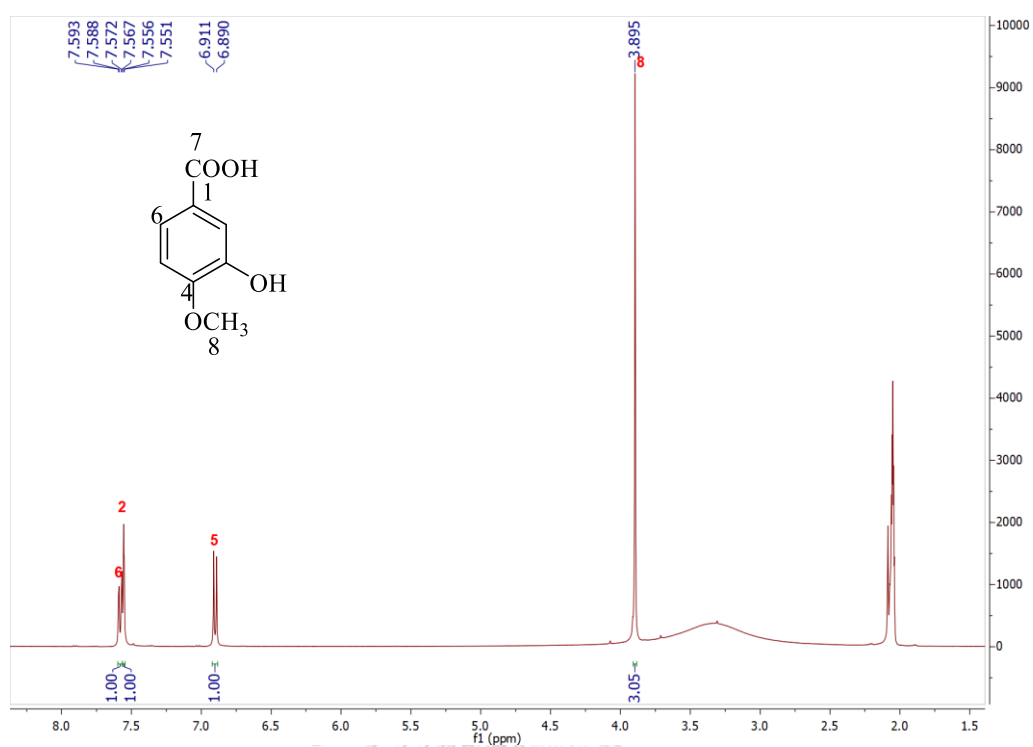
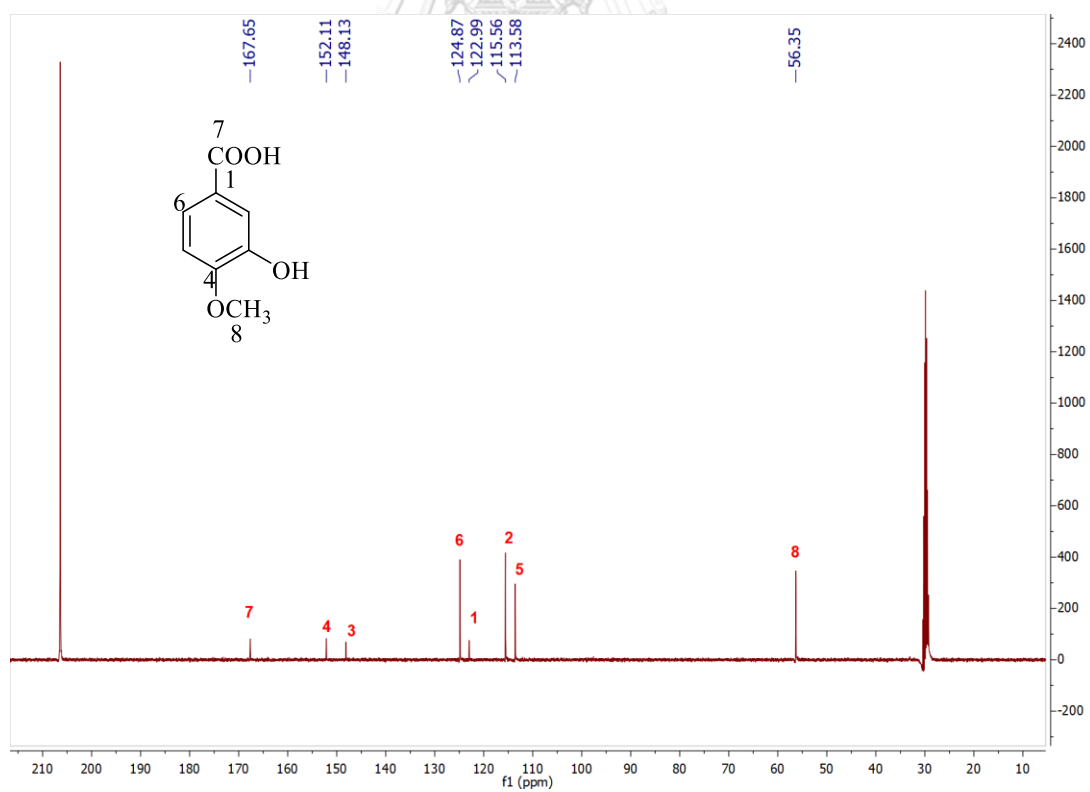


Figure A.28 The HMBC spectrum of 8 (acetone- d_6)

Figure A.29 The ^1H NMR (400 MHz) spectrum of 9 (acetone- d_6)Figure A.30 The ^{13}C NMR (100 MHz) spectrum of 9 (acetone- d_6)

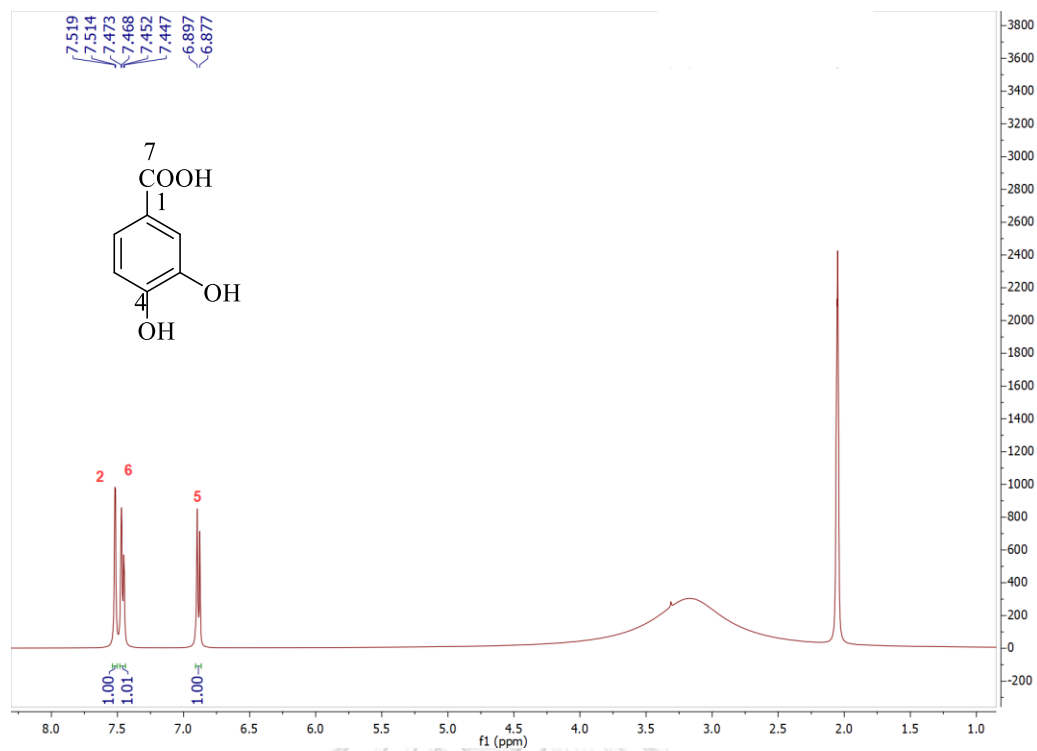


Figure A.31 The ^1H NMR (400 MHz) spectrum of **10** ($\text{acetone-}d_6$)

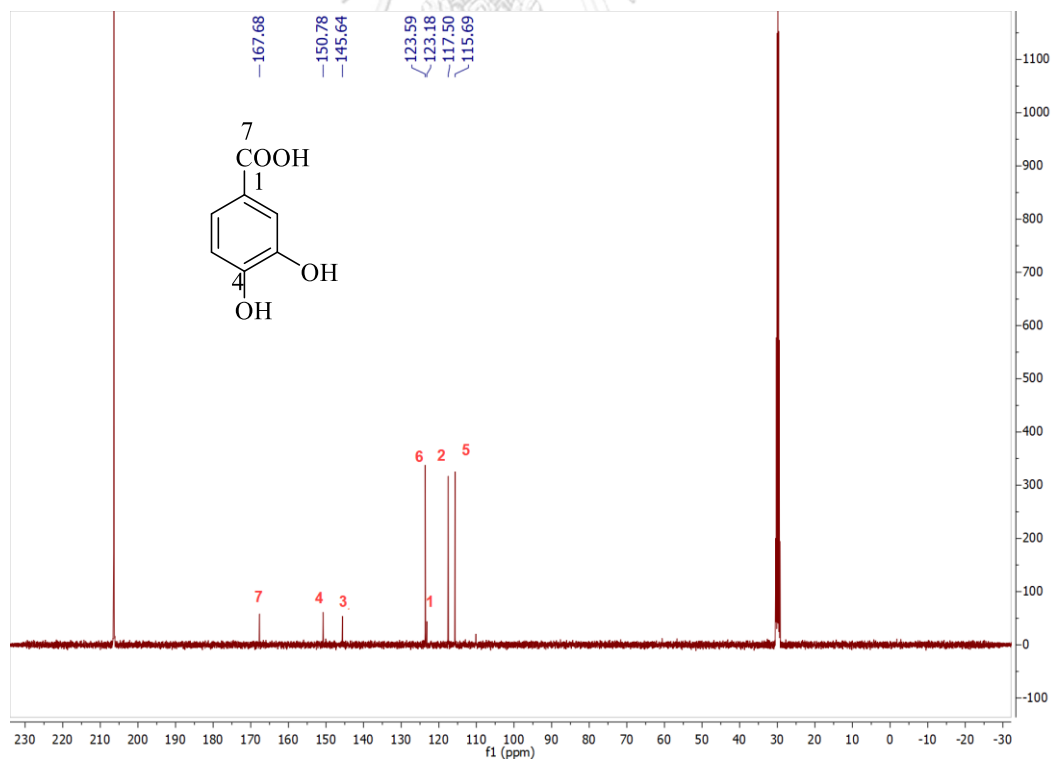


Figure A.32 The ^{13}C NMR (100 MHz) spectrum of **10** ($\text{acetone-}d_6$)

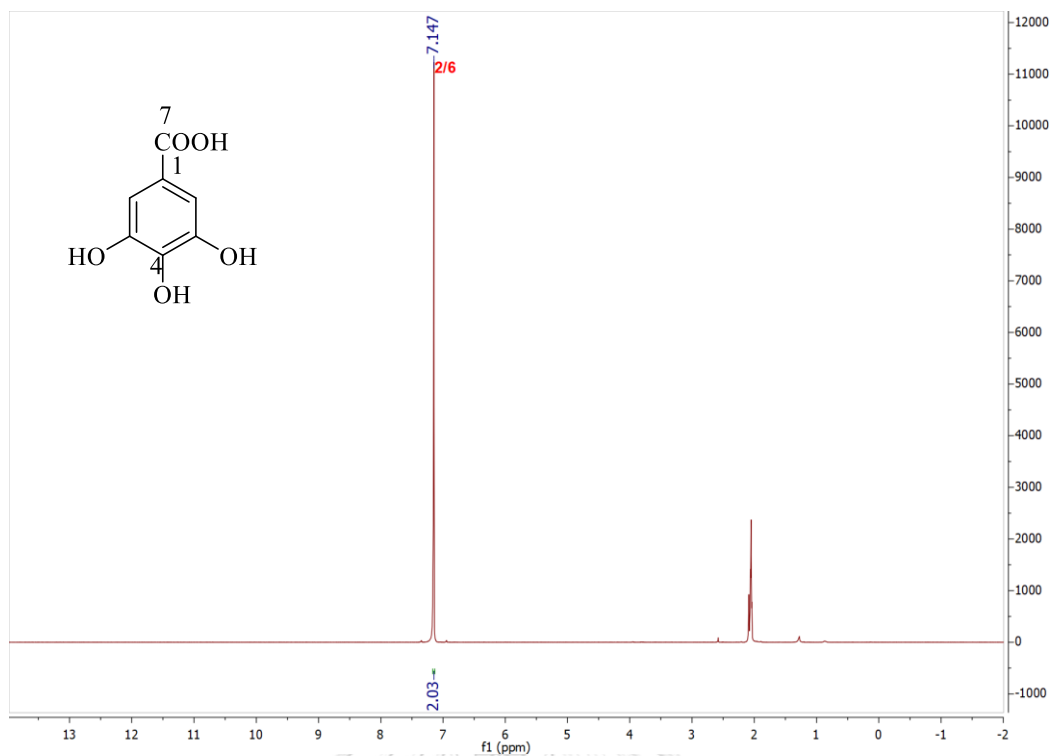


Figure A.33 The ^1H NMR (400 MHz) spectrum of **11** (acetone- d_6)

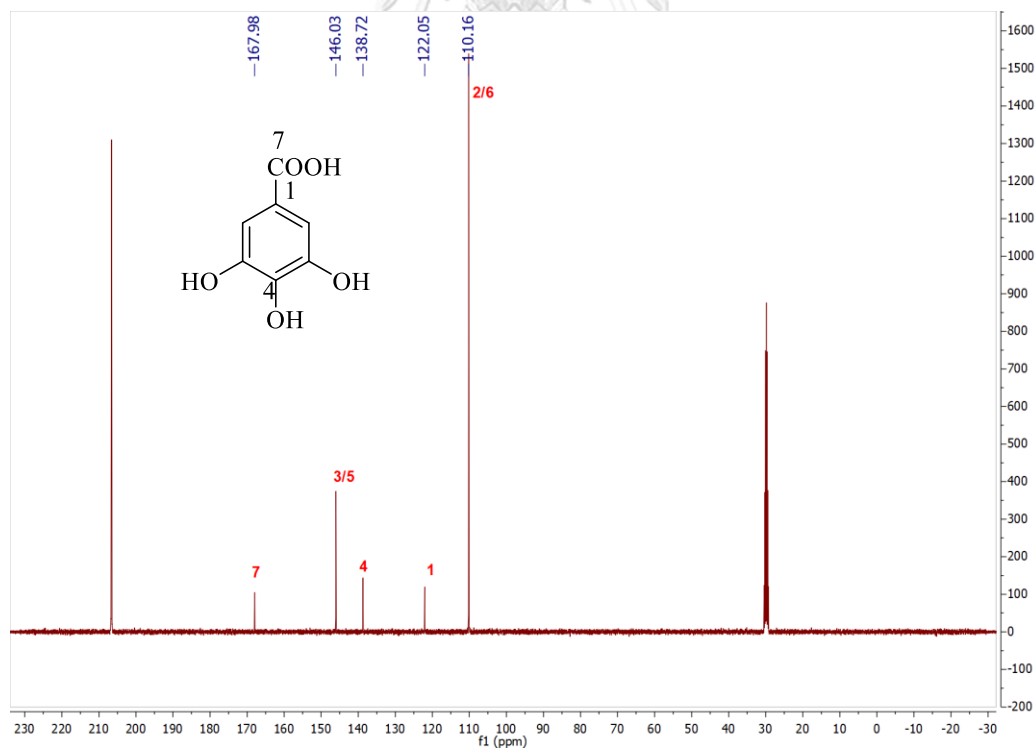


Figure A.34 The ^{13}C NMR (100 MHz) spectrum of **11** (acetone- d_6)

REFERENCES

1. Gaynes, R., The discovery of penicillin—new insights after more than 75 years of clinical use. *Emerging Infectious Diseases* **2017**, *23* (5), 849.
2. Dias, D. A.; Urban, S.; Roessner, U., A historical overview of natural products in drug discovery. *Metabolites* **2012**, *2* (2), 303-336.
3. Panthong, A.; Kanjanapothi, D.; Taylor, W., Ethnobotanical review of medicinal plants from Thai traditional books, Part I: Plants with anti-inflammatory, anti-asthmatic and antihypertensive properties. *Journal of Ethnopharmacology* **1986**, *18* (3), 213-228.
4. Phadungkit, M.; Rattarom, R.; Rattana, S., Phytochemical screening, antioxidant, antibacterial and cytotoxic activities of *Knema angustifolia* extracts. *Journal of Medicinal Plants Research* **2010**, *4* (13), 1269-1272.
5. Smitinand, T., Thai Plant Names. *Bangkok: Prachachon* **2001**, Revised Edition.
6. Chuakul, W.; Boonpleng, A., Survey on medicinal plants in Ubon Ratchathani province (Thailand). **2004**.
7. Ravi, K.; Ved, D., One hundred red listed medicinal plants of conservation concern in Southern India. *Bangalore, India: FRLHT* **2000**.
8. Pinto, M.; Kijjoa, A., Chemical study of *Knema* species from Thailand. *Quim Nova* **1990**, *13* (4), 243-4.
9. Perry, L. M., Medicinal Plants of East and Southeast Asia: Attributed Properties and Uses. *Cambridge: MIT Press* **1980**, 1st Edition.
10. Burkill, I. H., A dictionary of the economic products of the Malay Peninsula. *London: Crown Agents for the Colonies* **1935**.
11. Kijjoa, A.; Gonzalez, M. J. T.; Pinto, M. M.; Monanondra, O.; Herz, W., Constituents of *Knema laurina* and *Knema tenuinervia* ssp. *setosa*. *Planta medica* **1991**, *57* (06), 575-577.
12. González, M. J. T. G.; Pinto, M. M. M.; Kijjoa, A.; Anantachoke, C.; Herz, W., Stilbenes and other constituents of *Knema austrosiamensis*. *Phytochemistry* **1993**, *32* (2), 433-438.
13. Zahir, A.; Jossang, A.; Bodo, B.; Hadi, H. A.; Schaller, H.; Sevenet, T.,

- Knerachelins A and B, antibacterial phenylacylphenols from *Knema furfuracea*. *Journal of Natural Products* **1993**, *56* (9), 1634-1637.
14. Rangkaew, N.; Suttisri, R.; Moriyasu, M.; Kawanishi, K., A new acyclic diterpene acid and bioactive compounds from *Knema glauca*. *Archives of Pharmacal Research* **2009**, *32* (5), 685-692.
15. Zeng, L.; Gu, Z. M.; Fang, X. P.; McLaughlin, J. L., Kneglomeratanol, Kneglomeratanones A and B, and related bioactive compounds from *Knema glomerata*. *Journal of Natural Products* **1994**, *57* (3), 376-381.
16. Akhtar, M. N.; Lam, K. W.; Abas, F.; Ahmad, S.; Shah, S. A. A.; Choudhary, M. I.; Lajis, N. H., New class of acetylcholinesterase inhibitors from the stem bark of *Knema laurina* and their structural insights. *Bioorganic & medicinal chemistry letters* **2011**, *21* (13), 4097-4103.
17. Mei, W.-L.; Yang, Y.; Ni, W.; CHEN, C.-X., Flavonoids from *Knema globularia*. *Acta Botanica Yunnanica* **2000**, *22* (3), 358-360.
18. Mei, W.; Ni, W.; Hua, Y.; Chen, C., Flavonoids from *Knema globularia*. *Natural Product Research and Development* **2002**, *14* (5), 26-28.
19. Giap, T. H.; Thoa, H. T.; Oanh, V. T. K.; Hang, N. T. M.; Dang, N. H.; Thuc, D. N.; Hung, N. V.; Thanh, L. N., New acetophenone and cardanol derivatives from *Knema pachycarpa*. *Natural Product Communications* **2019**, *14* (6), 1934578X19850046.
20. Giap, T. H.; Duc, P. M.; Van The, N.; Popova, M.; Bankova, V.; Hue, C. T.; Kim Oanh, V. T.; Minh Hang, N. T.; Van, H. N.; Le, T. N., Chemical constituents and biological activities of the fruits of *Knema pachycarpa* de Wilde. *Natural Product Research* **2019**, 1-10.
21. Banik, D.; Bora, P. P., A taxonomic study on the diversity of Indian *Knema Lour.*(Myristicaceae). *Taiwania* **2016**, *61* (2), 141-158.
22. Ullah, S.; Son, S.; Yun, H. Y.; Kim, D. H.; Chun, P.; Moon, H. R., Tyrosinase inhibitors: a patent review (2011-2015). *Expert opinion on therapeutic patents* **2016**, *26* (3), 347-362.
23. Ruiz-Vargas, J. A.; Morales-Ferra, D. L.; Ramírez-Ávila, G.; Zamilpa, A.; Negrete-León, E.; Acevedo-Fernández, J. J.; Peña-Rodríguez, L. M., α -Glucosidase inhibitory activity and in vivo antihyperglycemic effect of secondary metabolites from the leaf

- infusion of *Ocimum campechianum* mill. *Journal of ethnopharmacology* **2019**, *243*, 112081.
24. Şöhretoğlu, D.; Sari, S., Flavonoids as alpha-glucosidase inhibitors: mechanistic approaches merged with enzyme kinetics and molecular modelling. *Phytochemistry Reviews* **2019**.
25. Yin, Z.; Zhang, W.; Feng, F.; Zhang, Y.; Kang, W., α -Glucosidase inhibitors isolated from medicinal plants. *Food Science and Human Wellness* **2014**, *3* (3-4), 136-174.
26. Anand, P.; Singh, B., A review on cholinesterase inhibitors for Alzheimer's disease. *Archives of pharmacal research* **2013**, *36* (4), 375-399.
27. Pohanka, M., Alzheimer's disease and oxidative stress: a review. *Current medicinal chemistry* **2014**, *21* (3), 356-364.
28. Larik, F. A.; Saeed, A.; Channar, P. A.; Muqadar, U.; Abbas, Q.; Hassan, M.; Seo, S.-Y.; Bolte, M., Design, synthesis, kinetic mechanism and molecular docking studies of novel 1-pentanoyl-3-arylthioureas as inhibitors of mushroom tyrosinase and free radical scavengers. *European Journal of Medicinal Chemistry* **2017**, *141*, 273-281.
29. Ramadhan, R.; Phuwapraisirisan, P., New arylalkanones from *Horsfieldia macrobotrys*, effective antidiabetic agents concomitantly inhibiting α -glucosidase and free radicals. *Bioorganic & Medicinal Chemistry Letters* **2015**, *25* (20), 4529-4533.
30. da Costa, R. C.; Santana, D. B.; Araujo, R. M.; de Paula, J. E.; do Nascimento, P. C.; Lopes, N. P.; Braz-Filho, R.; Espindola, L. S., Discovery of the rapanone and suberonone mixture as a motif for leishmanicidal and antifungal applications. *Bioorganic & medicinal chemistry* **2014**, *22* (1), 135-140.
31. Mahendran, S.; Badami, S.; Ravi, S.; Thippeswamy, B. S.; Veerapur, V. P., Synthesis and evaluation of analgesic and anti-inflammatory activities of most active free radical scavenging derivatives of Embelin—A Structure–Activity relationship. *Chemical and Pharmaceutical Bulletin* **2011**, *59* (8), 913-919.
32. Durg, S.; Kumar, N.; Vandal, R.; Dhadde, S. B.; Thippeswamy, B.; Veerapur, V. P.; Badami, S., Antipsychotic activity of embelin isolated from *Embelia ribes*: A preliminary study. *Biomedicine & Pharmacotherapy* **2017**, *90*, 328-331.
33. Choi, S.-J.; Tai, B. H.; Cuong, N. M.; Kim, Y.-H.; Jang, H.-D., Antioxidative and

anti-inflammatory effect of quercetin and its glycosides isolated from mampat (*Cratoxylum formosum*). *Food Science and Biotechnology* **2012**, *21* (2), 587-595.

34. Lin, L.-j.; Huang, X.-b.; Lv, Z.-c., Isolation and identification of flavonoids components from *Pteris vittata* L. *SpringerPlus* **2016**, *5* (1), 1649.

35. De Abreu, H. A.; Lago, I. A. d. S.; Souza, G. P.; Piló-Veloso, D.; Duarte, H. A.; Alcântara, A. F. d. C., Antioxidant activity of (+)-bergenin—a phytoconstituent isolated from the bark of *Sacoglottis uchi* Huber (Humireaceae). *Organic & biomolecular chemistry* **2008**, *6* (15), 2713-2718.

36. Khan, H.; Amin, H.; Ullah, A.; Saba, S.; Rafique, J.; Khan, K.; Ahmad, N.; Badshah, S. L., Antioxidant and antiplasmodial activities of bergenin and 11-O-galloylbergenin isolated from *Mallotus philippensis*. *Oxidative medicine and cellular longevity* **2016**, 2016.

37. Lakornwong, W.; Kanokmedhakul, K.; Kanokmedhakul, S., Chemical constituents from the roots of *Leea thorelii* Gagnep. *Natural product research* **2014**, *28* (13), 1015-1017.

38. Nyunt, K. S.; Elkhateeb, A.; Tosa, Y.; Nabata, K.; Katakura, K.; Matsuura, H., Isolation of antitrypanosomal compounds from *Vitis repens*, a medicinal plant of Myanmar. *Natural product communications* **2012**, *7* (5), 1934578X1200700516.

39. El-Razek, M. A., NMR assignments of four catechin epimers. *Asian Journal of Chemistry* **2007**, *19* (6), 4867.

40. Xiang, M.; Su, H.; Hu, J.; Yunjun, Y., Isolation, identification and determination of methyl caffeate, ethyl caffeate and other phenolic compounds from *Polygonum amplexicaule* var. *sinense*. *Journal of Medicinal Plants Research* **2011**, *5*, 1685-1691.

41. da Silva, L. A. L.; Faqueti, L. G.; Reginatto, F. H.; dos Santos, A. D. C.; Barison, A.; Biavatti, M. W., Phytochemical analysis of *Vernonanthura tweedieana* and a validated UPLC-PDA method for the quantification of eriodictyol. *Revista Brasileira de Farmacognosia* **2015**, *25* (4), 375-381.

42. Abri, A.; Maleki, M., Isolation and identification of gallic acid from the *elaegnus angustifolia* leaves and determination of total phenolic, flavonoids contents and investigation of antioxidant activity. *Iranian Chemical Communication* **2016**, *4*, 146-154.

43. Şöhretoğlu, D.; Sari, S.; Barut, B.; Özel, A., Tyrosinase inhibition by some

flavonoids: Inhibitory activity, mechanism by in vitro and in silico studies. *Bioorganic chemistry* **2018**, *81*, 168-174.

44. Naik, S. R.; Niture, N. T.; Ansari, A. A.; Shah, P. D., Anti-diabetic activity of embelin: involvement of cellular inflammatory mediators, oxidative stress and other biomarkers. *Phytomedicine* **2013**, *20* (10), 797-804.

45. Indrianingsih, A. W.; Tachibana, S.; Dewi, R. T.; Itoh, K., Antioxidant and α -glucosidase inhibitor activities of natural compounds isolated from *Quercus gilva* Blume leaves. *Asian Pacific Journal of Tropical Biomedicine* **2015**, *5* (9), 748-755.

46. Peng, X.; Zhang, G.; Liao, Y.; Gong, D., Inhibitory kinetics and mechanism of kaempferol on α -glucosidase. *Food chemistry* **2016**, *190*, 207-215.

47. Zhen, J.; Dai, Y.; Villani, T.; Giurleo, D.; Simon, J. E.; Wu, Q., Synthesis of novel flavonoid alkaloids as α -glucosidase inhibitors. *Bioorganic & medicinal chemistry* **2017**, *25* (20), 5355-5364.

48. Kashima, Y.; Yamaki, H.; Suzuki, T.; Miyazawa, M., Structure-activity relationships of bergenin derivatives effect on α -glucosidase inhibition. *Journal of enzyme inhibition and medicinal chemistry* **2013**, *28* (6), 1162-1170.

VITA

NAME Dung Le Thi Kim

DATE OF BIRTH 01 September 1994

PLACE OF BIRTH Quang Nam, Vietnam

INSTITUTIONS ATTENDED Department of Chemistry, University of Education, HCMC, Vietnam

HOME ADDRESS Room 1529, Chula International House, Chulalongkorn University, Bangkok, Thailand



จุฬาลงกรณ์มหาวิทยาลัย
CHULALONGKORN UNIVERSITY